INFORMATION TO USERS

This manuscript has been reproduced from the microfilm master. UMI films

the text directly from the original or copy submitted. Thus, some thesis and

dissertation copies are in typewriter face, while others may be from any type of

computer printer.

The quality of this reproduction is dependent upon the quality of the

copy submitted. Broken or indistinct print, colored or poor quality illustrations

and photographs, print bleedthrough, substandard margins, and improper

alignment can adversely affect reproduction.

In the unlikely event that the author did not send UMI a complete manuscript

and there are missing pages, these will be noted. Also, if unauthorized

copyright material had to be removed, a note will indicate the deletion.

Oversize materials (e.g., maps, drawings, charts) are reproduced by

sectioning the original, beginning at the upper left-hand corner and continuing

from left to right in equal sections with small overlaps.

Photographs included in the original manuscript have been reproduced

xerographically in this copy. Higher quality 6" x 9" black and white

photographic prints are available for any photographs or illustrations appearing

in this copy for an additional charge. Contact UMI directly to order.

Bell & Howell Information and Learning 300 North Zeeb Road, Ann Arbor, MI 48106-1346 USA

800-521-0600

UMI®

Design and Characterization of a Thermochemical High Performance Liquid Chromatography Flame Photometric Detector for the Detection Of Non-Volatile and /or Thermolabile Sulfur Compounds

by

Joël Bernard

Department of Food Science and Agricultural Chemistry McGill University

A thesis submitted to the Faculty of Graduate Studies and Research in partial Fulfillment of the requirement for the degree of Doctor in Philosophy



National Library of Canada

Acquisitions and Bibliographic Services

395 Weilington Street Ottawa ON K1A 0N4 Canada Bibliothèque nationale du Canada

Acquisitions et services bibliographiques

395, rue Wellington Ottawa ON K1A 0N4 Canada

Your file Votre référence

Our file Notre référence

The author has granted a nonexclusive licence allowing the National Library of Canada to reproduce, loan, distribute or sell copies of this thesis in microform, paper or electronic formats.

The author retains ownership of the copyright in this thesis. Neither the thesis nor substantial extracts from it may be printed or otherwise reproduced without the author's permission.

L'auteur a accordé une licence non exclusive permettant à la Bibliothèque nationale du Canada de reproduire, prêter, distribuer ou vendre des copies de cette thèse sous la forme de microfiche/film, de reproduction sur papier ou sur format électronique.

L'auteur conserve la propriété du droit d'auteur qui protège cette thèse. Ni la thèse ni des extraits substantiels de celle-ci ne doivent être imprimés ou autrement reproduits sans son autorisation.

0-612-55302-7



Suggested sort title: HPLC-FPD of sulfur compounds

Abstract

The need for selective and inexpensive detectors in liquid chromatography is of considerable interest in the determination of sulfur compounds. Of the available-selective sulfur methodologies, flame photometric detector coupled to gas chromatography is the most widely used. It has proven to be a sensitive and selective method for detection of heat stable and volatile sulfur compounds. Fundamentally, this technique is not applicable to high boiling and/or thermolabile sulfur compounds. More recently, hyphenated flame photometric detector has been utilized, with limited success, to monitor sulfur species in liquid chromatography. However, existing HPLC-FPD methodologies have never been applied to real samples, due to the low population of S₂, the emitting species, and the quenching effects of the other species present in the flame.

In this work, two total consumption high-performance liquid chromatography flame photometric (HPLC-FPD) interfaces compatible with either methanolic or aqueous mobile phases are described and optimized for monitoring low volatile and thermally fragile sulfur compounds in biological samples. Each interface was fuelled either by methanol or by hydrogen. The all quartz interfaces enclosed four consecutive thermal processes: (a) thermovaporization of the HPLC effluent; (b) pyrolysis of the organic matrix (including sulfur species) in a kinetic H₂/O₂ flame; (c) conversion of the oxidized sulfur compounds to H₂S in a reducing post-combustion stage fuelled by hydrogen; and (d) transport of the generated hydrides towards a hydrogen radical rich surrounding of an inverted hydrogen-oxygen diffusion flame. Chemiluminescence induced in the last step was integrated as a narrow beam in a light-guide positioned remotely from the analytical

cool flame and oriented towards a photomultiplier unit. Radioisotopic assays demonstrated that sulfur (as $H_2^{35}SO_4$) was transferred quantitatively to the analytical flame. Indirect evidence suggested that sulfur was hydrogenated in the post-combustion step via a thermochemical hydride generation process to mediate the formation of S_2 . The linearity of calibration graphs (0.9950 < r < 0.9986), where r is the correlation coefficient) and unprecedented HPLC-FPD limits of detection for sulfur compounds (1.5 $\eta g/s$ for 2-methylthiophene, 2.25 $\eta g/s$ for carbon disulfide, and 4.5 $\eta g/s$ for ethanesulfonic acid) allowed for the speciation of sulfur species in garlic extracts. Alternatively, modification of the methanol fuelled interface to a hydrogen fuelled reactor allowed detection of thiosulfinates and high molecular weight sulfur compounds in horse kidney and garlic extracts, respectively.

Résumé

L'élaboration d'un détecteur en chromatographie liquide qui soit à la fois sélectif et peu coûteux est particulièrement important pour la spéciation de produits soufrés. Parmi les méthodes actuelles de détection de ces produits, le détecteur photométrique à la flamme associé à la chromatographie en phase gazeuse est le plus utilisé. Il s'est avéré une méthode sensible et sélective pour la détection de produits soufrés volatilisables et thermostables. Cette technique n'est, cependant, pas applicable pour des produits non volatiles et instables à la chaleur. Plus récemment, on a proposé, avec un succès mitigé, plusieurs méthodologies utilisant le détecteur photométrique à la flamme couplé à la chromatographie liquide à haute performance. A cause de la faible population de l'espèce émettrice, S₂, et des effets inhibiteurs des autres espèces présents dans la flamme, ces techniques restent inapplicables à des échantillons biologiques.

Dans ce travail, deux interfaces, compatibles avec le méthanol ou des systèmes aqueux comme phases mobiles, sont décrites et optimisées pour la détection sélective, dans des échantillons biologiques, de produits soufrés instables à la chaleur ou non volatilisables en chromatographie gazeuse. Les interfaces proposées, reliant la chromatographie liquide au détecteur à la flamme, renferment quatre phénomènes thermiques successifs: a) thermovaporisation de la phase mobile, b) pyrolyse de la matrice organique (incluant les espèces soufrées) dans une chambre à combustion, c) volatilisation de radicaux de soufre dans une zone réductrice alimentée par de l'hydrogène, et d) transports des hydrures de soufre résultants dans une flamme analytique à alimentation inversée. La chimiluminescence induite dans la dernière étape a

été intégrée comme un faisceau étroit orienté vers un tube photomultiplicateur. Des expériences, utilisant H₂³⁵SO₄ comme marqueur isotopique, ont démontré que le soufre était transféré de façon quantitative à la flamme analytique. De plus, en faisant passer le courant gazeux, issu de l'interface, dans une solution d'acétate de plomb, nous avons pu démontrer que le soufre a été hydrogéné dans la chambre à combustion pour générer la formation de H₂S.

La linéarité des courbes de calibration (0.9950 < r < 0.9986), où r est le coefficient de corrélation) et les limites de détection obtenues pour des produits soufrés témoins (1.5 ηg/s pour le 2-methylthiophene, 2.25 ηg/s pour disulfite de carbone et 4.5 ηg/s pour l'acide éthanesulfonique) permettaient la spéciation de produits soufrés dans des extraits d'ail. Par ailleurs, en transformant l'interface à base de méthanol en une interface qui utilise l'hydrogène comme carburant, nous avons pu déterminer des thiosulfinates dans des extraits d'ail et des produits soufrés non volatiles en chromatographie gazeuse dans des extraits de reins de cheval.

This work is dedicated to my wife, Gisèle Savoie, my daughters, Chloé and Ariane, my sons, Jérémie and Théo, who gave me the inspiration and the strength to achieve this study.

Acknowledgements

I am grateful to my supervisor, Dr Jean-Simon Blais, for financial support, his guidance, his availability and flexibility throughout this study at McGill University. The following people also deserve my deep gratitude:

- •Dr W.D. Marshall for his precious advice and for his support during the radioisotopic assays.
- •Drs I.Alli and V. Yaylayan for helpful suggestions during my study.
- Antonio Nicodemo for assistance in the radioisotopic assays.
- •Dr Georges-Marie Momplaisir for introducing me at the Department of Food Science and Agricultural Chemistry of the McGill University.
- •Silvie Savoie for help with all the softwares used in this study.
- •Lise Steibel and Barbara Laplaine for their help with all the administrative procedures.
- •My parents, my sisters and my brothers who always encouraged me to pursue my studies.
- •Francine Savoie who reviewed the entire document and provided invaluable help and advice.

TABLE OF CONTENTS

Abstract			
Résumé			
Acknowledgements	viii		
List of Figures	xvi		
List of Tables	xvii		
List of Abbreviations and Symbols	xx		
Chapter I Literature review: Sulfur Occurrence, Metabolism, Bioavailability Analysis	and		
1. High Pressure Liquid Chromatography-Flame Photometric Detector for Speciation of Non-volatile and/or Heat Sensitive Sulfur Compounds	3		
1.1 Introduction	3		
1.2 The Fate of Metallothionein, Reduced Glutathione, and Taurine			
1.2.1 Metallothionein	4		
1.2.2 Functions of MT	5		
1.2.3 Methods for Detection and Quantification of MT	6		
1.3 Taurine	7		
1.3.1 Physicochemical Aspects of Taurine	9		
1.3.2 Functions of Taurine	9		
1.3.3 Methods for Determination of Taurine	11		
1.4 Glutathione and Its Functions	12		
1.4.1 Methods for Determination of Glutathione	13		
1.5 Overview of the Use of Garlic 15			

	1.5.1	Overview of Garlic Chemistry	16
		Methods for the Determination of Sulfur Compounds from Garlic	17
1.6	Importan	ce of Sulfur	20
1.7	History o	f Elemental Sulfur	20
1.8	Physical A	Aspects of Elemental Sulfur	20
1.9	Special C	haracteristics of Organosulfur Compounds	22
	Some Coo	mmon Characteristics of Sulfur and Other Members VIA	22
1.11	Sources	of Sulfur	24
	1.11.1	World Reserves of Sulfur	24
	1.11.2	Sulfur in Agriculture	25
	1.11.3	Sulfur in Soil	26
	1.11.4	Toxicity of Sulfur and Sulfur Compounds	27
1.12	Determin	nation of Sulfur Compounds by Molecular Emission	27
	1.12.1	Use of Molecular Emission in the Analysis of Sulfur Compounds	27
	1.12.2	Mechanisms Proposed for the S ₂ Formation	29
	1.12.3	Molecular Emission Cavity Analysis for Sulfur Detection	30
	1.12.4	Temperature-Resolved Molecular Emission Spectroscopy	30
	1.12.5	Hyphenated GC-FPD for Sulfur Detection	31
	1.12.6	Pulsed Flame Photometric Detection-GC for Sulfur Compounds	32
	1.12.7	GC-Sulphur Chemiluminescence for Sulfur Compounds	32
	1.12.8	Fluorine Induced Chemiluminescence for Sulfur Compounds	33
	1 13 0	Hyphanatad HDI C EDD for Sulfur Detection: Early Approaches	3/

Cł	apte	r II	Design, Characterization and Optimization of a Thermochemical High-Performance Liquid Chromatography Flame Photometric Detector Interface for the Speciation of Thermolabile and Low	
			Volatile Sulfur Compounds	38
2 (ptim	izatio	on of an Interface for HPLC-FPD	39
	2.	l Syr	nopsis	39
	2.2	2 The	ermochemical Interface for Sulfur hydrides Generation	39
		2.2.	I Technical Aspects of the Interface	45
	2.3	3 Ins	strumentation	46
	2.4	1 Re	agents, Standards, and Chromatography	47
	2.5	5 Tra	pping Experiments	48
	2.6	6 Op	timization of the Interface	50
	2.7	7 Re	sults and Discussion	50
		2.7.1	Radioisotopic Assays	50
		2.7.2	Thermospray Unit and Charaterization of the Intermediate Species Involved in the Formation of S_2	55
	2	2.7.3	Optimization of the Methanol Fuelled Interface for HPLC-FPD	57
		2.7.4	Flow Injection Calibration, Reproducibility, Linearization and Limit of Detection for S ₂ Response	60
		2.7.5	Determination of Thermolabile Sulfur Compounds from Garlic by HPLC-THG-FPD	67
	2.8	Limit	ations of the Methanol Fuelled Interface	69
	2.9	Conc	lusion	69
Ch	apter	·m	Design of a Hydrogen Fuelled Interface for the Determination of Sulfur Compounds from Biological Samples (Applications of the HPLC-THG-FPD to Horse Kidney and Garlic extracts)	71
3	Beha [,]	viour	of the HPLC-THG-FPD With Regard to Real Samples	72
	3.1	Introd	duction	72

3.2 Ma	terials and Methods	72
3.2.1	Reagents and Standards for the Characterization of the Fuelled Hydrogen HPLC-THG-FPD	72
3.2.2	Instrumental Components	73
3.2.3	Reagents and Standards for the Speciation of Sulfur Compounds from Horse Kidney Extracts	7 3
3.2.4	Sample Preparation and HPLC Conditions for the Speciation of Sulfur from Horse kidney Extracts	74
3.2.5	Reagents, Standards, and HPLC Conditions for the Separation of Sulfur Compounds from Garlic Extracts	74
3.2.6	Synthesis of Allicin	75
3.3 Resu	ilts and Discussion	75
3.3.1	Design of a Hydrogen Fuelled Interface	75
3.3.2	Optimization of a Hydrogen Fuelled HPLC-FPD Interface for Sulfur Dimer Emission	78
3.3.3	Reproducibility of the Hydrogen Fuelled Interface	83
3.3.4	Performance of the System With Regard to Potential Interferences: CN and NH	84
3.3.5	Choice of Ammonium Acetate as Eluent for the Speciation of Sulfur Compounds from Horse Kidney	86
3.3.6	Effects of Metals on the Emission of Sulfur Dimer	86
3.3.7	Limit of Detection and Level of the Three Target Analytes	87
3.3.8	Application of the HPLC-FPD System for the Determination of Taurine, Glutathione, and Metallothionein in Biological Matrices	89
3.3.9	Resolution of MT-I and MT-II and Chromatographic Behaviour of MTs, GSH, and Taurine on the G2000SW _{XL} Column	91
	termination of Allicin and Other Thiosulfinates from Garlic mogenates	94
3.4.1	Limit of Detection of Allicin Using the Hydrogen Fuelled Interface	94

3.4.2 Performance of the Hydrogen Fuelled Interface with Regard to Real Samples: Detection of Allicin and Other Thiosulfinates	94
3.5 Conclusion	96
Chapter IV Original Contributions to Knowledge and Suggestions for further Studies on Thermolabile and Low Volatile Sulfur Compounds using the HPLC-THG-FPD System	98
4.1 Contributions to Original Knowledge	99
4.2 Suggestions for Further Researches	99
4.2.1 Analysis of Garlic Products	99
4.2.2 Determination of Taurine in Fluids and Tissues Homogenates	100
Chapter V Appendix. Statistical Analyses Associated With the Optimization of the HPLC-THG-FPD System	101
Chapter VI References	141

List of Figures

Figure 1.1	Spectrum of S ₂ in Air-Hydrogen flame	28
Figure 2.1	Block Diagram of the HPLC-THG-FPD	41
Figure 2.2	Schematic Illustration of Thermospray Effects After Vaporization Process	42
Figure 2.3	Thermospray FPD System	43
Figure 2.4	Trapping Apparatus for Radiochemical Assay	49
Figure 2.5	Radiochemical Recoveries in Reactor Segments and chemical traps Measured After a Single Injection of H ₂ ³⁵ SO ₄ in Test THG unit Operated With A, 0.50, B,0.65 and C, 0.80 L/min of Pyrolysis Oxygen	51
Figure 2.6	Preliminary Design Used for the Classical Air-Hydrogen Diffusion Flame	54
Figure 2.7	Response Surface Models Depicting the Effects of Gas Flow Rates on Molecular Emission Response	58
Figure 2.8	Flow Injection Calibration of (A) 2-Methylthiophene, (B) Carbon Disulfide, and (C) Ethanesulfonic Acid	63
Figure 2.9	Regression Analysis for the Square Roots of the Peak Integrations versus Amounts of Injected Sulfur as (A) 2-Methylthiophene, (B) Carbon Disulfide, and (C) Ethanesulfonic Acid	64
Figure 2.10	Regression Analysis for the Logarithm of Peak Integrations versus Logarithm of Amounts of Sulfur Injected as (A) 2-Methylthiophene; (B) Carbon Disulfide; and (C) Ethanesulfonic Acid	65
Figure 2.11	Regression Analysis for the Chemical Linearization Obtained for 2-Methylthiophene	66
Figure 2.12	HPLC-THG-FPD Traces of an Aqueous Garlic Extracts: (a) Fresh Extracts; and (b) After Storage for 24 Hours at Room Temperature	68
Figure 3.1	Diagram of the THG-FPD Hydrogen System Compatible With Either Methanolic or Aqueous Mobile Phase	77
Figure 3.2	Surface Predicting Response to 16.33 ng of Sulfur as GSSG as a Function of Analytical Oxygen versus Helium Flow Rates in Flow Injection Mode (Mobile Phase:Pure Water, loop :20 µL)	81

Figure 3	3.3	Surface Predicting Response to 1.65 µg of Carbon as Ethanol as a Function of Analytical Oxygen versus Helium Flow Rates in Flow Injection Mode (Mobile Phase: Pure Water, Loop: 20 µL)	81
Figure	3.4	Surface Predicting Response Surface to 8.6 ppm of MetaLlothionein as a Function of Analytical Oxygen versus Helium Flow Rates in Flow Injection Mode (Mobile Phase : 10mM Ammonium Acetate, Loop: $20~\mu L$)	82
Figure	3.5	Surface Predicting Response Surface to 1.65 µg of Carbon as Ethanol as a Function of Analytical Oxygen versus Helium Flow Rates in Flow Injection Mode (Mobile Phase :10mM Ammonium Acetate, Loop: 20 µL)	82
Figure		HPLC-THG-FPD Responses for 20 Consecutive Injections of 25.4 ηg of Sulfur as GSSG (Conditions : flow injection Mode; Mobile Phase : 10 mM Ammonium Acetate; Loop : 97 μL)	84
Figure :	3.7	Performance of the System With Regard to CN and CH Emission (Flow Injection Mode, Mobile Phase :Pure Water)	85
Figure (3.8	Effects of Cadmium on the FPD Response of 20 ng of Sulfur as GSSG (Flow Injection Mode; Mobile phase : 10 mM Ammonium Acetate; Loop : 20µL)	87
Figure (HPLC-THG-FPD Response for Sulfur Compounds From Horse Kidney Extracts (1:100 Dilution): Mobile Phase, 10 mM Ammonium Acetate at 0.65mL/min; loop, 97 μL; Column, TSK G4000 PW _{XL}	n 90
Figure :	3.10	HPLC-THG-FPD Response for Sulfur Compounds From Horse Kidney Extract (1: 100 Dilution): Mobile Phase, 10 mM Ammonium Acetate at 0.65 mL/min; Loop, 97 µL; Column, TSK G2 000 SW _{XL}	93
Figure 3	3.11	C ₁₈ HPLC-FPD Chromatogram of Fresh Garlic Extracts Using Methanol-Water (60:40) as Eluent; loop 20 µL	95
Figure A	A- 1	Regression of Observed on Predicted Values for the Factorial Optimization of the Pure methanol fuelled interface 1	07
Figure A	\- 2	Residuals of Observed on Predicted Values for the Factorial Optimization of the Pure Methanol Interface 1	08
Figure A	A-3	Residuals for the Square Roots of Emission Intensity of Amounts of Sulfur Injected as 2-Methylthiophene 1	11

Figure A-4	Residuals for the Square Roots of Emission Intensity of Amounts of Sulfur Injected as Carbon Disulfide	113
Figure A-5	Residuals for the Square Roots of Emission Intensity of Amounts of Sulfur Injected as Ethanesulfonic Acid	115
Figure A-6	Residuals for the log Emission Intensity versus log Amounts of Sulfur Injected as 2-Methylthiophene	117
Figure A-7	Residuals for the log Emission Intensity versus log Amounts of Sulfu Injected as Carbon Disulfide	ır 119
Figure A-8	Residuals for the log Emission Intensity versus log Amounts of Sulfur Injected as Ethanesulfonic Acid	121
Figure A-9	Residuals for the Emission Intensity versus Amounts of Sulfur Injected as 2-Methylthiophene (Mobile Phase Doped With 20 of 2-Methylthiophene)	123
Figure A-10	Regression of Observed versus Predicted Values (Emission Intensity Sulfur Using Pure Water as Mobile Phase in Flow Injection Mode)	
Figure A-11	Residuals of Observed versus Predicted Values (Emission Intensity F Sulfur Using Pure Water as Mobile Phase in Flow Injection Mode)	rom 128
Figure A-12	Regression of Observed versus Predicted Values (Emission Intensity Using Water as Mobile Phase in Flow Injection Mode)	131
Figure A-13	Residuals of Observed <i>versus</i> Predicted Values (Emission Intensity From Carbon Using Pure Water as Mobile Phase in Flow Injection Mode)	132
Figure A-14	Regression of Observed versus Predicted Values (Emission Intensity From Sulfur Dimer Using 10 Mm Ammonium Acetate as Mobile Phase)	135
Figure A-15	Residuals of Observed versus Predicted Values (Emission Intensity From Sulfur Dimer Using 10 mM Ammonium Acetate as Mobile Phase)	136
Figure A-16	Regression of Observed versus Predicted Values (Emission Intensity From Carbon Using 10 Ammonium Acetate as Mobile Phase)	139
	Residuals of Observed versus Predicted Values (Emission Intensity From Carbon Dimer Using 10 mM Ammonium Acetate as Mobile Phase)	140

List of Tables

Table 1.1 Taurine Concentration in Some Species	8
Table 1.2 Some Physiological Actions of Taurine	10
Table 1.3 Volatile Compounds Isolated From Garlic Extracts Using GC	19
Table 1.4 Volatile Thiosulfinates Identified From Garlic Extracts Using HPLC	19
Table 1.5 Oxidation States of Sulfur in Covalent Compounds	21
Table 1.6 Bond Energies of Group VIA Elements	23
Table 1.7 Periodicity Among Group VIA Elements	23
Table 1.8 Natural Abundance of Sulfur	24
Table 1.9 Sulfur Content of Some Organic Materials	25
Table 1.10 Sulfur Amino Acid Content of Some Organic Materials	26
Table 2.1 Reproducibility of the HPLC-THG-FPD System in Flow Injection Mode at Various Concentrations of Analytes	62
Table 3.1 Recovery Test by Detection of MTs, GSH, and Taurine in Horse Kidney Tissues and Sums of MTs, GSH, and Taurine Contents in Kidney Tissues Plus Respective Additions	88
Table A-1 Obtained Counts Per Minute for 35S	102
Table A-2 Matrix of the 2 ⁴ Factorial Design	103
Table A-3 Observed and Predicted Results of the Factorial Experiment for the Methanol Fuelled Interface	104
Table A-4 Analysis of Variance for the Full Regression of Observed on Predicted Values (Sulfur Emission For the Optimization of the Methanol Fuelled Interface)	106
Table A-5 Factorial second order equations predicting the effect of selected variables on the emission of sulfur dimer for the pure methanol fuelled interface	109
Table A-6 Regression Analysis for the Square Roots of the Peak Integration versus Amounts of Sulfur Injected as 2-Methylthiophene	110
	xvii

Table A-7 Regression Analysis for the Square Roots of the Peak Integration versus Amounts of Sulfur Injected as Carbon Disulfide	112
Table A-8 Regression Analysis for the Square Roots of the Peak Integration versus Amounts of Sulfur Injected as Ethanesulfonic Acid	114
Table A-9 Regression Analysis for the log Emission Intensity versus log Amounts of Sulfur Injected as 2-Methylthiophene	116
Table A-10 Regression Analysis for the log Emission Intensity versus log Amounts of Sulfur Injected as Carbon Disulfide	118
Table A-11 Regression Analysis for the log Emission Intensity versus log Amounts of Sulfur Injected as Ethanesulfonic Acid	120
Table A-12 Regression Analysis for the Emission Intensity versus Amounts of Sulfur Injected as 2-Methylthiophene (Mobile Phase Doped With 20 ppm of 2-Methylthiophene)	122
Table A-13 Matrix of the 2 ² Factorial Design	124
Table A-14 Observed and Predicted Results of the Factorial Experiments for the Optimization of the Hydrogen Fuelled Interface Using Pure Water as Eluent (Emission Intensity for Sulphur)	125
Table A-15 Analysis of Variance for the Full Regression of Observed on Predicted Values (Sulfur Emission for the Optimization of the Hydrogen Fuelled Interface Using Pure Water as Mobile Phase)	126
Table A-16 Observed and Predicted Results of the Factorial Experiments for the Optimization of the Hydrogen Fuelled Interfaced Using Pure Water as Eluent (Emission Intensity for Carbon)	129
Table A-17 Analysis of Variance for the Full Regression of Observed on Predicted Values (Carbon Emission for the Optimization of the Hydrogen Fuelled Interface Using Water as Eluent)	130
Table A-18 Observed and Predicted Results for the Optimization of the Hydrogen Fuelled Interface for 10 mM Ammonium Acetate as Mobile Phase	133
Table A-19 Analysis of Variance for the Full Regression of Observed on Predicted Values (Sulfur Emission for the Optimization of the Hydrogen Fuelled Interface Using 10 mM Ammonium Acetate as Mobile Phase)	
Table A-20 Observed and Predicted Results for the Optimization of the Hydrogen Fuelled Interface for 10 mM Ammonium Acetate as Mobile Phase (Emission From Carbon)	137

Table A-21 Analysis of Variance for the Full Regression of Observed on Predicted Values (Emission From Carbon for the Optimization of the Hydrogen Fuelled Interface Using 10 mM Ammonium Acetate as Mobile Phase) 138

List of Abbreviation and Symbols

AAS Absorption Atomic Spectroscopy

Bq Becquerel

cm Centimetre

cp Centipoise

CZE Capillary Zone Electophoresis

DTNB 5,5'-Dithiobis-(2-Nitrobenzoic Acid)

FPD Flame Photometric Detector

GC Gas Chromatography

GR Glutathione Reductase

GSH Reduced glutathione

GSSG Oxidized Glutathione

HPCE High Performance Capillary Electrophoresis

HPLC High Performance Liquid Chromatography

ICP-AES Inductively-Coupled Plasma Atomic Emission Spectrometry

ICP-MS Inductively-Coupled Plasma-Mass Spectrometry

i.d. Internal Diameter

k Capacity Factor

LC Liquid Chromatography

mCi Millicurie

MECA Molecular Emission Cavity Analysis

MLP Metallothionein-Like Protein

Mol.wt. Molecular Weight

MS Mass Spectroscopy

MT Metallothionein

MTs Metallothioneins

N Number of Theoretical Plates

MW Molecular Weight

NADPH Nicotinamide Adenine Dinucleotide Phosphate (Reduced Form)

ηm Nanometer

Oanal Flow Rate of the Analytical Oxygen

Oox Flow Rate of the Thermospray Oxygen

OPA o-Phthaldehyde

OS Oxidation State

PFPD Pulsed Flame Photometric Detector

RP-HPLC Reverse-Phase HPLC

RSD Relative Standard Deviation

s Second

SEC Size Exclusion Chromatography

Tris Tris(hydroxymethyl)aminomethane

UV Ultra Violet

CHAPTER I LITERATURE REVIEW

SULFUR OCCURRENCE, BIOAVAILABILITY AND ANALYSIS

CHAPTER I LITERATURE REVIEW

SULFUR OCCURRENCE, BIOAVAILABILITY AND ANALYSIS

OBJECTIVES

The objectives of this work are to design, develop and optimize direct interfaces between high performance liquid chromatography and flame photometric detector for the separation and detection of thermally unstable and low volatile sulfur bearing-compounds.

1. High Performance Liquid Chromatography-Flame Photometric Detector for Speciation of Non Volatile and/or Heat Sensitive Sulfur Compounds

1.1 Introduction

Flame photometric detector (FPD) relies on a cool flame source to generate chemiluminescence from small molecules. The excited species have band emissions, made up of various combinations of rotational, vibrational, and electronic transitions. The use of FPD for the selective detection of sulfur compounds was first introduced in 1966 by Brody and Chaney. Since that time, this detector has found extensive applications for sulfur analysis. The flame photometric detector for sulfur detection is based on the principle found by Draeger and Draeger (1962) for selective detection of sulfur compounds in hydrogen-air flame. The FPD response to sulfur is due to the formation of activated sulfur dimers (S_2) and their subsequent chemiluminescence at 384 or 394 ηm . The molecular emission is monitored by a photomultiplier tube through an interference filter. Many applications of S₂-emission for the analysis of real samples have been reported, either for the determination of total or single sulfur in samples nebulized into the flame (Belcher et al., 1975; Schubert et al., 1979), or for selective speciation of sulfur compounds eluted from a gas chromatograph (GC) [Dressler, 1986; Raccio and Welton, 1985; Farwell and Baringa, 1986].

Speciation of thermolabile or non-volatile compounds requires the use of high performance liquid chromatography (HPLC). Although speciation of sulfur compounds have been performed by techniques allowing high selectivity and/or sensitivity (HPLC-ICP, HPLC-MS, HPLC-UV), the application of HPLC-FPD to real samples has never

been demonstrated. Several approaches have been reported on the HPLC-FPD for sulfur compounds. These systems were sensitive to sulfur compounds in synthetic samples, but were unusable for biological matrices.

The research aims to design, develop and optimize interfaces between high performance liquid chromatography and flame photometric detector for the separation and detection of nonvolatile and unstable sulfur containing-compounds in real samples. Non-volatile metallothioneins, glutathione, and taurine in horse kidney homogenates and unstable sulfur compounds from garlic extracts were the analytes chosen to test the feasibility of the system to analyze the two above classes of sulfur compounds in real samples.

1.2 The Fate of Metallothionein, Reduced Glutathione and Taurine

1.2.1 Metallothionein

Metallothionein (MT) from mammalian tissues is a single-chain polypeptide with a molecular weight of 6000-7000 daltons. MT was discovered in horse kidneys by Margoshes and Vallee (1957). This low molecular cysteine-rich protein is heat stable and has a single primary structure of 61 amino acids of which 20 are cysteines. MT is characterized by the absence of histidine and leucine as well as aromatic amino acid, including tyrosine, tryptophan, and phenylalanine. The sequence of the cysteines residues is strictly conserved along the protein (Fowler et al., 1987). MT has two majors isoforms (termed MT-I and MT-II), determined by elution profile in anion-exchange chromatography (Kägi and Kojima, 1987). 113Cd NMR spectroscopy revealed two

clusters within the structures of Metallothionein (MT), named cluster A and cluster B. Cluster A requires participation of eleven cysteines to bind four atoms of cadmium, while cluster B contains nine cysteines in the binding of three atoms of cadmium; both clusters adopt a tetrahedral conformation (Otvos and Armitage, 1980). Winge and Miklossy (1982) and Boulanger et al.(1982) suggest a two-domain model for MT. According to this model, the amino-terminal half of the protein (residues 1-30) constitutes the three-cadmium cluster and the carboxyl half forms the four-metal cluster.

Margoshes and Vallee (1957) were the first ones to initially identify metallothionein from horse kidney. Subsequently, this protein and similar polypeptides have been isolated from other mammals, marine and terrestrial invertebrates (Roesijadi et al. 1989; Dalinger et al., 1989; Bebianno et al., 1989; Martoja and Martin, 1985), in fish (Norey et al., 1989), in crab (Sparla and Overnell, 1990). The physical properties of these metallothionein-like proteins (MLP) are, in many ways, similar to those of mammalian MT, but differ, in some points, from mammalian MT. For example, the protein of crab *Scyla serrata* contains two three-metal clusters while mammalian MT adopts one three-and one four-metal cluster (Otvos et al., 1982); Nemer et al. (1985) reported that the amino acid sequence of sea urchin MT reveals variance from that of mammalian MT.

1.2.2 Functions of MT

Metallothionein (MT) is known to perform multiple functions. It can be used as a bioindicator of heavy metals, such as Cd, Hg, Cu, and Zn (Ariyoshi et al., 1990; Onosaka et al., 1989; Karasawa et al., 1987; Good and Vasak, 1986). Although MT

synthesis is induced in animals tissues by exposure to these metals (Kägi and Kojima, 1987), these metalloproteins have been suggested to be also constitutive polypeptides in organisms that had not been exposed previously to heavy metals; these endogenous MTs have been proposed to be involved in the cellular regulation and transport of zinc and copper (Cousins, 1985).

1.2.3 Methods for Detection and Quantification of MT

Numerous methods have been used to detect and quantify MT in biological samples. These techniques include: (a) HPLC coupled with fluorescence detection (Miyairi et al., 1998), HPLC-atomic absorption spectroscopy (AAS) using metal substitution techniques (Lehman and Klaassen, 1986), HPLC-inductively coupled plasma atomic emission spectrometry (ICP-AES) [Suzuki, 1991], or inductively coupled plasma mass spectrometry (ICP-MS) of protein fractions (Sunaga et al., 1987; Mason et al., 1990), metal saturation assay with radioactive (Patrierno et al., 1983) and nonradioactive metal (Onosaka and Cherian, 1981), and polarographic techniques (Onosaka and Cherian, 1982).

Metal substitution assays are indirect techniques used to determine and quantify MT in a variety of sources by means of metals bound to the protein. The basis of this technique lies in the detection of MT by substituting the native metals bound to cysteinyl thiol residues of MT with a different metal with a higher avidity for the binding site. The quantification of MT is based on known stochiometric relationships between cysteine ligands and the deplacing metal. Using ²⁰³Hg as substituting metal, this technique was

initially introduced by Piotrowski et al. (1974), and Zelazowski and Piotrowski (1977). Subsequently, Eaton and Toal (1982), Onosaka and Cherian (1982) extended this method to ¹⁰⁹Cd and ¹¹⁰Ag with increased sensitivity. However, metal substitution assays suffer from several limitations: [a] Silver is known to precipitate with halides, limiting the use of high halide concentration (Cherian, 1988), [b] because the affinity to bind to MT is lower in the case of cadmium than are mercury and copper, thereby incomplete displacement of these metals by cadmium saturation assays leads to underestimation of MT (Scheuhammer and Cherian, 1986), and [c] non-specific binding of metals to thiol-containing peptides cysteine and glutathione represents interferences leading to overestimation of MT concentration (Eaton and Toal, 1982; Eaton, 1985; Dieter and al., 1987).

1.3 Taurine

2-Aminoethanesulfonic acid, commonly named taurine, was initially isolated from ox bile more than 150 years ago (Demarcay, 1838), and has been regarded for a long time as an inert end product coming from sulfur metabolism. Taurine occurs at high levels in algae (Ericson and Carlson, 1954; Reynoso and Gamboa, 1982) and in most animals. It is present only at trace level in bacteria and plants (Huxtable, 1992). In mammals, taurine is abundant in brain, retina, heart, liver, skeletal muscle, and kidney tissues (Jacobsen and Smith, 1968). Taurine is also present in milk, urine, and the plasma of some mammalians. Up to 70 g of taurine is found in a 70-kg human body (Huxtable, 1992). Table 1.1 presents typical concentrations of taurine in some species and tissues.

Table 1.1 Taurine concentration in some species

Tissue	species	concentration (µmol/g wet weight)	Reference
Retina	Monkey	45.5	Sturman et al., 1988
Heart	Rat Monkey	17.7 10.3	Piao et al., 1990 Sturman et al., 1988
Liver	Man Rat Cat	0.3-1.8 2.0-8.2 2.0-5.0	Jacobsen and Smith, 1968 Worden and Stipanuk, 1985 Worden and Stipanuk, 1985
Brain	Man Rat	1.4-3.3 5.9-7.4	Sturman, 1986 Gustafson et al., 1986
Skeletal muscle	Man Rat Monkey	2.2-5.4 10.1 15.1	Jacobsen and Smith, 1968 Piao et al., 1990 Sturman et al., 1988
Seaweeds		0.015-0.998	Kataoka and Ohnishi, 1986
Pumpkin seeds		0.013	Pasantes et al., 1989
Shrimp		12	Pasantes et al., 1989
Clam		40	Pasantes et al., 1989
Crab		75.5	Evans, 1973
Honeybee		34.4	Frontali, 1964
Yellowtail		83	Sakaguchi et al, 1982
Plasma	Man Rat	5-22 (μmol/dL) 16.0 (")	Hayes, 1985 Piao et al., 1990

1.3.1 Physicochemical Aspects of Taurine

Taurine differs from other common amino acids by the presence in its structure of a sulfonic rather than an carboxylic group, and also by bearing a β -amino acid rather than an α -amino acid. Taurine exists as a zwitterion over the physiological pH range. Its zwitterionic nature confers a high water solubility and a low lipophilicity to this molecule (Huxtable, 1992).

1.3.2 Functions of Taurine

Many physiological functions have been attributed to taurine. This amino acid received widespread attention since Hayes et al. (1975) and Pion et al. (1987) reported that cats fed with a 2-aminoethanesulfonic acid deficient diet exhibited retinal degeneration and cardiomyopathy. Nutritional studies (Gaull et al. (1977) concluded that low birth-weight babies nourished with taurine free milk have lower urinary and plasma taurine level than breast-fed babies, because maternal milk contains a high taurine concentration. Currently taurine is added to all infant milk preparations. Many functions have been postulated for the biological actions of taurine, which include regulation of Ca²⁺ homeostasis (Lombardini, 1985), brain-retina development (Hayes et al., 1975), osmoregulation in the brain (Wade et al., 1988), and protection against toxic materials in cells (Alvarez et Storey, 1983). Table 1.2 gives an overview of some biological actions attributed to taurine.

Table 1.2 Some physiological actions of taurine

Action	References
Cardiovascular system	
Antiarrhythmic Positive inotropy at low calcium Antagonism of calcium paradox Hypotensive (central and peripheral action) Increased resistance of platelets to aggregation	Franconi et al., 1982 Khatter et al., 1981 Kramer et al., 1981 Abe et al., 1988 Hayes et al., 1989
Brain	
Anticonvulsant Maintenance of cerebellar function Thermoregulation	Huxtable, R.J., 1982 Sturman et al., 1985 Glyn and Lipton, 1981
Retina	
Maintenance of structure and function of photoreceptors	Pasantes and Cruz, 1984
Liver	
Bile salt synthesis	Huxtable, R.J., 1986
Reproductive system	
Sperm mobility factor	Ozasa and Gould, 1982
Muscle	
Muscle membrane stabilizer	Huxtable, R.J., 1976
General	
Osmoregulation Antioxidation Stimulation of glycolysis and glycogenesis Regulation of phosphorylation	Iwata et al., 1981 Thomas et al., 1985 Kulakowski, 1984 Lombardini, 1985

1.3.3 Methods for Determination of Taurine

Taurine is present in high concentration in mammalian tissues. This amino acid presents special chemical features that limit the use of standard detection and chromatographic methods: Taurine is not sufficiently volatile in GC procedures, it is non-fluorescent, and has low absorption by light in the low UV range.

One- and two-dimensional paper and thin layer chromatography followed by ninhydrin detection have been the earliest methods used for taurine determination (Dent, 1948). Paper chromatography was time consuming, requiring several hours for development. This technique gave limited resolution and suffered from interferences due to high concentration of salt or protein. Thin layer chromatography (TLC) is faster and provides improved results than paper chromatography; but without clean-up procedure TLC is still subject to interference.

Taurine has been separated from other amino acids in urine and tissues extracts on mini-columns of 2.5 cm packed with Dowex 50 W in the H⁺ form or Amberlite IR. In this technique, detection is performed by means of specific reactions of taurine with ninhydrin, dinitrofluorobenzene or florescamine (Pentz et. al, 1957; Sorbo, 1961).

An automated instrument, designed specially for taurine analysis has been proposed by Goodman et al. (1989). This procedure does not require sample clean-up. In this method, peptides and proteins are retained on a mixed bed of anion and cation exchange resins while taurine is eluted in a continuous flow system. Detection of taurine

is achieved by fluorimetry using post column derivatization with o-phthalaldehyde (OPA).

Amino acid analyzers have been used for analysis of taurine. The detection is based on detection of ninhydrin or OPA. But the instrument is expensive and the analysis is time consuming: the time required for an analysis varies from 1 to 6 hours.

Pre-column derivatization with 4-dimethylaminoazobene-4'-sulfonyl chloride (Futani et al, 1994) and 3,5-dinitobenzoyl chloride (Masuoka et al, 1994) in reversed phase HPLC have been successfully used in taurine analysis.

Among various methods for determination of taurine, analysis by GC/MS (after derivatization of taurine with N-pentafluorobenzoyl di-n-butylamine) appears to be the most promissing most with respect to convenience, resolution, and sensitivity (Fay et al., 1998)

1.4 Glutathione and Its Functions

Reduced glutathione (GSH) is a tripeptide containing the sequence y-glu-cys-gly. It has a high water solubility, which comes from its high content in hydrophilic functional groups, namely two peptide bonds, two carboxylic acid groups, one amino group, and one thiol group. The oxidized form of glutathione, usually denoted as GSSG, is always co-present with GSH in all tissues. However, GSH accounts for more than 99.5% of cells "total glutathione" (Anderson, 1985). The level of GSH, found in biological matrices is high and ranges from 0.5 to 10 mM (Meister and Anderson, 1983). GSH has several functions: it acts as co-enzyme for various enzymes, participates in

catalysis, amino acid transport, metabolism, and protects cells against foreign compounds, free radicals, and reactive oxygen compounds (Meister et al., 1976, 1983; Meister, 1981, 1983).

1.4.1 Methods for Determination of Glutathione

Several methods for the determination of GSH have been reported in the literature. Initially, thiols, including GSH, were determined by reaction with 5,5'-dithiobis-(2-nitrobenzoic acid) (DTNB) [Ellman, 1959]. Subsequently, OPA has been used to determine GSH or GSSG after alkylation of GSH with N-ethyleimide. But this procedure gave erroneously high GSSG values, since OPA reacts also with many primary amines (Cohn and Lyle, 1966; Hissin and Hilf, 1976; Beutler and West 1977).

The determination of glutathione disulfide (GSSG) in biological matrices is usually difficult since it is always present in cells at very much lower concentrations than those of GSH; in addition, oxidation of GSH can lead to overestimation of native GSSG. The DTNB-GSSG recycling assay, which is also valid for total glutathione, can be made specific for determination of GSSG. In this procedure, GSH is masked with either 2-vinylpyridine (Griffith, 1980) or N-ethylmaleimide (Akerboom and Sies, 1981).

Today, several precolumn and postcolumn chromatographic procedures for the determination and quantification of glutathione in biological matrices have been used in a number of HPLC procedures. The detection limits for these techniques range from 0.5 pmoles to 0.13µmol/L.These techniques include: HPLC with fluorescence detection (Newton et al., 1981; Gotti et al., 1994; Michelet et al., 1995; Dean et al., 1998;

Parmentier et al., 1998), HPLC-electrochemical detection (Mitton and Trevithick, 1994), HPLC-UV (Liu et al., 1996; Toshiki, 1996; Raggi et al., 1998).

Using a glassy carbon working electrode, detection limits of 6.0 and 22.0 pmol have been reported for cysteine and GSH respectively in human plasma (Carvalho et al., 1994). Besides the determination of glutathione, HPLC-pulse electrochemical detection has been demonstrated to be sensitive for the analysis of sulfur compounds (Catherine O. Dasenbrock and William R. LaCourse, 1998). This technique implies amperometric or coulometric detection coupled with pulsed potential cleaning. Sulfur compounds are detected by means of an oxide-catalyzed mechanism. Limit of quantification as low as 30 ppb (signal-to-noise ratio of 10) has been reported for this technique.

Enzymatic determination of GSH has been performed with glyoxylase (Woodward, 1935) or by method involving both glyoxylase and GSSG reductase (Bernt and Bergmeyer, 1974) and UV detection of GSH based on absorption of lactoyl-GSH at 280 nm. Enzymatic determination of GSSG used NADPH oxidation with glutathione reductase (GR) [Bernt and Bergmeyer, 1974]. Other enzymatic methods, based on spectrometric detection, used the requirement for GSH by maleylpyruvate isomerase (Lack and Smith, 1964), or by formaldehyde dehydrogenase (Koivusalo and Uotila, 1974). GSH has also been determined indirectly by using GSH S-transferase (Asaoka and Takahashi, 1981). In this method, GSH S-transferase is incubated with the test sample and O-dinitrobenzene, the released nitrile is determined with N-(1-naphthyl) ethylene diamine (Asaoka and Takahashi, 1981). In addition to the above stochiometric reactions, a recycling assay, which offers high sensitivity and specificity, has been used to determine

total glutathione (GSH + $\frac{1}{2}$ GSSG) in tissues. This procedure involves the colorimetric reaction of DTNB with GSH in the presence of NADPH and GR for the reduction of GSSG. The 5-thio-2-nitrobenzoic acid produced in this reaction is proportional to the total GSH and is detected spectrophotometrically at 412 η m (Owens and Belcher, 1965; Tietze, 1969).

GSH determination in real samples has been also performed by the use of high-performance capillary electrophoresis (HPCE) and UV detection based upon reaction of GSH with Ellman'reagent (Raggi et al., 1997). This separation technique combines high resolving power and high efficiency of capillary zone electrophoresis (CZE). Linearity was achieved over the range $0.1 - 1.0 \times 10^{-4} M$.

1.5 Overview of the Use of Garlic

There is likely no vegetable familiar to more people than garlic. Although most commonly used as flavour or aroma in different cultures, its preparations have been used, first of all, in folk medicine since antiquity. Regardless of one's personal likes or dislikes towards this plant, its medicinal features remain highly acclaimed. Pharmacological studies suggest that increased consumption of garlic could reduce cancer risks (Buiatti and Blot, 1989; Xing et al., 1982; You et al., 1989). Virtanen (1962, 1965), Nobel Laureate and a pioneer in garlic research, wrote: "Belief in the preventive or curative effect of vegetables towards disease has persisted for thousands of years. Garlic, onion, cress and cabbage are examples. In Eastern Europe and Asia Minor, large amounts of raw onion or garlic are a normal feature of diet. The science of nutrition has paid little attention to these beliefs, since, to some extent, they can be explained on the basis of the

vitamins and minerals contained in these vegetables, and because other alleged effects, if they exist, seem to be connected with substances better regarded as drugs than food".

1.5.1 Overview of Garlic Chemistry

The search for the compounds responsible for the medicinal and flavour properties of garlic has led to the identification of a multitude of sulfur-containing compounds. Efforts to understand the mechanism of their formation and their mode of action were contributed by several disciplines (Fenwick and Hanley, 1985, 1986; Brewster and Robinowitch, 1990). Research to isolate organic compounds from garlic go back to Wertheim (1844), who isolated diallyl sulfide from that vegetable. Subsequent analysis of garlic revealed that Wertheim had incorrectly identified diallyl disulfide as diallyl sulfide (Semmler, 1892). Further studies contributed to the eventual identification of di-, tri- and polysulfides. Cavailito and Bailey (1944) were the firsts to reveal the dual nature of sulfur compounds in garlic extracts. They observed that compounds extracted from frozen bulbs ice were odourless and yielded no sulfides. They demonstrated that these extracts could recover their usual odor and aroma if water is added to such extracts. These observations allowed the isolation of (+)-S-2-propenyl-L-cysteine-S-oxide (alliin) which is odorless and the precursor of 2-propenyl 2-propene thiosulfinate (allicin) and all the other thiosulfinates found in garlic extracts. These thiosulfinates are not present in intact garlic but result from decomposition of alliin and other related S-alk(en)yl-L-cysteine Soxide by action of alliinase. In intact cells of garlic, this enzyme is present in the vacuole while the S-alk(en)yl- L-cysteine S-oxides are located in the cytoplasm (Lancaster and Collin, 1981). When the bulb is disrupted or injured the action of alliinase on alliin and

related compounds gives rise to the biosynthesis of ammonia, pyruvate, and 2-propenesulfenic acid. Allicin is biosynthesized by the condensation of two molecules of 2-propenesulfenic acid. The combination of two molecules of 2-propenesulfenic acid yields all possible condensations of the corresponding thio sulfinates.

1.5.2 Methods for the Determination of Sulfur Compounds from Garlic

Initial methodologies for garlic analysis were focused on quantitative determinations of allicin by specific reactions of pyruvic acid with 2,4-dinitrophenylhydrazine (Jäger, 1955), sodium nitroprusside and iodine azide (Fujiwara et al., 1955) or N-ethylmaleimide and potassium hydroxide in 2-propanol (Fujiwara et al.,1955; Carson and Wong, 1955; Schwimmwer and Mazelis, 1963; Watanabe and Komade, 1960); Nakata et al.,1970). The weakness of these colorimetric methods comes from the instability of these coloured species and the lack of specificity of the cleavage of allicin by alliinase which cleaves also all the different alkyl-cysteine sulfoxides found in crushed garlic.

Recent developments for spectrophotometric analysis of garlic compounds have been reported. In a method described by Han et al. (1995), allicin is first reacted with an excess amount of cysteine and the residual concentration of cysteine is then quantified by reaction with DTNB. Another approach, reported by Miron et al. (1998), is based on specific reaction between allicin and 2-nitro-5- thiobenzoic acid.

Gas chromatography was used to analyse allyl and methyl mono-, di- and trisulfide in garlic (Brodnitz. et al., 1971; Schultz and Mohrmann, 1965; Tokarska and

Karwowska, 1983; Vernin et al.,1986; Block et al., 1988; Yu et al.,1989). Two sulphur cyclic compounds, 2-vinyl-4H-1,3 dithiin and 3-vinyl-4H-1,2 dithiin, were identified by GC (Brodnitz et al., 1971; Yu et al., Block et al., 1988). These two compounds were artefacts from diallyl thiosulfinate during GC analysis, usually performed at elevated injector and column temperature (Block et al., 1992). Table 1.3 lists various products (including sulfur compounds) typically identified in GC analysis of garlic extracts. Because of their suspected thermolabile nature, HPLC-UV determination of compounds in allium family has been suggested as a more relevant method (Wu and Wu, 1981). Presently, HPLC-UV, HPLC-MS, or HPLC-MS-MS approaches are the chief methodologies for the analysis of garlic extracts or garlic products (Miething, 1985; Knobloch, 1987; Lawson, 1990; Block, 1992; Calvey et al.,1998). LC detected none of sulfur compounds detected by GC, instead LC analysis revealed the presence of thiosulfinates in garlic homogenates. Table 1.4 lists the thiosulfinates usually found in crushed garlic.

Table 1.3 Volatile compounds isolated from garlic extract using GC (after Yu et al., 1989)

propene propenethiol 1,2-epithiopropane methyl allyl sulfide 2,4-dimethyl disulfide 2,4-dimethylfuran 2-propen-1-ol diallyl sulfide 2,5-dimethyl-tetrahydrothiophene C ₆ H ₁₀ S methyl propyl disulfide 3-methyl-2-cyclo-pentene 1-thione trans-1-propenyl methyl disulfide methyl allyl disulfide 1,3-dithiane aniline 1-beyanol	dimethyl trisulfide propyl allyl disulfide C ₆ H ₁₀ S ₂ diallyl disulfide unknown 1,2-dimercapto-cyclopentane unknown 4-methyl-5vinylthiazole methyl allyl trisulfide 2-methylbenzaldehyde 2,5-diethyl-1,2-4-trothiolane isobutyl isothiocyanate 3-vinyl-4H-1,2-dithiin unknown diallyl trisulfide unknown 2-vinyl-4H-1,3-dithiin
1-hexanol	unknown

Table 1.4 Volatile thiosulfinates identified from garlic extracts By HPLC

Diallyl
1-propenyl allyl
allyl 1-propenyl
allyl methyl
methyl allyl
1-propenyl methyl
methyl 1-propenyl
dimethyl

1.6 Importance of Sulfur

Sulfur is one of the elements essential to life and growth of all organisms. As a constituent of biological materials, it is widely distributed in plants and animal tissues. A large proportion of pesticides, a high portion of pharmaceutical and several food additives also contain sulfur in their molecular structure. Because sulfur holds such an important place in our environment, there is a need of improving methods for determination and quantification of sulfur containing-compounds.

1.7 History of Elemental Sulfur

Elemental sulphur has been known and used since antiquity. It was known as *lapis* ardens or brimstone. Because that element emits highly noxious fumes when burned, it was considered as a material with magical properties. Lavoisier (1794), who established the nature of sulfur studied the nature of the combination of sulfur oxygen.

1.8 Physical Aspects of Elemental Sulfur

Sulfur is the element number sixteen; with an atomic weight of thirty-two, it is the second element in-group VIA of the Periodic Table. It bears an electronegativity of 2.5 (Pauling scale) and may have oxidation numbers from -2 to +6 in its different compounds. At room temperature, the most stable compounds derive from three oxidation states, such metal sulfides (-2), elemental sulfur (0) and sulfates (+6) which are found in nature. Table 1.5 presents an overview of oxidation states (OS) of sulfur in covalent compounds. Modified solid crystallines sulfur contain: i) rings of sulfur atoms,

which may contain from 6 to 20 atoms, and ii) chains of sulfur atoms. The cyclooctasulfur, S_8 , is the most common form of sulphur, which occurs in three main allotropic species: orthorhombic α -sulfur, the most stable allotrope, exists as yellow crystals in volcanic deposits. At 95.5°C, this allotrope is converted to monoclinic β -sulfur that melts at 119°C. The third, a monoclinic form, γ -sulfur, is obtained by recrystallization of α -sulfur from ethanolic ammonium polysulfide (Meyer, 1976) and melts at 107°C.

Table 1.5 Oxidation States (OS) of Sulphur in covalent Compounds

os	S-compounds	S-compounds
		0
-1 (net charge)	_	$S - S - CH_2 - CH = CH_2$
-2	R - S - H (thiol)	R - S - R (sulfides)
0	R - S - OH (sulfenic acid)	O R - S - R' (sulfoxides)
+2	O R - S - OH	O R - S - R' O
	(sulfinic acid)	(sulfone)
+4	O H O- S - OH (sulfurous acid)	
		(surrounc acid)
+6	HO - SO ₂ - OF	H RO - S - OR'
	(sulfuric acid)	

1.9 Special Characteristics of Organosulfur Compounds

In-group VIA of the Periodic Table, sulfur is located below oxygen and is followed by selenium, tellurium and polonium. Accordingly, the chemistry of organo-sulfur compounds is best understood by comparing these compounds with their oxygen or carbon-substituted analogues. There are many common features between sulfur and their oxygen compounds analogues, as is the case for the numerous similarities of thiols and alcohols, or sulfides (thioethers) and ethers. However, many differences are accounted for the unique characteristics of organosulfur chemistry. The difference between oxygen and sulfur comes from the fact that sulfur has an additional inner-electron shell beneath the outer. Sulfur possesses a larger atomic core than oxygen (1.02 Vs 0.73Å). Another important feature of sulfur arises from the fact that the outer shell in this element can use not only the s and p orbitals but also the d orbital. Consequently, the valence is not restricted to two, as in the case of oxygen, since the d orbitals may be used in bonding by acting as receptors of the covalent electrons. In this way, sulfur can form many hypervalent compounds like, SO₃, SF₄, sulphoxides and sulphones.

1.10 Some Common Characteristics of Sulfur and Other Members of Group VIA

Oxygen, selenium, and tellurium are the elements to which sulfur bears the greatest physical similarity, although its differences from these elements are clearly evident. The likeness between sulfur and selenium is more marked in a number of respects than the one between sulfur and oxygen or sulfur and tellurium. The periodicity in properties found In-Group VIA is shown in Table 1.6 and 1.7 (Pauling, 1960).

Table 1.6 Bond Energies of Group VIA Elements.

Bond	Energies (Kcal/mole)
0-0	33.2
S-S	50.9
Se-Se	44.0
Te-Te	33.0

Table 1.7 Periodicity among Group VIA Elements

	Oxygen	Sulfur	Selenium	Tellurium
Electron configuration	2-6	2-8-6	2-8-18-6	2-8-18-18-6
Covalent radius, Å	0.74 ⁻	1.04	1.17	1.37
Electronegativity	3.5	2.5	2.4	2.1
(Pauling scale)				

1.11 Sources of Sulfur

1.11.1 World Reserves of Sulfur

Sulfur exists in four isotopic forms (³²S, ³³S, ³⁴S, ³⁵S), the natural abundance of each isotope is presented in Table 1.8. It occurs in the biosphere in the following forms: elemental sulfur, hydrogen sulfide occurring in natural gases, sulfur compounds in petroleum and various metal sulfides (FeS, CuS,...). The most important commercially exploitable forms of sulfur are gypsum (CaSO₄), coal and oil shales (Bixby, 1970).

 Table 1.8
 Natural Abundance of Sulfur (Heathcock, 1976)

·	Sulfur isotope	%	
	32 _S	95.00	
	33 _S	0.76	
	34 _S	4.22	
	35 _S	0.014	

1.11.2 Sulfur in Agriculture

Biological tissues are noted for the diversity of sulfur compounds that they contain. But only a few sulfur compounds have been recognized as essential constituents of animal and vegetal cells. The most important sulfur containing compounds include S-adenosylmethionine, cysteine, cystine, glutathione, methionine, and co-factors, thiamine-pyrophosphate, biotin, lipoic acid and co-enzyme A, sulfolipids of the chloroplast. Table 1.9 and 1.10 present some representative concentrations of sulfur in organic materials.

Table 1.9 Sulfur Content of some organic Materials (after Allaway, 1966; Lemoine, 1973; Beaton, 1974)*

Material S	ulfur content	Material Su	lfur content
Animal tissues	s %(W/W)	Plant tissues	%(W/W)
Brain	1.10	Barley	0.25
Albumen	1.77	Oats	0.41
Milk	0.95	Clover	0.79
Egg White	1.60	Parsnip	0.61
Muscle	1.10	Peas	0.76
Kidney	1.00	Apple	0.45

Table 1.10 Sulfur Amino Acid Content of some Organic Materials (after Allaway, 1966; Lemoine, 1973; Beaton, 1974)*

Foed stuff	%Sulfur- Amino Acid(w/w)	Plant and Ani- mal Residue	%Sulfur- Amino Acid(w/w)
Milk	1.16	Fish meal	0.70
Cheese	7.87	Milk powder	1.30
Egg	5.50	Fresh blood	0.008
Beef	3.74	Egg yellow	0.14
Chicken	3.07	Malt	0.15
Bread	1.05	Sugar pulp	0.65
Beans	4.88	Linseed	0.36
Peanut Flour	7.78	Cabbage	0.31
Soybean flour	r 14.00	Rice	0.20
Wheat flour	4.90	Corn	0.25

^{*} cited by Meyer, B. (1977)

1.11.3 Sulfur in Soil

Fertile soils contain between 0.01 and 0.5% sulfur (Chapman, 1961). In humid regions, sulfur occurs not only as inorganic but also in the form of organic matter which is oxidized to sulfate making the element available to plants (Harward, 1966; Starkey, 1966; Li, 1966; Bloomfied, 1967).

1.11.4 Toxicity of Sulfur and Sulfur Compounds

In contrast to selenium, elemental sulfur is not toxic (Denis, 1927; Dziewiawki, 1962), but it becomes active when its oxidation state changes. For example, gaseous sulfur compounds are toxic in general. Carbonyl sulfide, in high concentration, is a narcotic and hydrogen sulfide is considered as the most dangerous gaseous sulfur compound. Fortunately, most of these gases have a strong nauseating odors that allow their detection well before they reach a fatal concentration. The smell of hydrogen sulfide is noticeable at a concentration of about 0.02 ppm. Unfortunately, the odor of these gases does not increase with the concentration. The upper concentration limit for exposure to hydrogen sulfide is 30 ppm in air, otherwise headache, vomiting and intestinal pain will result (Denis, 1927).

1.12 Determination of Sulfur Compounds by Molecular Emission

1.12.1 Use of Molecular Emission in the Analysis of Sulfur Compounds

The principal absorption line of sulfur lies at 180 nm in the vacuum region of the electromagnetic spectrum where flames gases and atmospheric oxygen absorb appreciably (L'Vov, 1970; Kirkbright, 1972). In other respects, it was known a long time ago that traces of sulfur compounds, regardless of their chemical structure, also colour flames blue. Salet (1869) was first to describe this chemiluminescent phenomenon. But this spectral characteristic of sulfur was first described by Brody and Chaney (1966) followed by Dagnall et al (1967), Syty and Dean (1968), and by Aldous et al. (1970), as a selective and sensitive flame photometric detection method for sulfur compounds. This

detection is based on the formation of excited sulfur dimer (S_2) by chemiluminescent reactions exclusively in cool (around 400°C) reducing flames. All commercial GC-FPD take advantage of this physical feature and we used the same approach in our proposed HPLC-FPD. Low flame temperatures are obtained by the use of an inert gas (supported with air or oxygen)-hydrogen flame. The excited species emits its characteristic emission bands from 276.9 to 616.6 η m (Dagnall et al., 1968) in the visible region of the electromagnetic spectrum when it returns to the lower electronic state. The analytically advantageous region of the spectrum falls around 384 η m and is shown in the Figure 1.1. In this region, the problems associated with absorption by atmospheric oxygen and flame gases are reduced.

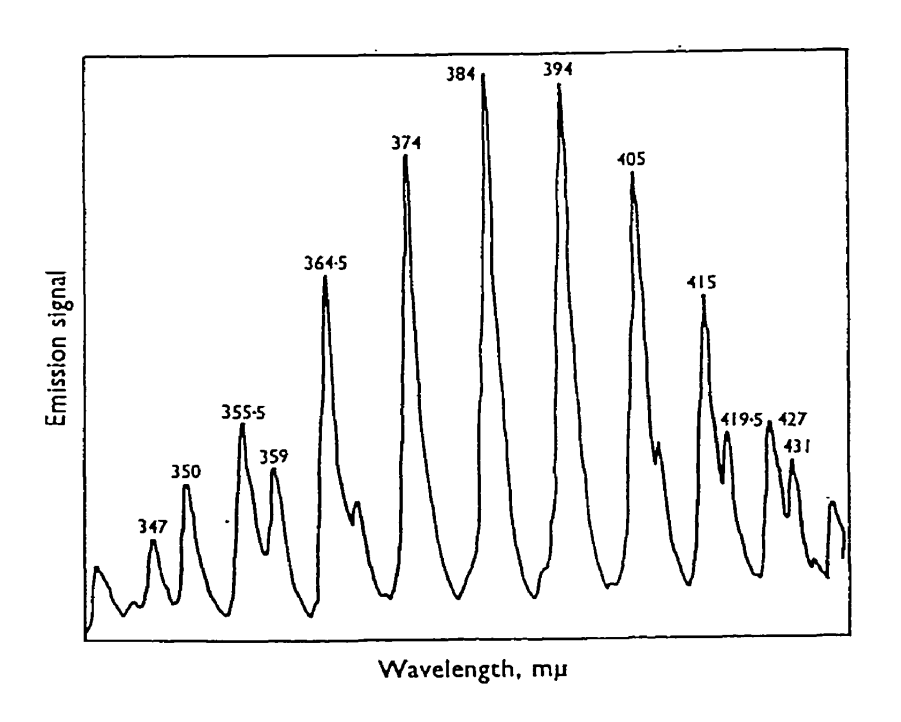


Figure 1.1

Spectrum of S₂ in an air-hydrogen flame (according to Dagnall et al., 1968)

1.12.2 Mechanism Proposed for the S₂ Formation

According to current models (Thosiaki et al, 1973; Patterson et al, 1978), the formation of the sulfur dimer requires prior degradation of the sulfur containing compounds in a hydrogen rich flame. The reactions that are presumed to occur when a sulfur compound reaches a hydrogen based flame are as follows:

$$\begin{array}{c} \text{heat} \\ \text{Sulfur compound} & \longrightarrow & \text{H}_2\text{S} \end{array}$$
 (1.1)

$$H_2S + H^{\bullet} \longrightarrow SH^{\bullet} + H_2$$
 (1.2)

$$SH^{\bullet} + S^{\bullet} \longrightarrow S_2 + H^{\bullet}$$
 (1.3)

$$H^{\bullet} + H^{\bullet} + S_2 \rightarrow S_2^{\star} + H_2 \qquad (1.4)$$

$$S_2^* \longrightarrow S_2 + hv$$
 (1.5)

Other groups suggested an excitation mechanism based on two or three body recombinations (Farwell et al., 1981; Sugiyama et al., 1973):

$$S^{\bullet} + S^{\bullet} \longrightarrow S^{\star}_{2} \qquad (1.6)$$

or
$$S^{\bullet} + S^{\bullet} + M \longrightarrow S_{2}^{*} + M$$
 (1.7)

Where M is a third body, and finally:

$$S_2^* \longrightarrow S_2 + hv$$
 (1.8)

The emission is first filtered by means of an appropriate filter and detected by a photomultiplier tube. Since two atoms of sulfur are required to generate the chemiluminescence, the response signal is quadratic. However, the linearization of the calibration curve can easily be performed as per the square root of the response (mathematical transformation is obtained electronically in commercial GC-FPD) or by doping the analytical flame with a small concentration of any sulfur compound (Crider and Slater, 1969; Flinn, 1978; Cardel and Marriott, 1982) to engender a pseudo-first-order reaction.

1.12.3 Molecular Emission Cavity Analysis for Sulfur Detection

Molecular emission cavity analysis (MECA) is a well established technique for determination of various sulfur compounds. The principles of this technique are based on the formation and chemiluminescence of sulfur dimers in a hydrogen rich-flame. In this technique, the sample is placed in a small cavity at the end of a metal rod, introduced into a cool flame on line with a monochromator, and the intensity of the resulting emission is recorded. MECA has been applied to the analysis of many organic and inorganic sulfurbearing compounds (Belcher et al., 1973). In general, this technique is restricted to samples which contain only one species or for total sulfur analysis.

1.12.4 Temperature-Resolved Molecular Emission Spectroscopy

Temperature-Resolved Molecular Emission Spectroscopy (TRMES) is used for the analysis of solid and liquid samples. The technique is very similar to MECA and has been designed for the analysis of total sulfur. In TRMES the sample is decomposed in an electrically heated graphite cup and the resulting gaseous sulfur species are transported by an inert gas into a cool hydrogen flame. The Chemiluminescence of S₂, involved in the flame, passes through an interference filter before striking the cathode surface of a phomultiplier tube. Detection limit of 50 ηg of sulfur might be obtained using TRMER (Johnson et al., 1998).

1.12.5 Hyphenated GC-FPD for Sulphur Detection

Hyphenated chromatography/spectroscopy techniques (Ebdon et al., 1986, 1987) are now recognized as valid tools for the speciation of biologically important metallic, metalloid, and non-metallic elements. Initially, the spectroscopic transparency of inert carrier gases used in GC allowed for direct coupling of GC with MECA. Flame photometric detectors (FPD) commonly used in commercial GC systems make use of the thermochemical formation of chemiluminescent molecular species from sulfur compounds. The analytes are burned in a relatively cool hydrogen rich flame where chemiluminescent S₂ molecules are generated in a series of radical-mediated reactions (section 1.12.2., equations 1.1 to 1.8). A simple photometric unit fitted with the appropriate optical filter detects the molecular emissions. All major companies marketing analytical instruments (Varian, Perkin Elmer, Carla Erba, Hewlett Packard, Tracor,

Shimadzu...) offer GC instruments with FPD as a selective and inexpensive detector for sulfur compounds. All these instruments contain an hydrogen/oxygen burner, an optical filter, and a photomultiplier tube. This resemblance in FPD design comes from the fact that all these commercial GC-FPDs share the same principles of S₂ photometric detection. However, GC, which usually performs at high injector and column temperatures is unfit to volatilize some classes of molecules, and is not suited for approaching the analysis of thermally instable and/or poorly volatile sulfur compounds.

Attempts were made to use FPD in capillary supercritical fluid chromatography (Markides et al., 1986). The fact the supercritical fluid, CO₂, quenched the emitted signal, limited the application of that technique to real samples

1.12.6 Pulsed Flame Photometric detection – GC for sulfur compounds

The FPD technique has been improved to allow enhanced selectivity and sensitivity for sulfur compounds. This technique, referred to pulsed flame photometric detection (PFPD), uses two chambers: a continuous igniter filament housing in an ignition chamber and a combustion chamber on line to a photomultiplier tube. The principle of the technique is based on a low (< 50mL/min.) gases flow rate insufficient to supply a continuous flame. Ignition of the flame takes place in the ignition chamber, the flame moves to the combustion chamber, combusts the sulfur compounds, and finally goes out, generating about 2-4 pulses per second of light emission. GC-PFPD, is now commercially available from Varian instruments. According to this manufacturer, under optimum conditions, PFPD permits detectivity of 1pg S/sec and selectivity of 10⁶ S/C.

1.12.7 GC - Sulfur Chemiluminescence Detection

Another sulfur-selective detection method has recently become commercially available. Sulfur chemiluminescence detection (SCD), compatible to most gas chromatographs, uses a reducing flame for generating SO. SO reacts with ozone in a reaction chamber to form electronically SO_2^{\bullet} , which emits a strong blue signal at 340 ηm . The Sulfur compounds, in a reducing flame and in presence of ozone, are presumed to undergo the following reactions (Hills et al., 1998):

Sulfur compound
$$\rightarrow$$
 SO

$$SO + O_3 \rightarrow SO_2^{\bullet} + O_2$$

$$SO_2^{\bullet} \rightarrow SO_2 + hv$$

SCD was coupled to GC for specific analysis of sulfur compounds (Johansen and Birks, 1991; Shearer, 1992; Ryerson et al., 1994), the SCD response is linear and equimolar. These characteristics are useful for speciation of sulfur compounds. For these reasons, various methods, among them ASTM method D5623-94 (1994), suggest a single sulfur compound for calibration of all sulfur species. The SCD was reported to allow a limit of detection of 80 pptv (Bernner and Stedman, 1990).

1.12.8 Fluorine Induced Chemiluminescence Detector for Sulfur Compounds

Fluorine induced chemiluminescence detector has been proposed for gas chromatography for the analysis of reduced sulfur compounds (Nelson et al., 1983, Hills

et al., 1998). The principle of this technique is based upon chemiluminescence of HF (λ = 660-750 η m) after reaction of molecular fluorine and sulfur compounds. This reaction requires that the S atom must be bonded to a carbon bonded, in turn, to at least one hydrogen atom (i.e. H-C-S).

One mechanism proposed for the formation of HF is as follows (Nelson et al., 1983, Hills et al., 1998):

Hills et al. have developed a high speed sensor for dimethyl sulfide based on its reaction with molecular fluorine. Limits of detection range of 36, 12, and 4 pptv were reported for this sulfur compound for 0.1-, 1-, and 10-s integration times, respectively.

1.12.9 Hyphenated HPLC-FPD for Sulfur Detection: Early Approaches

Although most sulfur biogenics can be detected in HPLC column effluent using standard UV spectrophotometry, sulfur specific detection offers two major advantages:

(a) increased selectivity of detection allows for the analysis of crude samples, simplifying isolation protocols and reducing the losses of labile species; and (b) organo-sulfur compounds containing poor or no UV chromophores may be quantified with higher sensitivity using a specific detector.

Biological species containing complexed metals or covalently bound heteroatoms are generally non-volatile or thermally labile, prohibiting their separation in gas phase, and justifying the development of hyphenated HPLC-spectroscopy systems (Ebdon, 1987). These analytes range from ubiquitous biomolecules, such as phospholipids and sulfur amino acids, to trace organometalloids including biogenic selenium and arsonium species (Blais, 1990; 1991), arsenolecithin (Marafante, 1984), seleno animoacids (Stadtman, 1979), and selenonucleosides (Whitter, 1984).

Flame photometric detectors have been used extensively as sulfur selective detectors for gas chromatography. The development of this detector was facilitated by the fact that the carrier gases in GC (nitrogen, helium, argon) are chemically inert and transparent to these selective detectors. However, attempts to couple FPD to HPLC has been more problematic since the low temperature (300-400°C at the centre) of the analytical diffusion flame makes it very unstable in the presence of large concentrations of solvent. Aside from disrupting a fragile thermochemical equilibrium, hydrocarbons and organic solvents physically quench the excited species (Fredriksson, 1981; Patterson, 1978) and produce background emissions from CH/C2 radicals (Patteron, 1978) and from carbon oxides (Markides, 1986; Olesik,1989) during pyrolysis. The combination of these impediments may explain why relatively few HPLC-FPD coupling approaches have been attempted (Julin, 1975; Chester,1980; Karnicky, 1987; Kientz, 1989).

HPLC-FPD techniques have been developed with moderate success and limited applicability. Direct connection of a HPLC system (Julin, 1975) or micro-HPLC system (McGuffin and Novotny, 1981; Kientz et al., 1989) or indirect approaches such as

ultrasonic micronebulization (Karnicky et al.,1987) have been reported. At present, these concepts are far from routine and have never been applied to real samples.

Although larger, the first generation of HPLC-FPD burners were essentially similar to GC-FPD configurations, both in terms of construction and of limitations. As in GC-FPD system (Patterson, 1978; Fredricksson, 1981) single-flame HPLC-FPD units (Julin, 1975; McGuffin, 1981) proved to be highly sensitive to organic solvents, whereas a double-flame system considerably reduced quenching by organics (Chester, 1980). Both approaches used conventional pneumatic nebulization chambers to convert the HPLC effluent to a polydispersed aerosol from which only a small proportion reached the analytical flame. A second generation of HPLC-FPD systems involved the interfacing of micro-bore HPLC systems with smaller burners. In either direct-introduction (McGuffin and Novotny, 1981) or ultrasonic-nebulization mode (Karnicki, 1987), the lower flow rates (10µL/min) used in micro-HPLC reduced problems associated with the use of phases. Limited sample-loading capacity and the fact that methanolic mobile conventional HPLC pumps are not designed to reproducibly deliver at such low flow rates are significant factors limiting the applicability of this approach for routine work. All but one (Julin et al., 1975) of the above-mentioned HPLC-FPD studies used phosphorus species (500-600nm emission bands, Dagnall, 1968) as test analytes. The above techniques give rise to the following limitations: a) poor limit of detection; b) limited to pure aqueous solvent; c) methanol, even at very low concentration in aqueous mobile phase, quenches the signal severely; with pure methanol, essentially no sulfur emission is observed; d) impossibility to detect sulfur compound in biological samples.

Most of these shortcomings can be related to the fact that, in both single and dual flame, hydrogen sulfide, responsible for the formation of the sulfur dimer, accounts for less than 0.5 % of the total sulfur introduced into FPD flames (Sugden et al., 1962). The results of calculations by Kramlich (1980) for equilibrated species of sulfur in hydrogenrich flame indicated that SO₂ and SO represent around 85% of the total sulfur, whereas S₂ was predicted to account for only a few parts-per-million. Thus, unfortunately, hydrogen sulfide is not the ultimate product of all sulfur introduced into the hydrogenrich flames. In addition to the low level of hydrogen sulfide available in FPD, organic degradation compounds quench the excited species and, by this fact, decrease the performance of existing HPLC-FPD systems for sulfur detection. It is considered that a successful HPLC-FPD coupling should imply high production of hydrogen sulfide.

CHAPTER II

Design, Characterization and Optimization of a Thermochemical High-Performance

Liquid Chromatography Flame Photometric Detector Interface for the Speciation of

Thermolabile and Non-Volatile Sulfur Compounds.

2 Optimization of an Interface for HPLC-FPD

2.1 Synopsis

An interface compatible with mobile phases delivered at conventional HPLC flow rates and containing up to 100% methanol is described and optimized for the analysis of low volatile or thermolabile sulfur compounds. The thermospray effect has been applied to introduce column eluate in a continuous and pulseless mode into the FPD. The thermospray effect was performed by using a fused silica capillary (50 µm i.d.) heated quartz tube. The capillary was connected to the injector or to the outlet of the column. Blais et al. (1990) have determined selenium by HPLC-thermochemical hydride generator (THG) using a quartz interface on line with an atomic absorption instrument. The fact that sulfur behaves like selenium in many aspects (section 1.10) led us to propose the same principles of hydrides generation in a HPLC-flame photometic detector tandem to detect chemiluminescence from the sulfur dimer. The quartz interface encompassed four consecutive thermal steps: nebulization of the HPLC mobile phase, thermal degradation of the organic matrix as well as the sulfur compounds in a laminar flow chamber, reduction of the generated sulfur radicals to H₂S, and generation of the sulfur dimer in a hydrogen rich flame. Sulfur emission induced in the last step was detected with a flame photomultiplier tube.

2.2 Thermospray Interface for Sulfur Hydrides Generation

The Figures 2.1 and 2.2 give respectively a block diagram of the HPLC-THG-FPD system and a schematic description of the transport mechanism in the thermospray

effect (Schwartz and Meyer, 1986). The HPLC-THG-FPD unit comprised three modules (Figure 2.3): a quartz tube assembly, a light-shielded molecular emission cell, and a photomultiplier unit fitted with an interferometric filter. The HPLC eluent (typically 85-100% methanol, at 0.65-1.00mL/min) emerging from a column or from the injector (flow injection mode) was channelled to a silica capillary tube (A. 50 um i.d. x 20 cm deactivated silica connected via a 1.6-0.8 mm reducing union; Chromatographic Specialities, Brockville, Ontario, Canada). The capillary was inserted into a quartz guide-tube (B, 2 mm i.d. x 3.2 mm o.d. x 10 cm, with outlet bore constricted to 1 mm using a glass blowing torch), which served to center the capillary within a thermospray tube (D, 4 mm i.d. x 6 mm o.d. x 8 cm) using Swagelok fittings (C. Blais, 1990). The thermospray tube (D) was heated to 750-800°C (external wall temperature) by a coil of resistance wire (E, 40 cm of Kanthal A-1 wire, 4.53 Ω m-1, 0.7 mm diameter, Pyrodia, Montreal, Canada) powered by an alternating current variable transformer, and insulated with refractive wool (Fiberfrax, The Carborundum Co., Niagara Falls, NY, USA) and two cylindrical firebrick segments held together by a screw-clip. The physical processes inducing the thermospray effect in this particular thermoelectric design have been characterized previously by Blais et al. (1993). The vaporized HPLC effluent fuelled a pyrolytic flame supported by a continuous stream of O₂, which was introduced to the combustion chamber (F, 9 mm i.d. X 11 mm o.d. X 5 cm) via an inlet tube (G, 2 mm i.d. X 3.2 mm o.d. X 5cm).

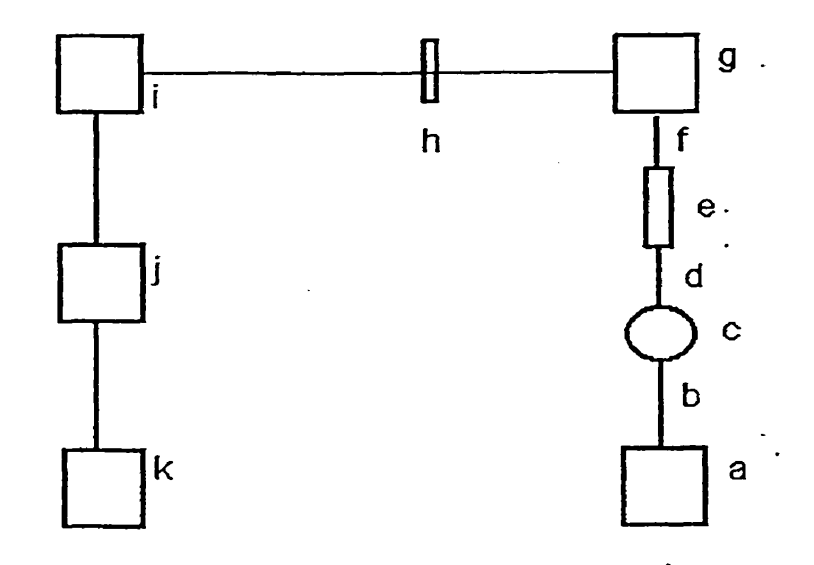


Figure 2.1

Block diagram of the HPLC-THG-FPD: a, HPLC pump; b, d, f, transfer line; c,injector; e, column; g, interface; h, filter; i, photomultiplier tube; j, photomultiplier tube power supply; k, integrator.

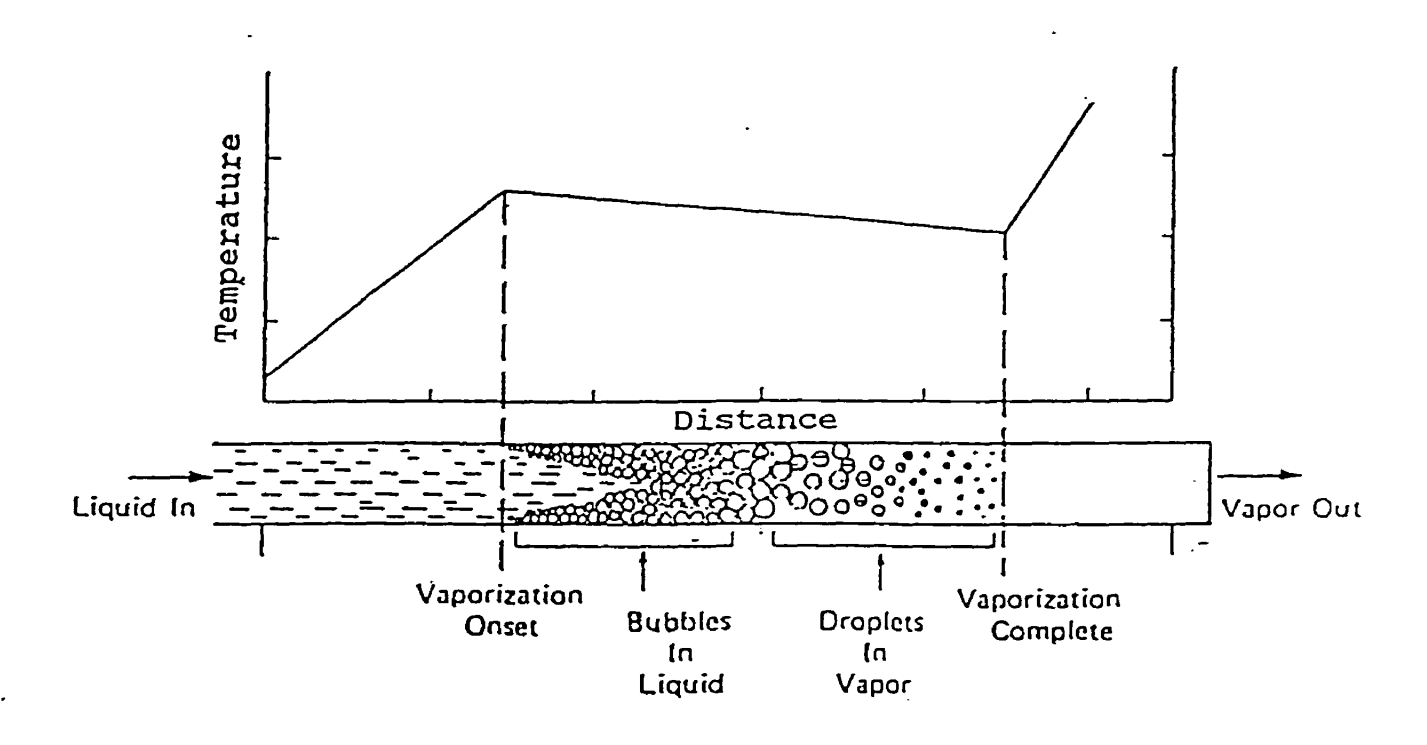


Figure 2.2
Schematic illustration of thermospray effect after vaporization process (Schwartz and Meyer, 1986)

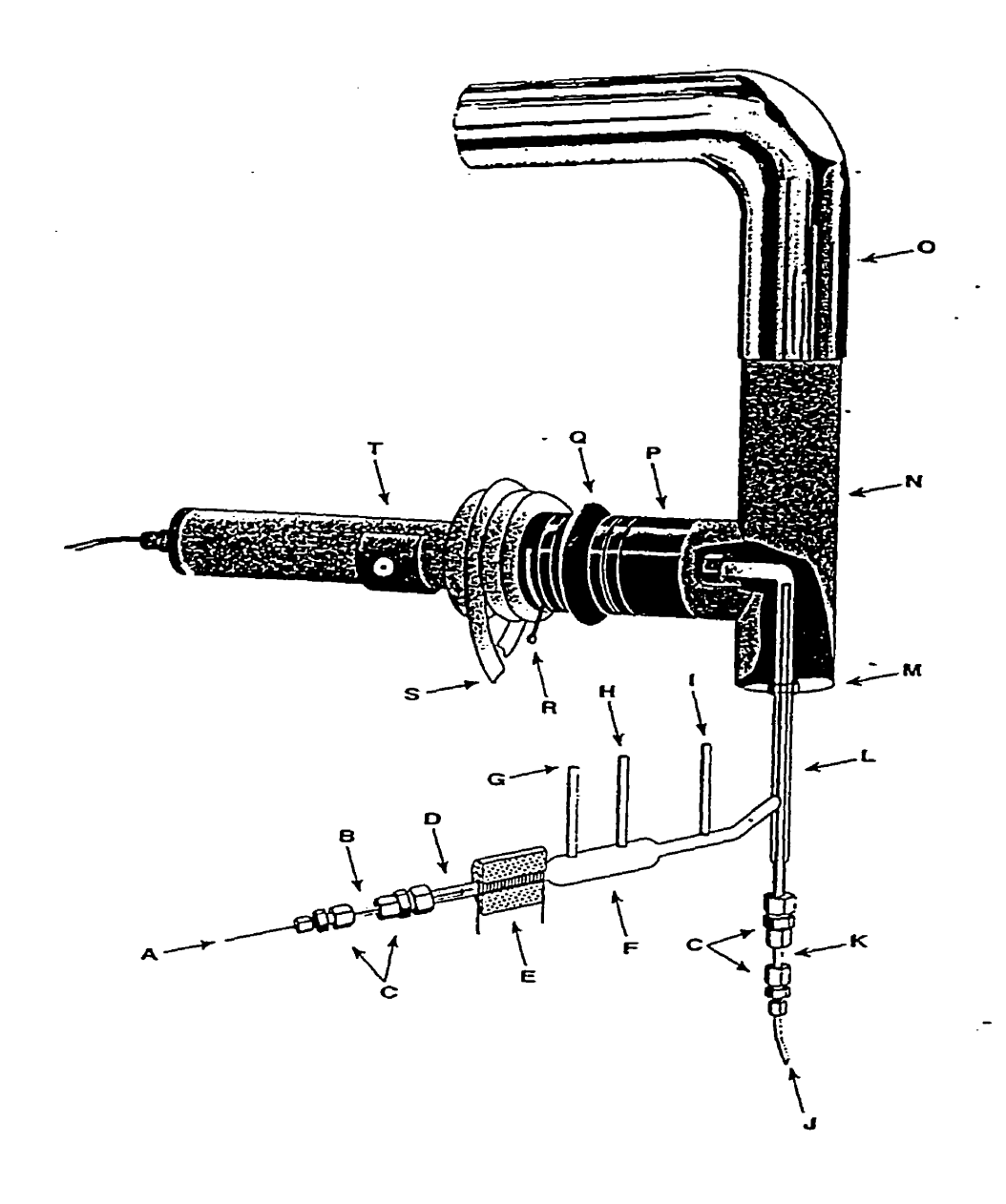


Figure 2.3

Thermospray FPD system comprising: A, 50 µm i.d. capillary transfer line (from the HPLC column); B, silica guide-tube; C, Swagelok fittings; D, heated thermospray chamber; E, insulated thermoelectric coil; F, combustion chamber; G, pyrolysis O₂ inlet; H, post-combustion H₂ inlet; I, helium inlet; J and K, analytical O₂ inlet; L, vertical silica tube/molecular emission chamber; M, cover plate; N, photometric chamber; O, chimney; P, window holder; Q, rubber joint; R, iris diaphragm; S, water-cooling coil; and T, filter holder and photomultiplier unit.

The key component of this system was a reducing post-combustion stage fuelled by hydrogen, which was introduced 2.5 cm downstream via an inlet tube (H) similar in dimensions to the oxygen inlet (G). The gas stream was diluted and cooled with helium, which was introduced 4 cm downstream via an inlet tube I, 4 mm i.d. X 6 mm o.d. X 5 cm). This stream emerged in a vertical tube (L, 7 mm i.d. X 9 mm o.d. X 20 cm) leading to the photometric detector. This tube (L) was constricted at one end with a short segment of silica tubing (4 mm i.d. X 6 mm o.d. X 1.5 cm) to allow for the installation of the Swagelok fittings (C) used to introduce the concentric analytical oxygen inlet tube (K, 2 mm i.d. X 3.2 mm o.d. X 15 cm), and bent to a 90° elbow at the other end. The analytical diffusion flame burning at the tip of the oxygen inlet tube (K) was positioned 5 mm beneath the elbow. Molecular emission occurred in the elbow joint and following 6 cm horizontal tube section (optical tube). The upper portion of the assembly was inserted into a custom-built modular photometric cell composed of welded aluminium pipes (N; vertical, 5 cm i.d. X 4.4 cm o.d. X 15 cm; horizontal, 6 cm). An aluminium inlet plate (M) and galvanized steel elbow chimney (O) were pressure-fitted on the cell (N) and secured with clips. The photometric assembly was built from modular optics purchased from Oriel (Statford, CT, USA). The assembly was composed of a 2.5 cm spacer tube (P) fitted with seal silica window, a flexible rubber joint (O) used to minimize conductive heat transfer to an iris diaphragm (R), and an interference filter for sulfur detection, which was inserted in the phototube (T) compartment (Figure 2.3). The optical filter and photocathode were kept cool by using a water circulation coil (S, 0.9 mm i.d. Tygon tubing). The system was secured at the following four points: the thermospray Swagelok fittings (C), the vertical tube (L), the photometric cell (N), and the phototube (T). The

thermospray-pyrolysis chamber assembly was operated at internal flame temperatures(>1800°C), which maintained the walls of the combustion chamber at around the softening point (about 1500°C). To prevent eventual distortion in the assembly, it was essential to fasten the supports without causing build-up of residual static stress.

2.2.1 Technical Aspects of the Interface

Reflection of external light through the emission cell was minimized using a series of light shields. All internal surfaces of the photometric cell (M,N,O, Figure 2.3) were covered with heat-resistant black paint and the lower and upper (up to elbow) portions of the tube (L) were shielded with graphite foil (0.254 mm thick, Johnson Matthey, Ward Hill, MA, USA). Light that was guided up to the end edges of the optical tube by internal reflection inside the quartz wall was masked using a screw (7 mm, i.d., pressure-fitted with a graphite foil liner), leaving an observation window of diameter equal to the internal diameter of the tube.

Smooth ignition of the FPD unit was obtained using the following sequence. (a) The photometric unit was separated from the cell (at P-N joint, Figure 2.3), giving direct access to the optical tube outlet. (b) The flow rate of pyrolysis oxygen was adjusted to 500 mL/min. (c) The current to the thermospray heating element was set to 6A. (d) After 1-2 min (thermospray tube outer-surface temperature, 800-900°C), the capillary transfer line (A) was introduced 0.3-0.8 cm into the heated portion of the thermospray tube (B). (e) The HPLC pump flow rate (85-100% methanol) was rapidly adjusted to 0.5 mL/min., causing ignition of the pyrolysis flame. Insufficient thermoelectric heating

of the thermospray tube or inserting the capillary tube further than the recommended depth may delay ignition, causing accumulation of the methanol vapours, which may then ignite explosively. (f) Hydrogen was then introduced at a flow rate of 1.2 L/min. (g) Excess hydrogen was ignited at the end of the optical tube (L). (h) The flow rate of the analytical oxygen [introduced via a poly(tetrafluorethylene) (PTFE) line] (J)] was then adjusted to 80 mL/min (or higher) until the analytical flame ignited at the tip of the concentric tube (K). The helium flow rate meter was then adjusted to a nominal flow rate of 7.33 L/min. causing extinction of the flame at the end of the optical tube. Fine adjustments such as capillary depth, HPLC eluent, pyrolysis oxygen flow rates (to obtain a stable thermospray effect), and flow rates of other gases were performed after joining the phototube and analytical cell assembly.

Instrumentation shut-down was performed smoothly by following this procedure in reverse sequence. The capillary was removed from the heating section of the thermospray tube immediately after HPLC pump shut-down. To avoid irreversible damage to the phototube, the photometric assembly must be in idle mode when separated from analytical cell. Shut-down of the HPLC system and heating element caused the pyrolytic flame front to move under the hydrogen inlet; this is a desirable feature, which allows for smooth recovery when the HPLC pump and heater are turned back on.

2.3 Instrumentation

The HPLC mobile phase was delivered by a Model 305/306 dual-pump system (Gilson, Worthington, OH, USA). The sample injection volume was 20 μ L. The

photomultiplier tube (PMT) was powered and monitored by PMT radiometric unit (Oriol, Stratford, CT,USA, and Leatherhead, Surrey, UK). The analogue, Kioto, Japan output was connected to a Model C-R3A integrator (Shimadzu, Kyoto, Japan). The interference filter for sulfur detection (367.5-427.5 nm at 0.5 peak width) was purchased from Oriel (Stratford, CT, USA). Hydrogen, oxygen and helium were delivered from calibrated flow meters fitted with micrometric valves (Matheson, Toronto, Ontario, Canada).

2.4 Reagents, Standards, and Chromatography

All chemicals used in this study were ACS reagent grade or better. H₂³⁵SO₄ (702 mci/mL), used in the radioisotopic assays, was purchase from ICN Radiochemicals. Lead acetate trihydrate, 2-methylthiophene, carbon disulfide, and ethanesulfonic acid were purchased from Aldrich (Milwaukee, WI, USA). Methanol, distilled in glass, was purchased from BDH, Montreal, Quebec, Canada). Water was distilled and deionized to 18 MΩ cm at 25°C (Milli-Q system, Millipore Corp., Montreal, Que.). Garlic cloves were purchased in a local market. Peeled whole garlic was chopped, homogenized in 10 mL of water per gram of garlic with a Polytron homogenizer, and left to stand at room temperature for 30 minutes to allow maximum production of thiosulfinates, as described by Ibert et al (1990). After centrifugation (2000g for 5 minutes) and filtration (0.45μm), the extracts were directly injected into the HPLC-THG-FPD system, which was fitted with a 20 μL injector. The LC column consisted in a C₁₈ column (250 X 4.6 mm i.d., 5 μm particles) and a guard column (30 X 4.6 mm i.d.) (CSC, Montreal, Quebec,

Canada). The mobile phases were methanol (100%), or methanol-water (85:15 v/v). The flow rate was 0.65 mL/min.

2.5 Trapping Experiments

The thermochemical behaviour of sulfur in the combustion chamber and downstream tubes was studied by the flow injection of H₂3⁵SO₄ (1μg, 15540 Bq, in methanol) into a test reactor (Figure 2.4), identical to the thermal reactor depicted in Figure 2.3 [horizontal assembly A to L without the helium finlet (I)]. The gas stream was channelled via PTFE tubing (2.48 mm i.d. X 4 mm o.d. X 30 cm, Cole-Parmer, Chicago, IL, USA) into two sequential chemical traps (250 mL Erlenmeyer flasks with magnetic stirrers at full speed) containing 150 mL of 1.0 M/L NaOH. The test radioisotope was injected into the system at 0.65 mL/min. using pure methanol as eluent. After each test, the reactor was dismantled and cut into 3.5 cm segments, which were then placed in scintillation cocktail (3⁵S). After an equilibration period of 24 hours, the samples (including aliquots from chemical traps) were analysed by liquid scintillation. The thermochemical fate of the analytes was tested at constant hydrogen flow rate (1.7 L/min) and three oxygen flow rates: 0.50, 0.65, 0.80 L/min.

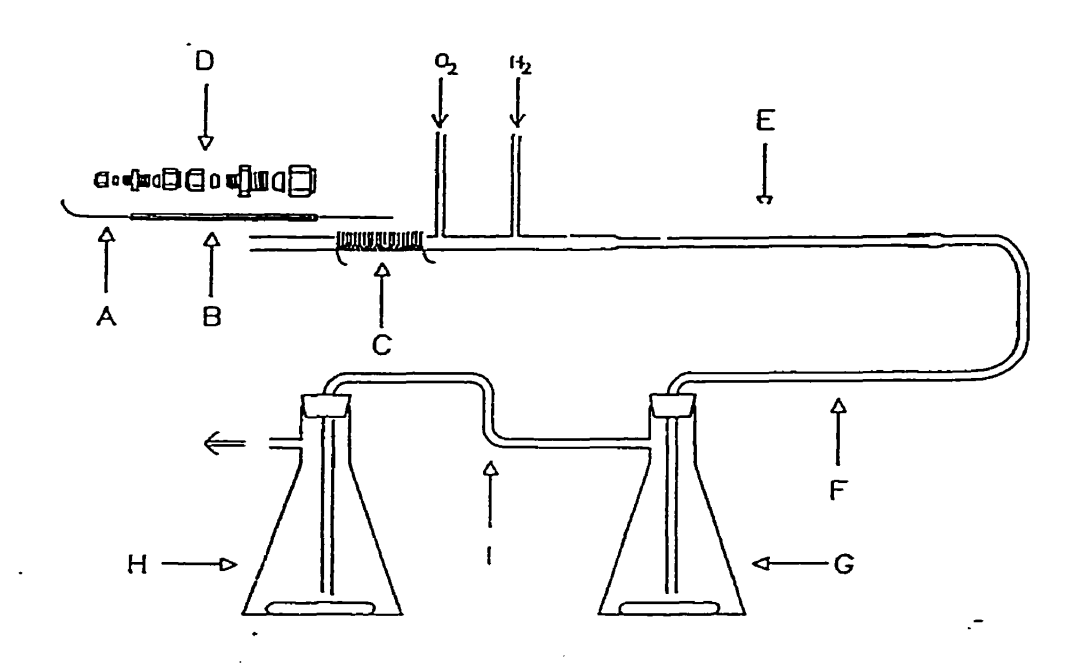


Figure 2.4

Trapping apparatus for radiochemical assay: (A) silica capillary; (B) guide tube; (C) thermoelectric coil; (D) Swaggelok fittings; (E) Quartz tube; (,F,I) Teflon tubes; (G,H) Erlenmeyer flasks containing 1M NaOH.

2.6 Optimization of the Interface

Pyrolytic oxygen, hydrogen, helium, and analytical oxygen flow rates were optimized as a function of FPD response to 2-methylthiophene (5.07 µg in flow injection mode) using a multivariate factorial 2⁴ composite design (Hill, 1966). The multivariable response model was obtained by multiple regression of factor level versus the integrated FPD responses.

2.7 Results and Discussion

2.7.1 Radioisotopic Assays

Preliminary sulfur volatilization experiments were followed by a quantitative study aimed at determining the proportion of analyte deposited in the interface during the transport to the analytical flame. Radiolabelled sulfur as $H_2^{35}SO_4$ was injected into test thermospray THG units (Figure 2.4, horizontal section A to L of the Figure 2.3) with an outlet emerging in two serially connected alkaline chemical traps each containing solution of 1.0 M NaOH. A deposition profile across the combustion chamber and downstream section was obtained by cutting the unit into short segments (3.5 cm), which were subjected to radiochemical analysis (along with aliquots from the chemical traps).

The test (H₂3⁵SO₄) compound in which sulfur was at its highest oxidation states was selected to test the reducing capacity of the THG process under different conditions.

The temperature of the pyrolysis flame was varied using three oxygen flow rates,

resulting in fuel-rich, quasi-stoichiometric, and oxygen-rich flames. At the higher oxygen flow rate, a secondary hydrogen/ oxygen flame was present at the hydrogen inlet, increasing the surface temperature of the quartz reactor near melting point (1665°C). The radiochemical recovery profiles found in the reactors and the traps are presented graphically in Figure 2.5. The recorded counts per minute for ³⁵S are listed in appendix (Table A-1).

S-35 Recovery in Reactor and Traps

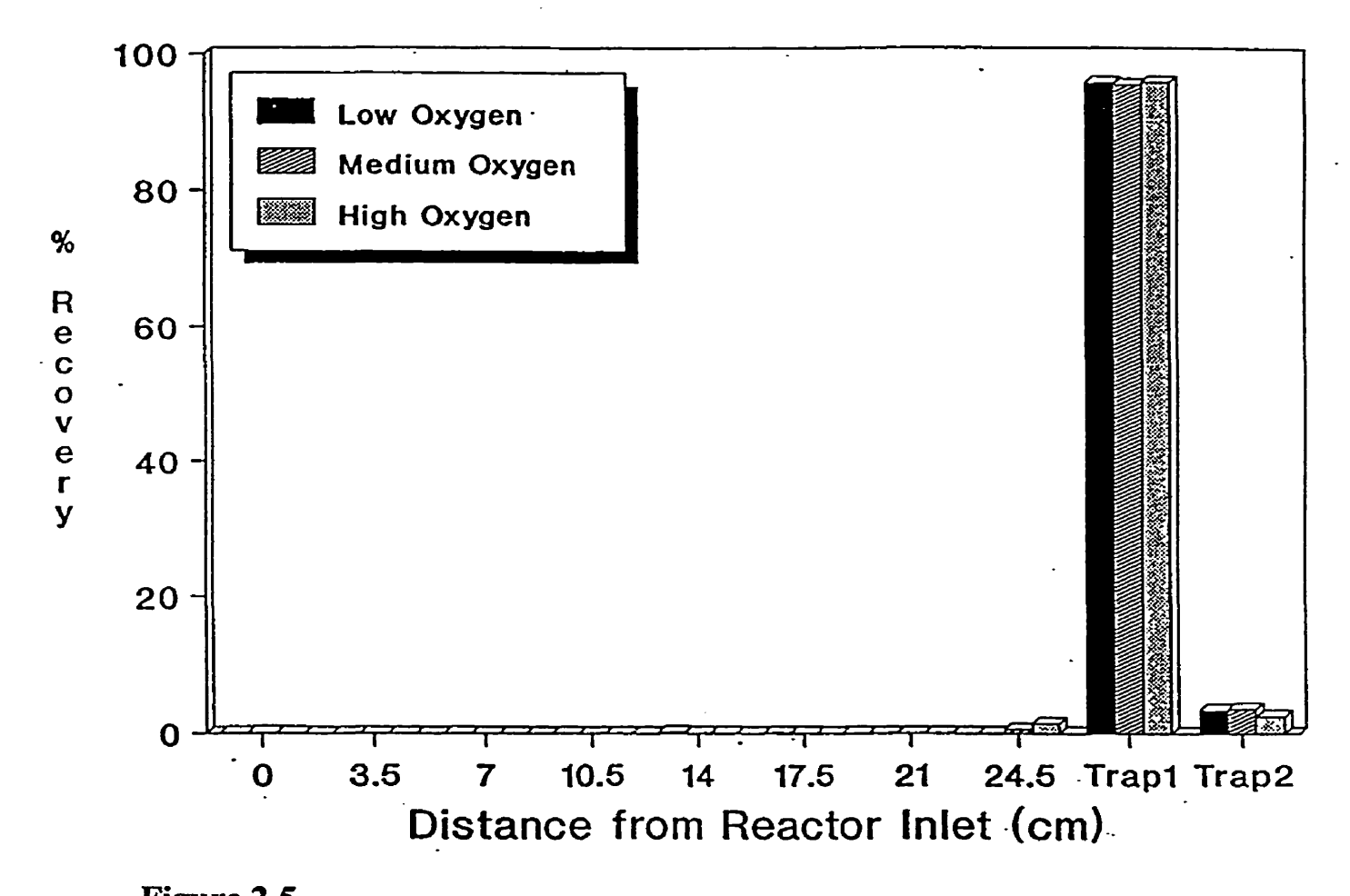


Figure 2.5

Radiochemical recoveries in reactor segments and chemical traps measured after a single injection of H₂³⁵SO₄ in test THG unit operated with A, 0.50, B, 0.65 and C, 0.80 L/min of pyrolysis oxygen.

At the three pyrolysis chamber temperatures tested, sulfur was recovered almost quantitatively in the alkaline chemical traps 1 (95.5-95.9%) and 2 (3.4-3.6%). With evidence that sulfur was transferred quantitatively from the thermospray THG section to the photometric cell, the molecular emission step appeared to be the critical component affecting the sensitivity of the system. Collisional quenching of sulfur dimer in excited state by carbon dioxide and water vapours (Weber, 1980) and the short residence time of the analyte in the analytical flame, which is inherent to the high flow rates of the gases, were expected to be limiting factors.

Previous HPLC-FPD detectors operating under conventional HPLC flow rates (Julin, 1975; Chester, 1980) involved a pneumatic nebulization step in which the mobile phase was converted into an aerosol of which a large proportion did not reach the analytical flame. The particle size distribution in venturi aerosols is affected by changes in solvent viscosity and vapour pressure, which occur during gradient HPLC elution (Hill, 1966). This complicates optimization and calibration procedures. Peakbroadening effects are inherent to the large dead volumes of these nebulizers, which may also be prone to flame-back when used to nebulize flammable solvents (Chester, 1980).

In GC-FPD detectors, emission background and quenching of chemiluminescence due to organics have been reduced conveniently using a double-flame configuration where a primary hydrogen-air diffusion flame oxidizes hydrocarbons (Patterson, 1978; Fredriksson, 1981). Primary H₂-air diffusion flames have been used in HPLC-FPD design either in normal (Karnicky, 1987) or inverted (Chester, 1980) modes. By

definition, these flames remain reducing and relatively cool (300-400°C at the centre), and are rapidly saturated by organic solvents. This problem is reflected by increased background emission or decreased signal response with elevated levels of methanol in HPLC mobile phases (Chester, 1980; McGuffin, 1981; Karnicky). Almost all published work on HPLD- FPD designs was based on phosphorus compounds as test analytes. Saturation of the primary diffusion flame by organic solvent would be more evident in sulfur detection mode, since the emission background from hydrocarbons is relatively intense at the lower analytical bands (347-431 μm) used to monitor S₂ emissions (Patterson, 1978).

A preliminary design illustrated in Figure 2.6 used the classical air-hydrogen diffusion flame burning at the tip of the tube (L) without elbow and positioned in the PMT observation window. Air was introduced at a controlled flow rate via a porous PTFE membrane, which minimized turbulence efficiently. Dilution of air with helium decreased the temperature of the outer primary reaction layer of the flame and associated UV emission continuum to the optimum level for S₂ formation. Dilution of air with helium further decreased the intensity of the background emission continuum from the outer layer allowing slightly higher PMT voltages (600-650 V) to be used. This background emission, which prohibited operation of the PMT at optimum voltage, and the difficulty of focusing the photocathode in order to observe the S₂ emissions quantitatively, limited the detectability of carbon disulfide to approximately 1 μg/S in flow injection mode.

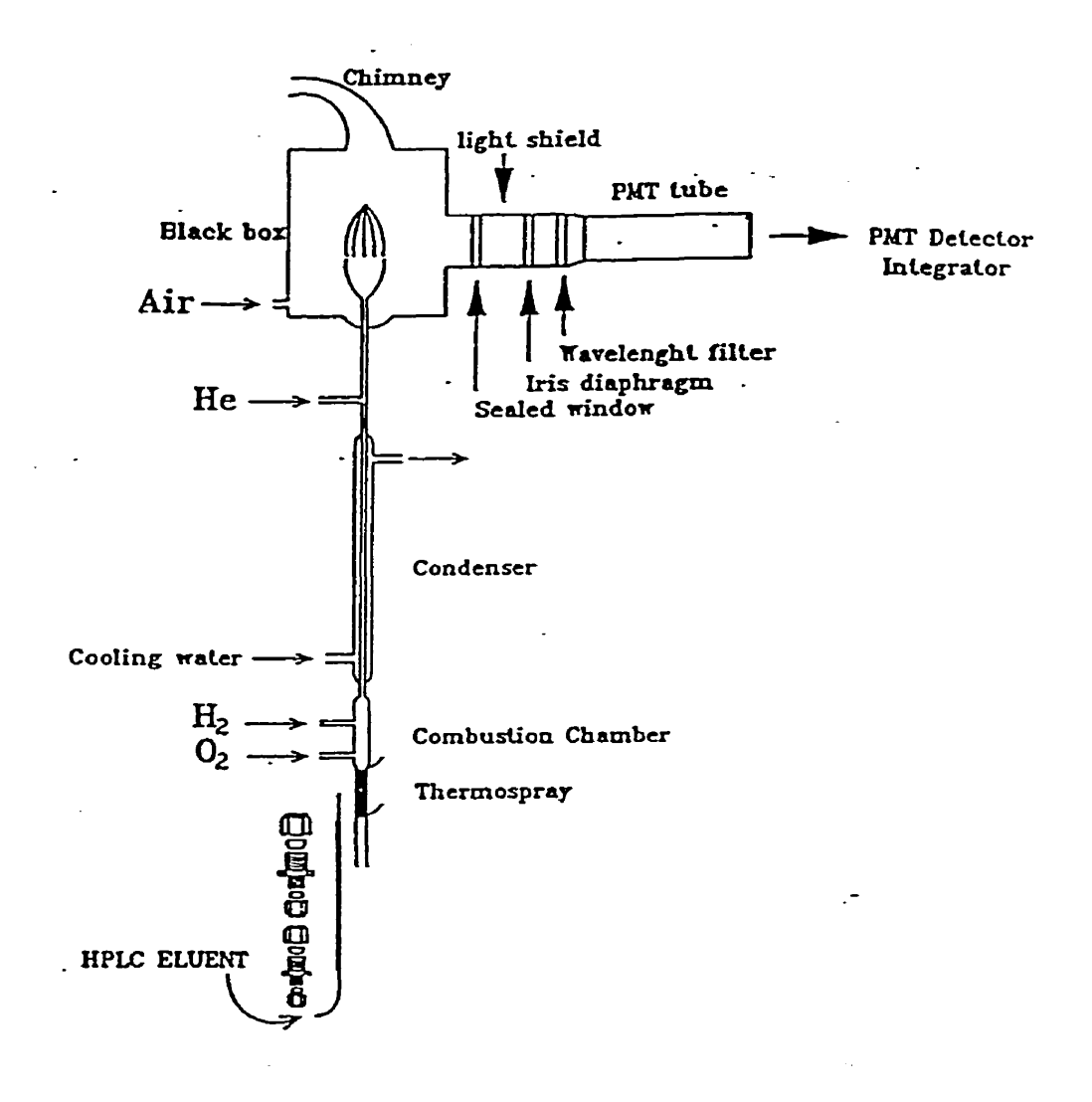


Figure 2.6

Preliminary design used for the classical air-hydrogen diffusion flame

2.7.2 Thermospray Unit and Characterization of the Intermediate Species Involved in the Formation of S₂

The present design included two thermal steps, which overcame the sample introduction and interference problems inherent to HPLC-FPD designs described above. The HPLC effluent was introduced quantitatively via a total consumption thermospray unit (Figure 2.3, A-E). This total-consumption introduction approach minimized post-chromatography peak broadening effects, and allowed for a rapid mixing of methanol vapours and oxygen, which resulted in a stable pyrolysis flame. Methanolic HPLC mobiles phases delivered at conventional flow rates (0.65 – 1.00 mL/min.) were pyrolysed efficiently in the oxygen supported kinetic flame at temperatures exceeding 1800°C at the center [commercially available platinum group alloy (as thin wires) that were used to estimate the temperature melted in the flame]. In comparison with the relatively cool diffusion flames used in previous designs, this highly oxidizing flame efficiently combusted interfering methanol and hydrocarbons to carbon dioxide and water vapours.

Previous HPLC-AAS applications of a similar design with selenium and arsenic (Blais, 1990; 1991) suggested that the reducing post-combustion stage fuelled by hydrogen would be essential to maintain pyrolysed sulfur in the gas phase during transport to the analytical flame. In their studies, Blais, et al., demonstrated, by means of chemical trapping experiments, that various selenium species were converted to volatile H₂Se in a reaction that was termed "thermochemical hydride generation (THG)". Likewise, we found during the present work that various sulfur compounds (carbon disulfide, ethanesulfonic acid, and 2-methylthiophene) processed in this reactor were

trapped in a lead acetate solution as a black precipitate. The precipitate was characterized to be lead sulfate (PbS) by its insolubility in water, its solubility in cool HNO₃ and hot HCl (The Merck index, Merck & Co, Tenth Edition, 1983, Rahway, N.J., USA), and finally, by its high melting point: no melting was observed around 600°C. The melting point reported for PbS is 1114°C (Handbook of Chemistry and physics, CRC, 64TH Edition, 1983-84, p. B-104).

$$Pb(CH_3COO)_2 + H_2S \rightarrow 2 CH_3COOH + PbS\downarrow$$

This reaction indicates that hydrogen sulfide (H₂S) is the key intermediate for the formation of sulfur dimer (H₂S) and may corroborate the mechanism proposed by Toshiaki (1973) and by Patterson (1978).

The photometric section of the system (Figure 2.3) used an inverted micro flame (1-2 mm length) burning at the outlet of a small concentric quartz tube (Figure 2.3, K) and positioned in the light-shielded section below the observation plane of the phototube. In this configuration, only a faint reflection from the analytical flame was detected by the phototube, which could be zeroed at maximum voltage (1000 V). As discussed by Blais et al. (1991), Dedina (1992), in a previous application of this approach for the atomization of selenium hydride, and by Rupprecht and Phillips (1969) in GC-FPD analysis of sulfur compounds, the inverted microflame supports a peripheral zone that is rich in hydrogen radicals. Hence, this peripheral core is essentially similar, in its chemical composition and temperature, to the inner core of the classical diffusion flame. The

horizontal emission tube integrated the chemiluminescence plume as a narrow beam, which was easily directed onto the phototube.

2.7.3 Optimization of the Methanol Fuelled Interface for HPLC-FPD

A multivariate model was used to optimize the gas flow rates in order to account for simple and quadratic effects of individual variables as well as inter-variable interaction effects. The model obtained by multiple regression of the 2^4 composite factorial design was reasonably accurate. Considering the interactive effects of the four gases on the state of the analytical flame, observed versus predicted values were relatively well correlated (r = 0.9304, slope = 1). More importantly, the error between observed and predicted values was normally distributed, excluding systematic lack-of-fit deviations from the model. The resulting response surface models depicting the combined effect of pyrolysis oxygen-hydrogen, hydrogen-analytical oxygen, and helium-analytical oxygen flow rates on the intensity of molecular emission are presented in Figure 2.7.

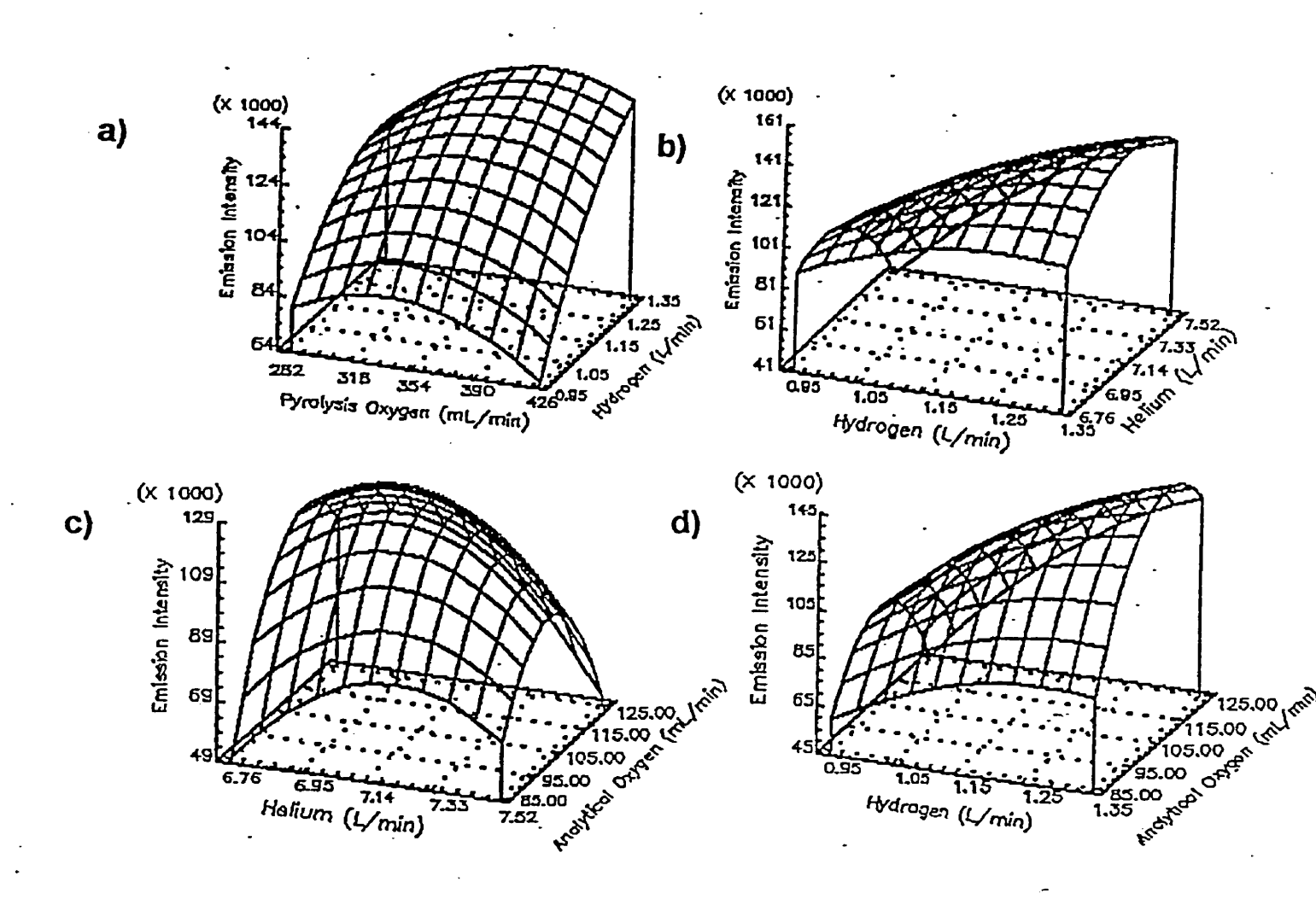


Figure 2.7

Response surface models depicting the effects of gas flow rates on molecular emission response. (a) Pyrolysis oxygen-hydrogen; (b) hydrogen-helium; (c) helium-analytical oxygen; and (d) hydrogen-analytical oxygen. In each instance, the flow rates of the two other gases were adjusted to the near-optimum values.

This modelling approach allowed for plotting response surfaces under conditions where two variables were set far from optimum values while the values of the two other variables were fixed at the model centroid values. These latter values were set for near maximum response as determined by preliminary univariate optimization experiments. The shape of the pyrolysis oxygen-hydrogen response surface [Figure 2.7(a)] was similar to those previously observed from arsenic (Blais, 1990), and, to a lesser extent, for selenium (Blais, 1991). As the efficiency of the THG process did not appear to be sensitive to changes in combustion/post combustion conditions [Figure 2.7(b)], the variation in response was interpreted in terms of effects on the status of the analytical flame. A lower response was observed when high pyrolytic oxygen flow rates were combined with decreased hydrogen flow rates [Figure 2.7(a)]: a condition under which the amount of hydrogen escaping from the post-combustion step was barely sufficient to sustain the analytical flame. A low pyrolytic oxygen flow rate resulted in significant background emissions, indicating incomplete combustion of methanol, which appeared to quench S₂ emissions. An interaction between hydrogen and helium flow rates [Figure 2.7(b)] was reflected by a distortion of the response surface in the region corresponding to the lower hydrogen: helium ratios where higher dilution of hydrogen decreased the temperature and reactivity of the analytical flame. The drastic effects of analytical oxygen flow rate on response surface [Figure 2.7(c) and (d)] demonstrated that this was the critical variable. The helium versus analytical oxygen flow rate [Figure 2.7(c)] showed that with the two other variables set at near optimum centroid values, the system would not be considerably affected by small variations in helium flow rate

within the studied range. This desirable trend was also observed for the hydrogen flow rate [Figure 2.7(d)].

Optimum flow rates determined using the model were estimated as follows: pyrolytic oxygen, 450 mL/min.; hydrogen, 1.35L/min.; helium, 7.33 L/min. and analytical oxygen 115 mL/ min., with the phototube operated at 900 V. Statistics related to the optimization of the methanolic fuelled interface are presented in appendix, in Tables A-2 to A-5 and in Figures A-1 and A-2.

2.7.4 Flow Injection Calibrations, Reproducibility, Linearization and Limit of Detection for S₂ Response

The HPLC-FPD system was calibrated in flow injection mode for three test analytes: 2-methylthiophene, carbon disulfide, and ethanesulfonic acid (Figure 2.8). All the three calibration curves exhibit a quadratic relationship between the concentrations and the response for the three test analytes. The short term repeatability of the system at various amounts of the three tests analytes is expressed in term of relative standard deviation (RSD) based on triplicate analysis (Table 2.1). The limits of detection (LODs), determined as two standard deviations above the average background signal, were 1.5ng/s for 2-methylthiophene, 2.5 ng/s of sulfur for carbon disulfide, and 4.5ng/s of sulfur for ethanesulfonic acid. The response varied as a function of bonding energy and oxidation state of sulfur. This phenomenon has been observed previously in GC-FPD (Farwell, 1986) and in HPLC-THG-AAS applications (Blais, 1990; 1991). These limits of detection were obtained using pure methanol as mobile phase, which was reported to inhibit sulfur dimer emissions in previous HPLC-FPD system optimized for sulfur

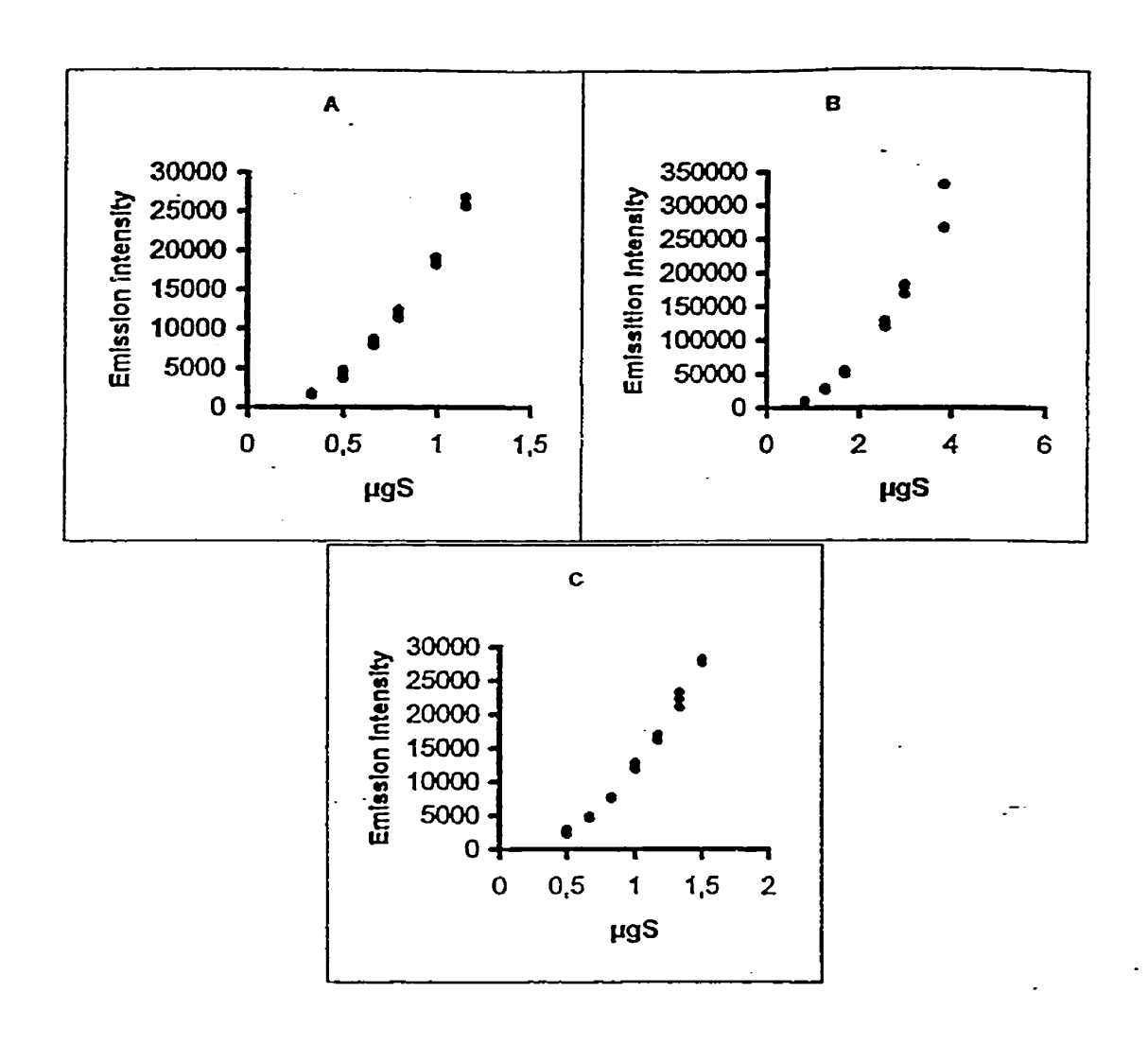
analysis (Julin et al., 1975). The quadratic nature of the S₂ formation process required a square-root transformation of the response data before analysis by linear regression (Figure 2.9). The square roots of the peak integrations versus amounts of sulfur injected were linearly correlated (r = 0.9985, 0.9950, and 0.9986), for respectively 2methylthiophene, carbon disulfide, and ethanesulfonic acid, over the concentration ranges studied (Tables A-6 to A-8). The graph of log signal versus log sulfur concentration resulted in a linear relationship with a slope of 2.2 for each of the three tests sulfur compounds studied (Tables A-9 to A-11). The Figure 2.10 illustrates the log-log relationship for these compounds. The slope of log-log curves for sulfur dimer emission is commonly referred to n-value, exponential proportionality constant, or linearity factor. The theoretical value for the slope is exactly 2, self quenching effects from the emitting species (S2) might account for the observed deviation from the theoretical value in our system. Values usually reported in the literature for this number range from 1 to greater than 2 (Selucky, 1971; Farwell et al., 1981; Burnett et al., 1977; Marriott and Cardwell, 1981). The deviation from the theoretical n-value of 2 are thought to be associated to non-optimal flame conditions, compound-dependent decomposition, experimental imprecision. In addition to square-root transformation and log-log relationship, chemical response linearization was obtained for 2-methylthiophene (Figure 2.11) [r=0.9975] by spiking the mobile phase with 2-methylthiophene (20 ppm), which causes the formation of sulfur dimer under pseudo-first-order conditions (Farwell and Barina, 1986). Statistics related to these calibrations are presented in Appendix (Figures A-3 to A-9, Tables A-6 to A-12).

Table 2.1 Reproducibility of the HPLC-THG-FPD system in flow injection mode at various concentrations of analytes

Analyte	Concentration ppm	RSD %
2-Methylthiophene	20.3 (0.33) ^a	7.13
	30.4 (0.50)	12.55
	40.6 (̀0.66)́	4.61
	48.7 (0.79)	4.36
	60.8 (0.99)	2.67
	71.0 (1.15)	2.29
2-Methylthiophene ^b	30.4 (0.50)	5.90
	40.6 (0.66)	2.43
	48.7 (O.79)	1.40
	60.8 (0.99)	1.70
	81.1 (1.32)	2 .66
Carbon disulfide	20.3 (0.85)	8.39
	30.4 (1.28)	4.15
	40.5 (1.71)	4.67
	60.8 (2.56)	3.50
	70.9 (2.99)	3.96
	91.1 (3.84)	12.88
Ethanesulfonic acid	34.4 (0.50)	12.48
	45.8 (0.67)	2.75
	57.3 (0.83)	1.31
	68.8 (1.00)	3.64
	80.2 (1.17)	2.37
	91.7 (1.33)	4.85
	103.7 (1.50)	0.96

a: values in parentheses represent micrograms of sulfur per mL

b:eluent doped with 20 ppm of 2-methylthiophene



Flow injection calibration of (A) 2-methylthiophene, (B) carbon disulfide, and (C) ethanesulfonic acid.

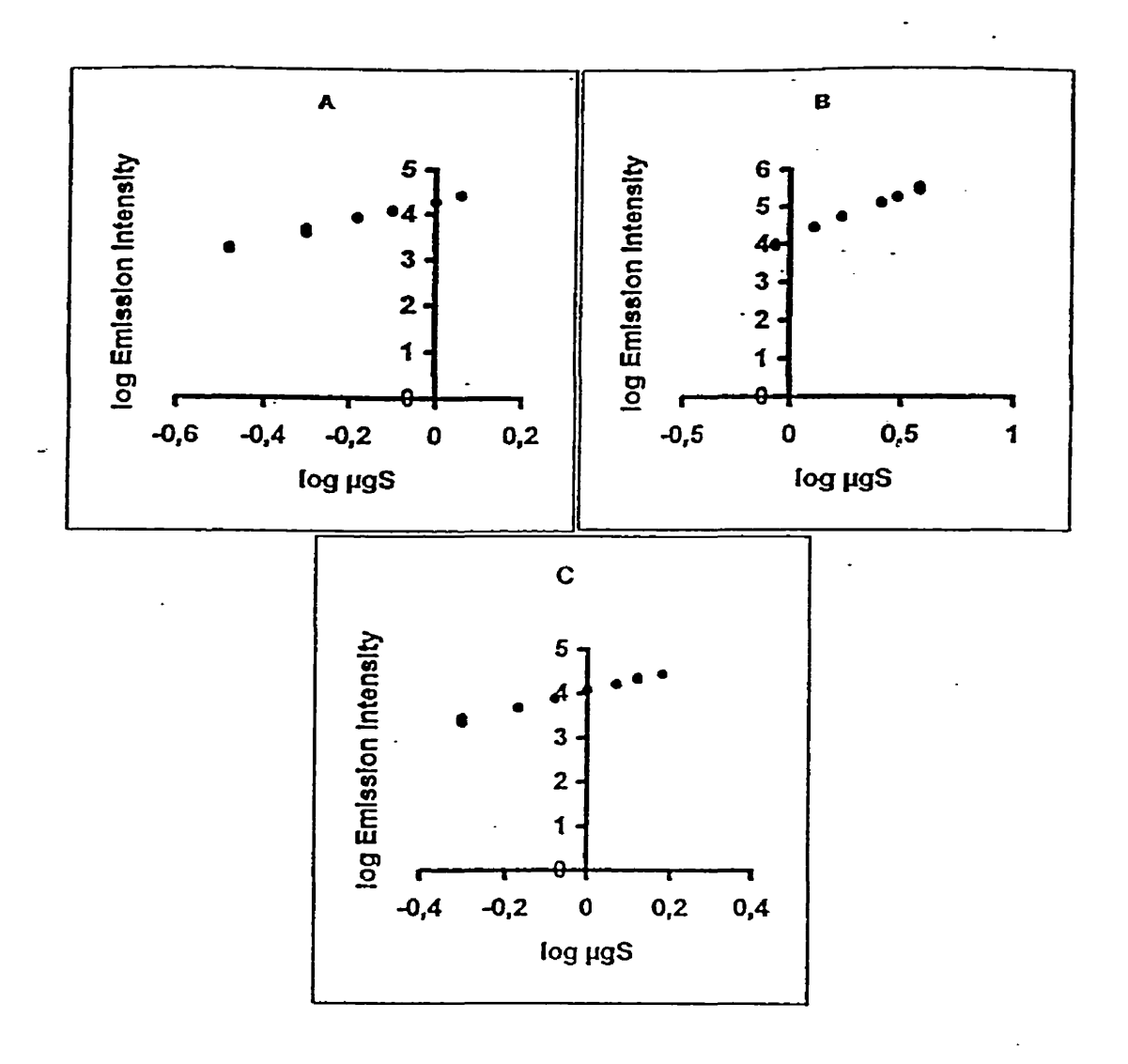


Figure 2.10

Regression analysis for the logarithm of the peak integrations versus logarithm of amounts of sulfur injected as (A) 2-methylthiophene, n = 2.19; (B) carbon disulfide, n = 2.24; and (C) ethanesulfonic acid, n = 2.21.

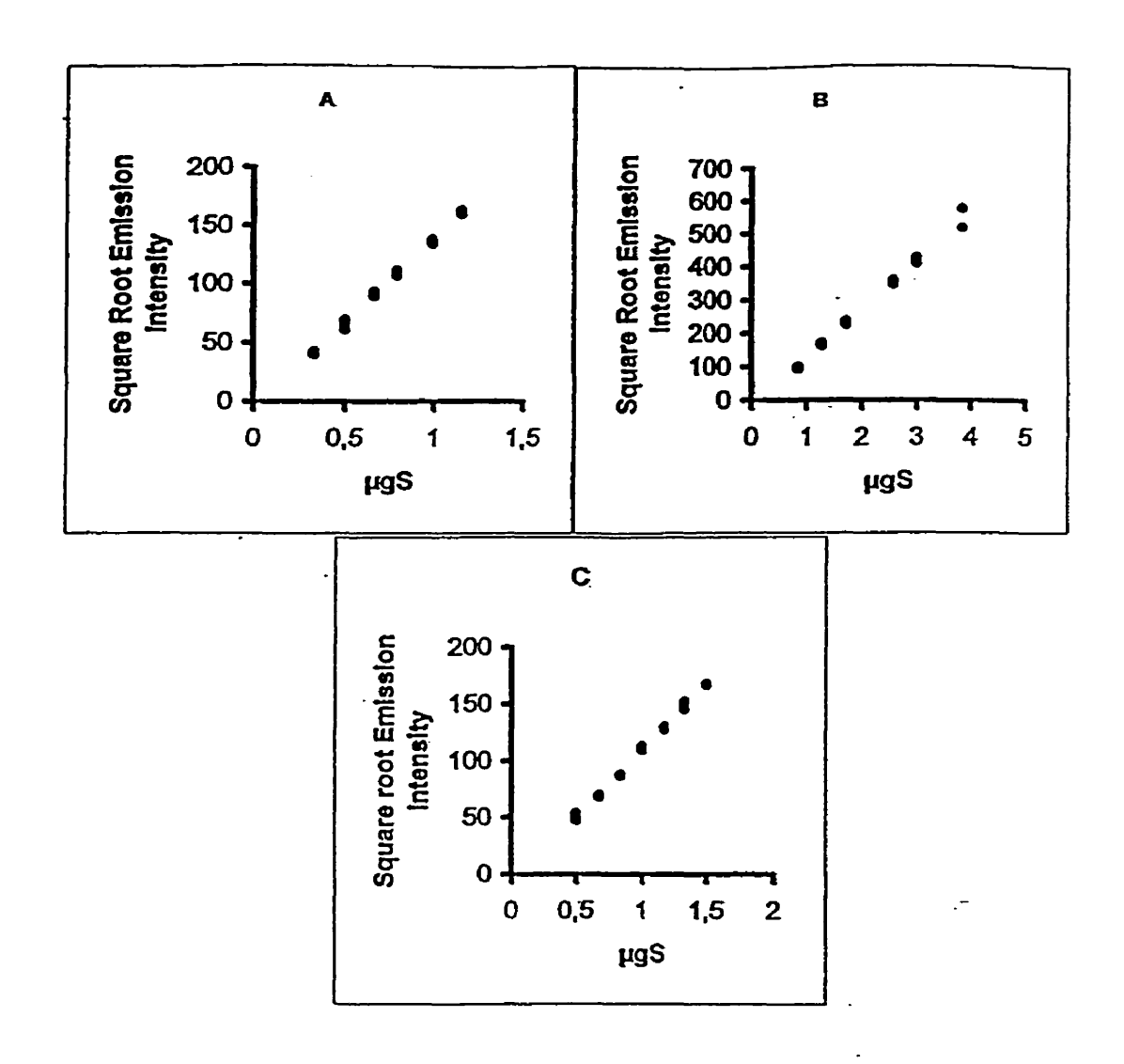


Figure 2.9

Regression analysis for the square roots of the peak integrations versus amounts of sulfur injected as (A) 2-methylthiophene, (B) carbon disulfide, and (C) ethanesulfonic acid.

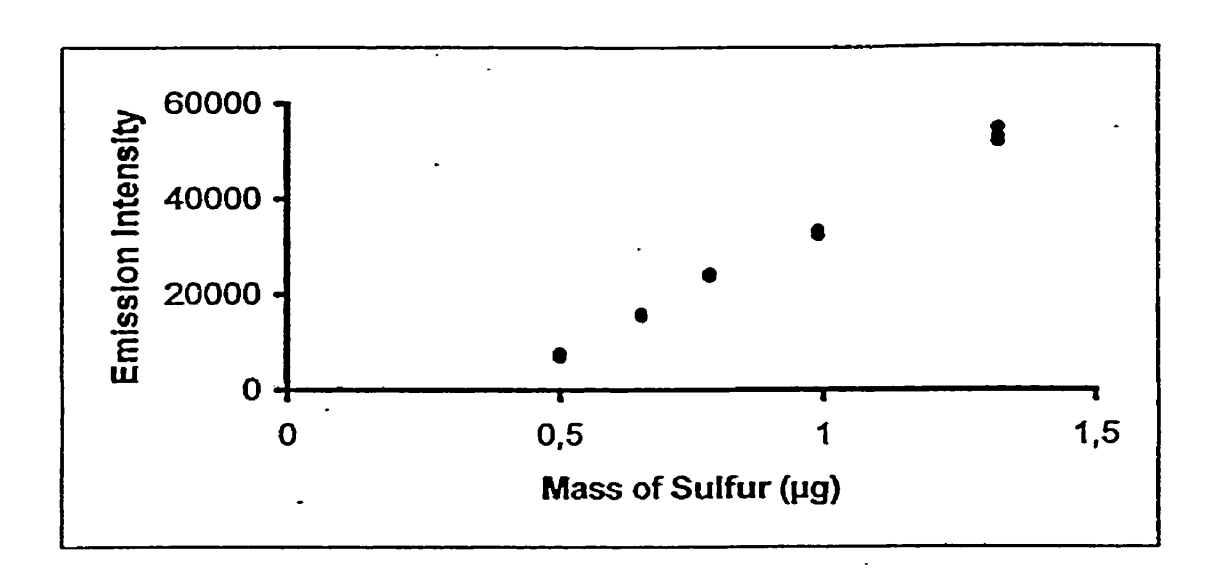


Figure 2.11

Regression analysis for the chemical linearization obtained for 2-methylthiophene

Since two atoms of sulfur are required to produce emission (of sulfur dimer), it was surprising that carbon disulfide did not exhibit a direct linear relationship of the emission response with concentrations (Figure 2.8, B). Instead, the relationship between the intensity of the sulfur dimer emission and the concentrations of carbon disulfide followed a quadratic behaviour similar to that of any sulfur compounds containing only one atom of sulfur. The fact that the formation of sulfur dimer is a non-quantitative reaction in hydrogen-rich flames accounts for this behaviour. As reported by Farwell and

Barinaga (1986), by Kramlich (1980), and by Fowler and Vaidya (1931), several sulfur containing-species, such SO, SH, SO₂, CS, CS₂, OCS..., coexist with the sulphur dimer in the analytical flame. According to Bornhop et al. (1989), in a hydrogen-rich flame, SO₂ is the major species and SO accounts for around 20%, while S₂ represents less than 1% of the total subproducts.

2.7.5 Determination of Thermolabile Sulfur Compounds from Garlic by HPLC-THG-FPD

The HPLC-THG-FPD system was assembled specifically for the analysis of heatlabile sulfur compounds. Garlic was chosen in our studies as a means to demonstrate the utility of the HPLC-THG-FPD system with biological samples as a selective detector for heat unstable sulfur compounds. Member of the genus Allium, garlic contains a high concentration of biologically active organo-sulfur species (Whitaker, Thiosulfinates comprise the major proportion of the organosulfur pool in freshly crushed garlic (Sendl et al., 1992; Block et al., 1992; Weinberg et al., 1993). Gas chromatography with flame photometric detection has been excluded as a reliable analytical tool for the determination of sulfur species in garlic due to formation of thermally induced artefacts such as polysulfides and thiophenes. It is generally recognized that the speciation of thiosulfinate in garlic extracts depends largely on the extraction conditions (Sendl et., 1992; Block et al., 1992). Organic or aqueous extracts from garlic are prone to degradation or rearrangements of sulfur species, especially when chemically sample clean-up steps are attempted. We anticipated that the formation of artifacts might be reduced by direct injection of a crude extract into the HPLC-FPD system.

A HPLC-FPD trace of a fresh water extract from garlic analysed during our feasibility study is shown in Figure 2.12a. Aqueous extract of fresh garlic contains a large proportion of thiosulfinates, and as such we assumed that the single peak observed under these chromatographic conditions (C₁₈ column, 85% methanol-15% water, room temperature) included a series of thiosulfinates. The labile character of these species in solution (Block et al, 1992; Weinberg et al, 1993) was corroborated by analysing the same extract after storage for 24 hours at room temperature. The actual chromatogram (Figure 2.12b) showed several new peaks which were absent from the former chromatogram.

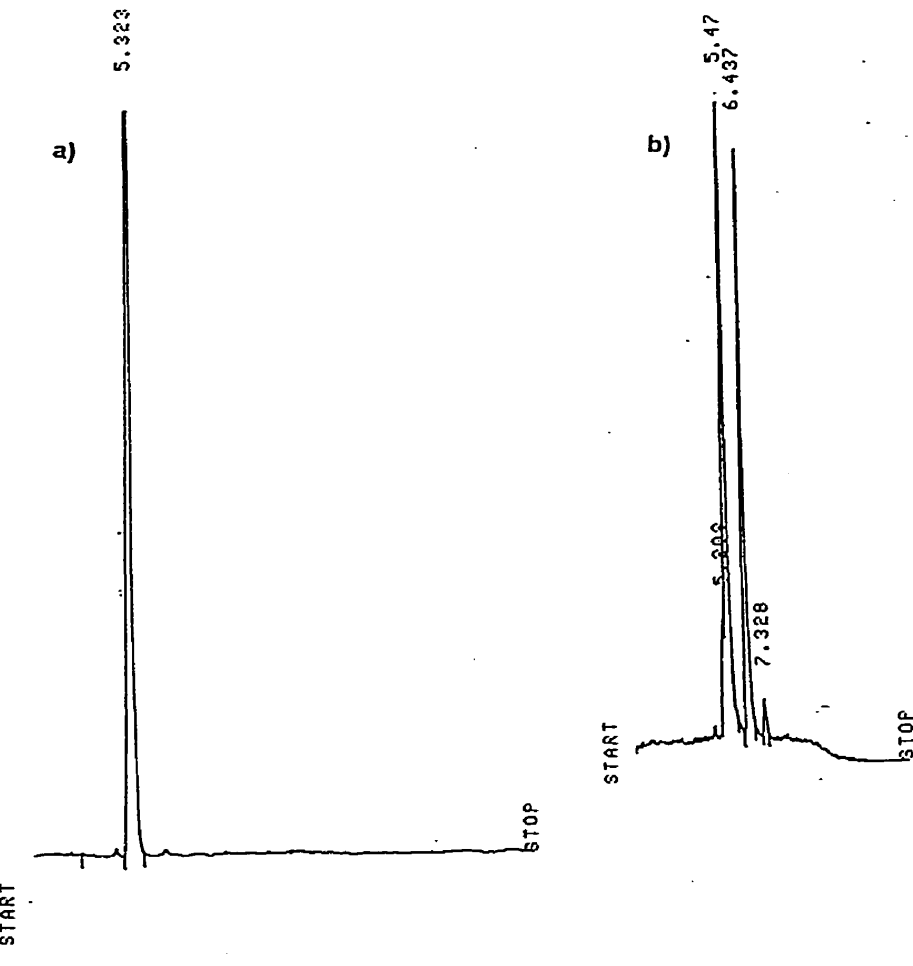


Figure 2.12

. HPLC-THG-FPD traces of an aqueous garlic extract: (a) fresh extract; and (b) after storage for 24 hours at room temperature.

2.8 Limitations of the Methanol Fuelled Interface

In this interface, the methanol is used as mobile phase as well as fuel for the pyrolytic flame. However, only up to 15% of water can be used without involving a high pressure in the system when higher percentages of water are used for improving separation of the analytes. This high pressure is due to the change in the viscosity of the mobile phase. Three methods can be used to improve separation and resolution in a chromatographic procedure. These methods are based on the modulation of the following parameters: the number of theoretical plates (N), the selectivity factor (α), and finally the capacity factor (k). Among these parameters, the latter is the most easily manipulated because of its strong dependence on the composition of the mobile phase. Separation of thiosulfinates from garlic extracts can be performed by using a 50:50 methanol-water mobile phase (Block, 1992, Lawson et al., 1990). However, the design of this actual interface does not allow handling of such a mobile phase and cannot be applied to speciation of hydrophilic molecules which are best resolved with high content of water in a mobile phase. Since the requirement of methanol as mobile phase limits the use of this interface, a modified interface fuelled by hydrogen has consequently been designed for handling high water content (more than 15%) in the methanolic mobile phase (Chapter Π).

2.9 Conclusion

The thermospray pyrolysis THG train, used to pyrolyze the methanolic HPLC mobile phase, efficiently volatilized sulfur species, which were detected by an FPD system with limits of detection that appeared to be suitable for the speciation of sulfur in

garlic. In the present configuration, the design was not appropriate for speciation: methanol, used not only as fuel but also as mobile phase, can not be diluted apreciably with water for improving separation. To extend the compatibility of the system to aqueous HPLC mobile phases, it was expected that the introduction of a hydrogen fuelled thermospray micro atomizer system (High et al., 1992) to eliminate the requirement for methanol will allow more flexibility in the composition of mobile phases.

Although methanol is a limitation for this design, the use of this mobile phase in HPLC-FPD methodologies is a precedent in the literature and led us to investigate the applicability of the HPLC-THG-FPD to real samples.

CHAPTER III

Design of a Hydrogen Fuelled Interface for the Determination of Sulfur Compounds from Biological Samples (Applications of the HPLC-THG-FPD to Horse kidney and Garlic extracts)

3. Behaviour of the HPLC-THG-FPD With Regard to Real Samples

3.1 Introduction

This chapter describes the feasibility of using HPLC/THG/FPD fuelled with hydrogen for separation and subsequent detection of reduced glutathione, metallothioneins, taurine in horse kidney extracts, and thiosulfinates in garlic extracts. Due to their non volatility or heat instability, the analysis of these compounds is not feasible by GC-FPD methodologies. The determination of these analytes was impossible using the previous methanolic interface (see Chapter II) due to the generation of a high pressure when high water level was used in the mobile phase.

The selectivity of the technique has been demonstrated by determination of sulfur compounds of biological interest that are either non-volatile (MT, GSH, Taurine) in GC procedures, or required UV/visible or fluorescent detection (GSH, taurine) after LC separation. The results showed that the proposed HPLC-THG-FPD system is an inexpensive, sensitive and selective tool for the determination of these species in biological samples.

3.2 Materials and Methods

3.2.1 Reagents and Standards for the Characterization of the Fuelled Hydrogen HPLC-THG-FPD System

Ethanol was HPLC grade (BDH, Inc., Montreal, Que). Ethanolamine, copper acetate, cadmium acetate, zinc acetate dihydrate, mercury acetate, and glutathione disulfide

(GSSG) were purchased from Aldrich (Milwaukee, WI, USA). Pure water was prepared by running tap water at 25°C through Milli-Q system (Millipore, Mississauga, Ontario). All solutions were deoxygenated with helium before use.

3.2.2 Instrumental Components

The instruments and data acquisition systems used for this study were as described previously (Section 2.3). Optimization experiments were performed without a column (in flow injection mode). A block diagram of the system is illustrated in Figure 2.1 (Chapter II), with the exception that, for these studies, the methanol fuelled interface was replaced by a hydrogen fuelled pyrolysis unit.

3.2.3 Reagents, Standards for the Speciation of Sulfur Compounds from Horse Kidney Extracts

All reagents used in this study were at least 98% pure and used without purification. Reduced glutathione (GSH), ammonium acetate, and 2-aminoethanesulfonic acid (taurine) were purchased from Aldrich, Chemical Co. (Milwaukee, WI). Horse kidney metallothionein I and II isoform as well as metallothionein containing both forms I and II were purchased from Sigma Chemicals Co., St Louis, MI. Tris(2-amino-2-(hydroxymethyl)-1,3-propanediol was from BDH, Montreal, PQ. The kidney used as matrix in this study came from a twenty-eight years old horse. Water was deonized to 18 MΩ cm at 25°C by Milli-Q (Millipore, Mississauga, Ontario). All solutions were deoxygenated before use.

3.2.4 Sample Preparation and HPLC Conditions for the Speciation of Sulfur Compounds from Horse Kidney Extracts

Horse kidneys were homogenized under helium in 0.03 M TRIS-HCl (2:1,v/m) at pH 8.6 using a polytron homogeneizer. Aliquots of the horse kidney homogenate were heated at 70°C for 5 minutes, then cool on ice for 10 minutes, and ultracentrifuged at 145,000g for 90 min. The supernatant was used for HPLC experiments. The sulfur compounds from the extract were separated on a Progel-TSK G2000SW (5 μm, 300 X 7.8 mm i.d.) and a Progel-TSK SW guard column (40 X 6mm i.d; Supelco, Miss., Ont., Canada) or a Progel TSK G4000 PWxL using a loop of 97 μL and 10 mM ammonium acetate, pH 6.0, as mobile phase that was delivered by a dual pump HPLC system (Gilson, model 305/306 Worthington, OH, USA) at 0.70 mL/min.

3.2.5 Reagents, Standards, and HPLC Conditions for the Separation of Sulfur Compounds from Garlic Extracts

Methanol used in this study was HPLC grade (BDH, Inc., Montreal, Que). Diallyl disulfide, sodium hydrogen carbonate, m-chloroperbenzoic acid and chloroform used for the synthesis of allicin were purchased from Aldrich. The LC column consisted in a C₁₈ column (250 X 4.6 mm i.d., 5 μm particles) and a guard column (30 X 4.6 mm i.d.) (CSC, Montreal, Quebec, Canada). The mobile phase, delivered at 0.50 mL/min, methanol-water (60:40 v/v) using a 20 μL loop. Garlic extract was prepared as described in Section 2.4. To allow maximum production of thiosulfinate, the homogenate was left to stand at room temperature for 30 minutes as described by Iberl et al., 1990.

3.2.6 Synthesis of Allicin

Allicin was not available commercially and was prepared by oxidation of diallyl disulfide with m-chlroperbenzoic acid in chloroform, according to the method of Jansen et al. (1987). To a solution of diallyl disulfide (0.01 mol) in chloroform (100 mL) at 0°C was added a solution of m-chloroperbenzoic acid (0.01 mole) in chloroform (100 mL). The reaction mixture was stirred for 30 minutes, permitted to react at room temperature for an additional 30 minutes, added to a solution of 5% sodium hydrogen carbonate in water and then extracted with chloroform. The solvent was removed under vacuum at room temperature. The resulting oily residue was extracted ten times with 20 mL of water. The aqueous fractions were combined and then extracted 10 times with ether. The organic layers were combined and the ether was removed under vacuum at room temperature. The residue was characterized by FT-IR (Jarsen et al., 1987). The principal feature of the spectrum is a strong absorption at 1090 cm⁻¹ (> S = O).

3.3 Results and Discussion

3.3.1 Design of a Hydrogen Fuelled Interface

Since the viscosity of water (1.002 cp at 20°C) is higher than that of methanol (0.597 cp at 20°C), the thermospray of aqueous mobile phase could not be achieved efficiently with the previous design. A hydrogen fuelled interface (Figure 3.1) was designed from quartz tubes. The aqueous mobile phase (water, water modified with methanol or with a salt) was heated (via the capillary) with thermoelectric element coiled around the thermospray inlet tube. The tip of the silica capillary tube received additional

thermal energy from the hot fuel introduced from the heated hydrogen inlet (H). In this configuration, the HPLC effluent underwent four consecutive processes: thermovaporization of the aqueous mobile phase, pyrolysis of the organic matrix in a kinetic hydrogen-oxygen flame, hydrogenation of the resulting sulfur radicals, and transport of the generated sulfur hydrides to an analytical inverted hydrogen-oxygen diffusion flame. This design permitted vaporization of the mobile phase inside the silica tube (B) and an efficient thermospray in the combustion chamber (F, 9mm i.d. X 11 mm o.d. X 5 cm). The oxidant (oxygen) inlet (G, 2mm i.d. X 3.2 mm o.d. X 6 cm) is located at a 900 in the combustion chamber, the optical part of this interface was identical to the previous methanolic fuelled interface. Under this geometry, the fine aerosol coming from the capillary was converted efficient into a thermospray in the combustion chamber without increasing the pressure of the system.

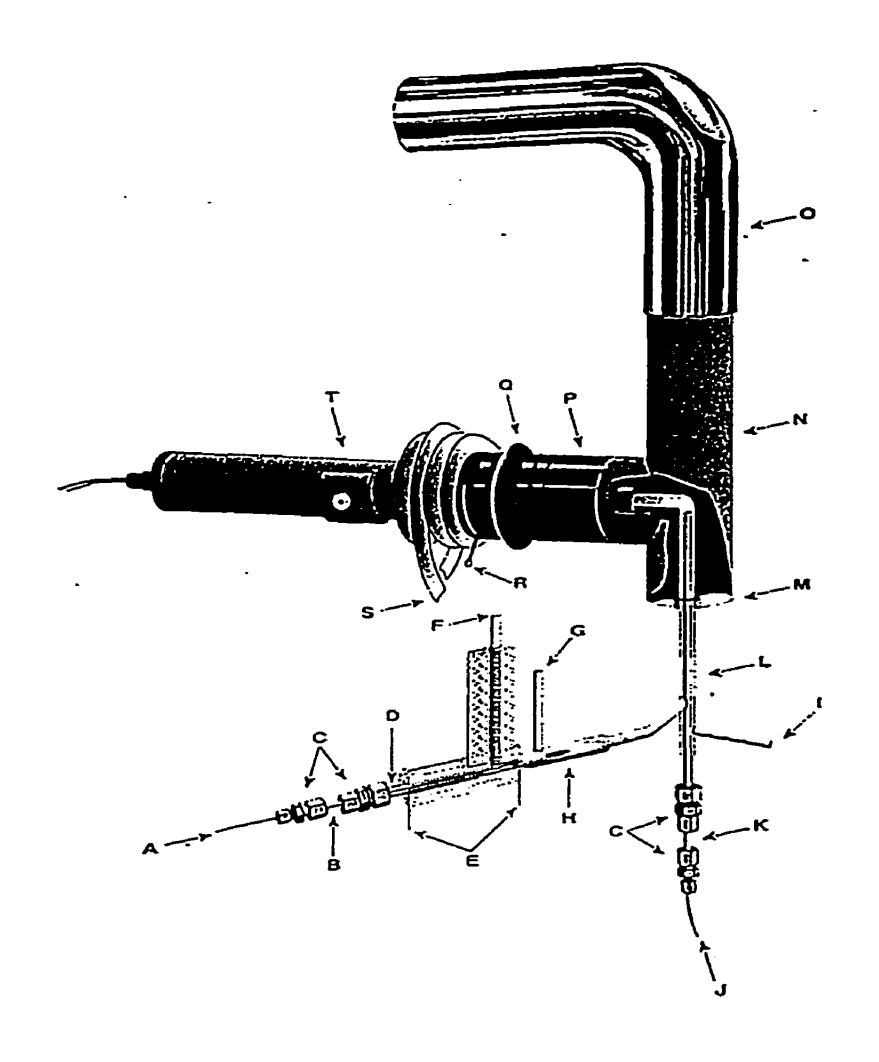


Figure 3.1

Diagram of the THG-FPD hydrogen system compatible with either methanolic or aqueous mobile phase. The thermospray-FPD system consisting of: (A) 50 µm i.d. capillary transfer line (from the HPLC column or from the injector; (B) silica guide tube; (C) Swagelock fitting; (D) heated thermospray chamber; (E) insulated thermoelectric coil; (F) H₂ inlet; (G) pyrolysis O₂; (H) post-combustion chamber; (I) helium inlet; (J) and (K), analytical O₂ inlet; (L) vertical silica tube/molecular emission chamber; (M) cover plate; (N) photometric chamber; (O) chimney; (P) window holder; (Q) rubber joint; (R) iris diaphragm; (S)water cooling coil; and (T) filter holder and photometric unit.

3.3.2 Optimization of an Hydrogen Fuelled HPLC-FPD Interface for Sulfur Dimer Emission

The hydrogen fuelled HPLC-FPD interface was optimized by using a multivariate factorial 2². The composite design accounted for the hydrogen, pyrolysis oxygen, analytical oxygen and helium effects on the FPD signal to 16.33 ηg of sulfur as glutathione disulfide using pure water as eluent or to 8.6 ppm of metalloprotein using 10 mM ammonium acetate as eluent. The optimization experiment was carried in flow injection mode using a loop of 20 μL . The phototube was operated at 900 V, at minimum sensitivity, with a interferometric filter having a band width of 60.0 ηm and a nominal wavelength at 397.5 ηm .

Optimum flow rates for the determination of sulfur-containing compounds, when the hydrogen fuelled interface was used with pure or modified water as eluent, were determined from surface response plots of analytical oxygen versus helium at different levels. Since the analytical oxygen and helium flow rates were shown to be the two critical variables on the status of the analytical flame (Section 2.7.3), the other two parameters (pyrolysis oxygen and hydrogen) are maintained constant during the experiment. The optimum parameters (pyrolytic oxygen and hydrogen) were kept constant at optimum values (pyrolytic oxygen = 280 mL/min and hydrogen = 1.5L/min), as determined by preliminary experiments.

The study of Dagnall and al. (1969), Mc Grea and Light (1967) on the emission spectra produced by non-sulfur organic compounds revealed observation of CH emission with a maximum at 431 nm. Since the spectral bandwidth of the filter used is found

between 367.5 and 427.5 nm, the spectral slit width is theoretically between 337.5 and 457.5 nm, thus the signal observed for sulfur dimer could contain positive interference from the emission of CH. In addition to this effect, the presence of non-sulfur-bearing organic compounds is known to affect the S₂ emission intensity (Rupprecht and Phillips, 1969; Belcher et al., 1974; Dressler, 1963). Therefore, a discussion on the chemiluminescence of sulfur dimer in cool flame would not be complete without considering the contribution produced by the interference of carbon response on the observed signal. Figures 3.3 and 3.5 illustrate the response surface obtained for CH, as 20% ethanol in water, during the optimization procedure. In generating the response surfaces for the optimum flow rates for sulfur detection, either with pure water or with 10mM ammonium acetate, the CH emissions were generated under the same conditions used for the above two eluents. The responses were compared with those obtained from the optimization results for sulfur detection. Evaluation of minimum conditions for CH emissions intensity was a necessary condition for the selectivity of system to sulfur detection. This optimization procedure required that the CH itself not be a significant emitter at the relevant oxygen (analytical) and helium flow rates for sulfur dimer emission. Figures 3.3 and 3.5 showed that the emission from CH is optimum at elevated oxygen flow rates (hot flame). Fredriksson and Cedergren (1981) had observed this behaviour previously. The results from the two systems indicated that the minimum emission from carbon was obtained in the absence of helium with the analytical oxygen operated at 8.00 mL/min. As a consequence, evaluation of the surface responses displayed in Figures 3.2 and 3.4 allowed us to estimate the optimum flow rates for maximum sensitivity and selectivity for sulfur detection to 8.00 mL/min for analytical

oxygen flow rate and absence of helium when water was used as mobile phase and to 8.00 mL/min for analytical oxygen and to 5.82 L/min for helium when 10mM ammonium acetate was used as eluent. Statistical analyses related to these optimizations are presented in the appendices (in Tables A-13 to A-21 and in Figures A-15 to A-17).

The intervariable interaction effects of analytical oxygen versus helium (Figure 3.2) on the molecular emission suggested that pure water had a cooling effect on the analytical flame in such a way helium was not required for this purpose. However when the water mobile phase was modified with ammonium acetate (Figure 3.4), the chemical and physical equilibrium of the cool analytical flame was disrupted by the presence of the salt that quenched the molecular emission of S₂. As demonstrated in Figure 3.4, presenting the effect of helium and analytical oxygen flow rates on the surface response, helium restored the optimum conditions of the analytical flame in the presence of ammonium acetate. Since the pyrolysis chamber conditions, described above for the optimization using pure water as eluent, still permitted atomization of the salt modified pure water mobile phase, the same 2² factorial composite design was used for the optimization of helium and analytical flow rates when 10 mM ammonium acetate was used as mobile phase.

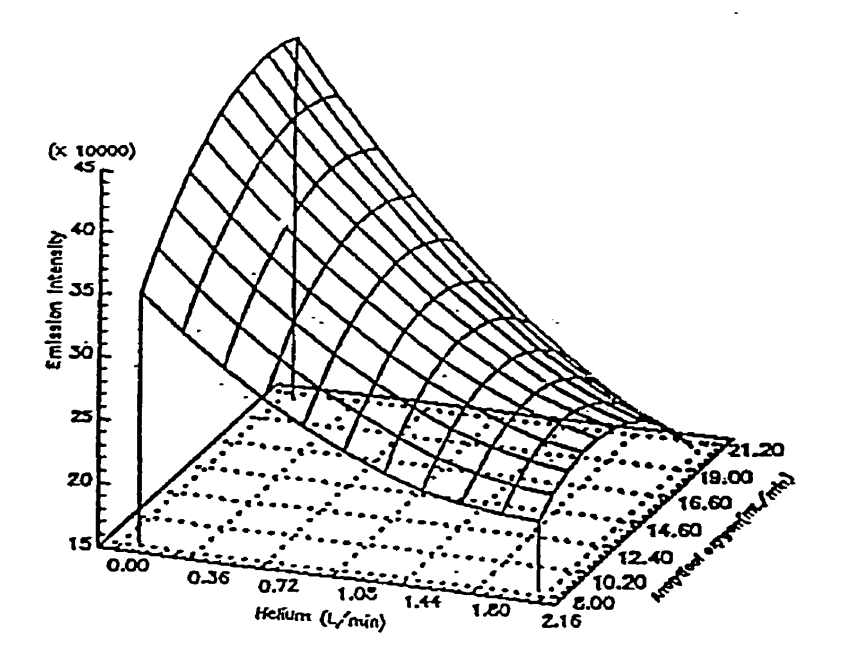


Figure 3.2

Predicted response surface to 16.33 ηg of sulfur as a function of analytical oxygen versus helium flow rates in flow injection mode (mobile phase: pure water, loop: 20 μL)

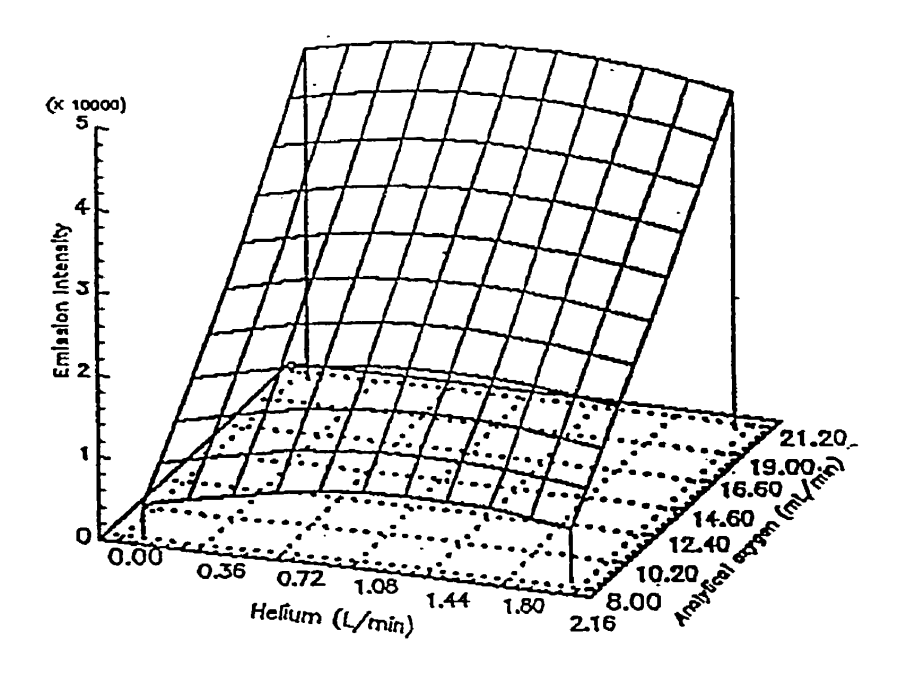


Figure 3.3

Predicted response surface to 1.65 μg of carbon as ethanol as a function of analytical oxygen *versus* helium flow rates in flow injection mode (mobile phase : pure water, loop: $20~\mu L$)

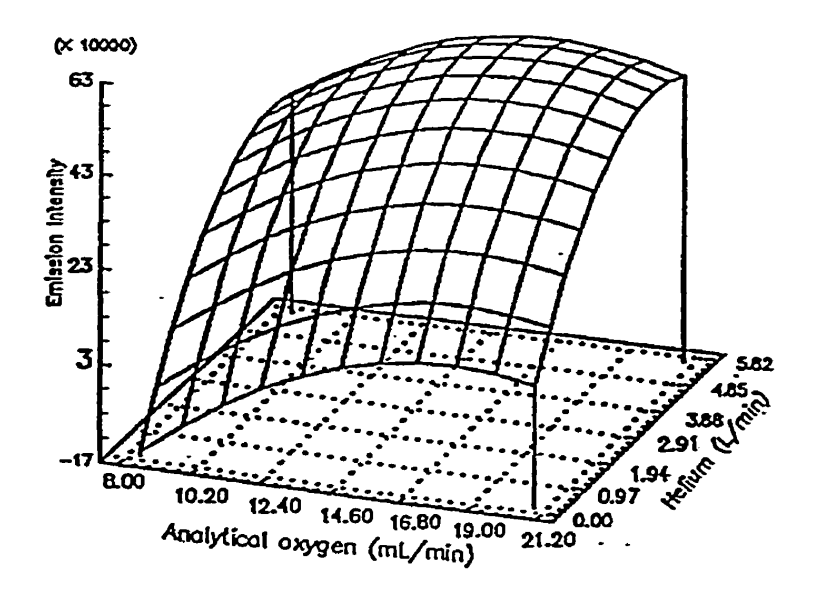


Figure 3.4

Predicted response surface to 8.6 ppm of metallothionein as a function of analytical oxygen versus helium flow rates in flow injection mode (mobile phase: 10 mM ammonium acetate, loop: 20 μ L)

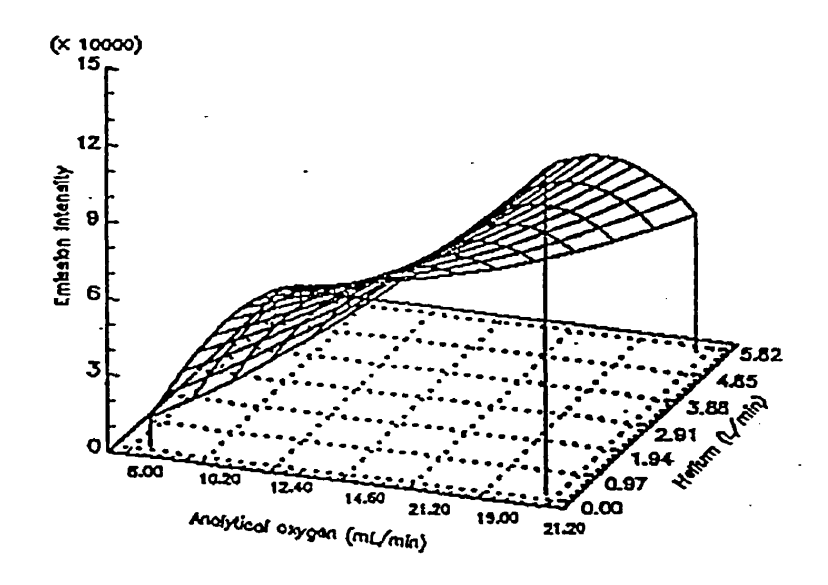


Figure 3.5

Predicted response surface to 1.65 μg of carbon as ethanol as a function of analytical oxygen *versus* helium flow rates in flow injection mode. (mobile phase: 10 mM ammonium acetate, loop: 20 μL)

3.3.3 Reproducibility of the Hydrogen Fuelled Interface

Figure 3.6 illustrates the HPLC-THG-FPD response for 20 consecutive injections of 2.18 ppm of oxidized glutathione (GSSG) [22.13 ng of sulfur]. Statistical evaluation of the surface gave excellent short term repeatability with a relative standard deviation (RSD) of 3.7%. However poor repeatability and sensitivity were obtained when we operated a freshly constructed interface. The response became optimal and repeatable only after several injections of any kind of sulfur compound until an adsorbed layer of sulfur had formed on the walls of the optical tube. This situation was also reported by Bogdanski et al. (1982) who attributed this enhancement to the fact that two sulfur radicals can give more than one photon by the generation of the following reactions:

$$S_n$$
 + HS + HS \rightarrow S_{n-2} + S_2 + S_2 + H_2 4.1

$$S_n + HS + HS \rightarrow S_{n-4} + S_2 + S_2 + S_2 + H_2$$
 4.2

$$S_n$$
 + HS \rightarrow S_{n-2} + S_2 + HS (regeneration of HS) 4.3

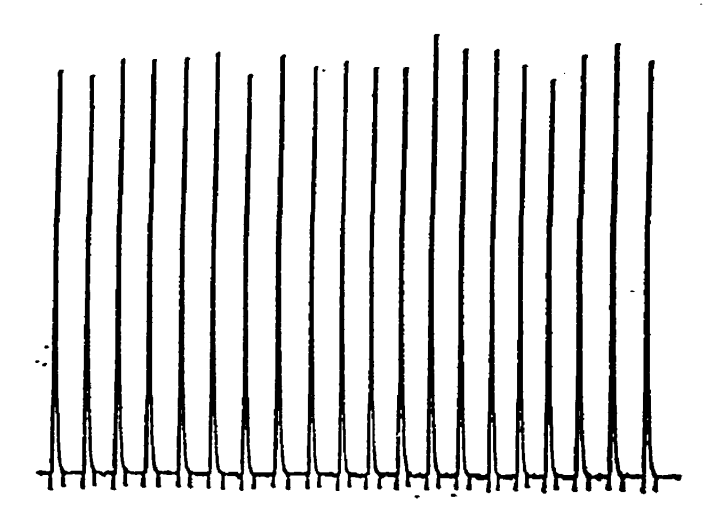


Figure 3.6

HPLC-THG-FPD response for 20 consecutive injections of 12.13 ηg of sulfur as GSSG (conditions: flow injection mode; mobile phase: 10 mM ammonium acetate; loop: 97 μL)

3.3.4 Performance of the System With Regard to Two Other Potential Interferences :CN and NH

In addition to CH, two other species, CN at 360 ηm and NH at 337 ηm , emitting at the same wavelength as S_2 , have been reported to produce chemiluminescence in the region of interest (Dagnall et al., 1969). The behaviour of the system with regard to these species is illustrated in the Figure 3.7. Triplicate injection of 1.65 μg of carbon as ethanol and 4.64 μg of nitrogen as ethanolamine (7.95 μg of carbon) demonstrated no appreciable positive interference of these species on the signal to 4 or 7 ηg of sulfur (conditions: flow injection mode; mobile phase: pure water). The differences in emissive

performance between the studied species are explained by the difference in temperature and chemistry of the analytical flame towards these species. Whereas the emissions of CH, CN, and NH are maximized in a hot and oxygen-rich flame, emission from the S_2 species is maximized in a relatively cool (300-400°C) and hydrogen-rich flame. Due to the wide bandwidth of our filter (80 η m), it was impossible to evaluate CN (360 η m) and NH (337 η m) emissions separately, thus the signal observed for ethanolamine was attributed to both CN and NH.

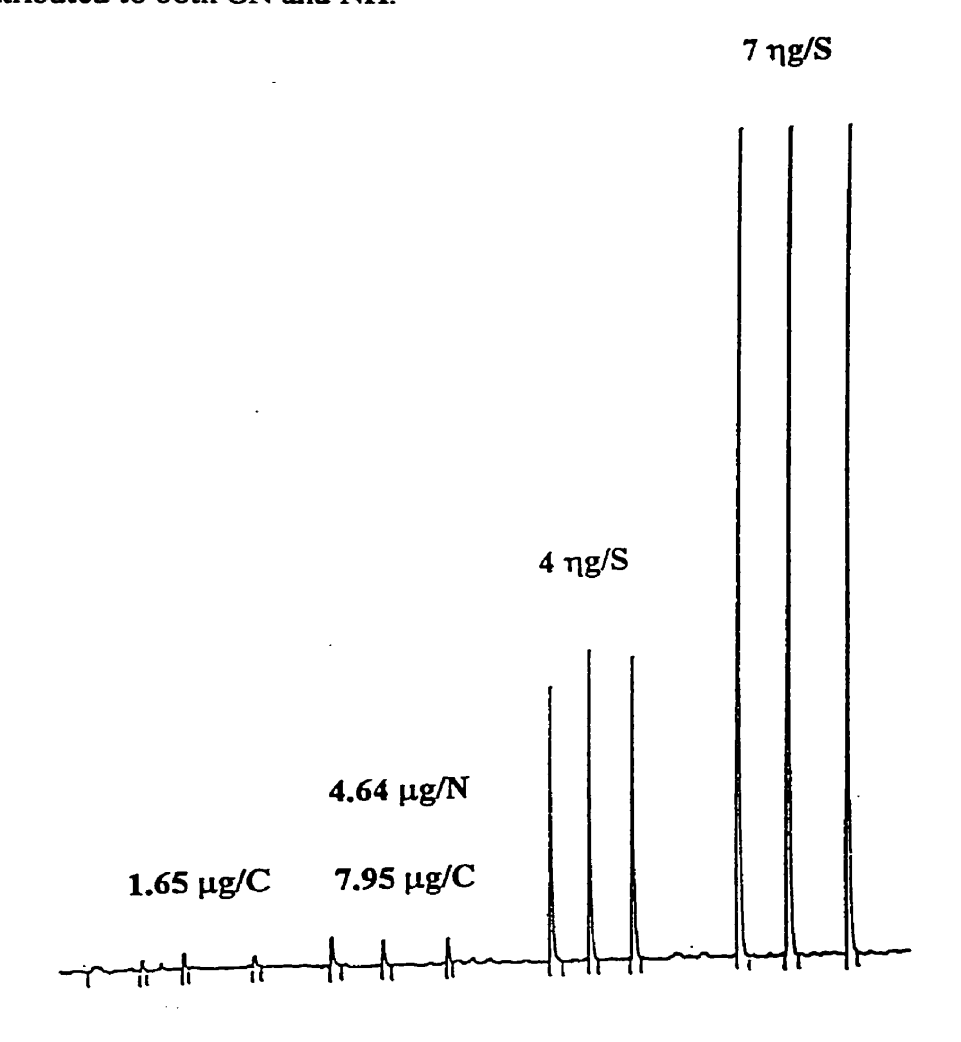


Figure 3.7

Performance of the system (flow injection mode) with respect to CH and CN. (Mobile phase: pure water)

3.3.5 Choice of Ammonium Acetate as Eluent for the speciation of sulfur compounds from horse kidney

Tris-HCl is usually used as eluent and buffer solution in most HPLC procedures for the determination of MT in biological matrices, but the use of Tris-HCl as eluent, in our system, resulted in a base line drift because this buffer readily clogged the capillary transfer line. This partial clogging increased the FPD noise and, consequently, was expected to decrease the sensitivity of the system. Rydén and Deutsch (1978) determined the molecular weight of MT by size exclusion chromatography and ammonium acetate solution as eluent. Using 10 mM ammonium acetate as mobile phase, it was possible to utilize the system for extended periods without clogging the capillary or without base line drift.

3.3.6 Effects of Metals on the Emission of Sulfur Dimer

Since metals are usually associated with MT, additional characterization studies of possible analytical interference were required. The effect of copper, cadmium, zinc and mercury on the response of sulfur was evaluated. Coinjection of 20 ng/S as GSH with respectively 3.09, 6.18, 9.26, 12.66, and 15.75 ng/Cd as cadmium acetate reduced the magnitude of the sulfur emission (Figure 3.8). This situation might be attributed to the formation of metals sulfide such as CdS in the pyrolysis chamber and/or in the analytical flame, and to changes in the temperature and flame chemistry of the analytical flame. Each of tested metals, copper acetate, zinc acetate dihydrate, or mercury acetate, resulted a similar diminution of the sulfur response. Similar effects had been observed previously during the characterization of a HPLC-AAS interface for selective detection of cadmium (High, K. et al, 1992).

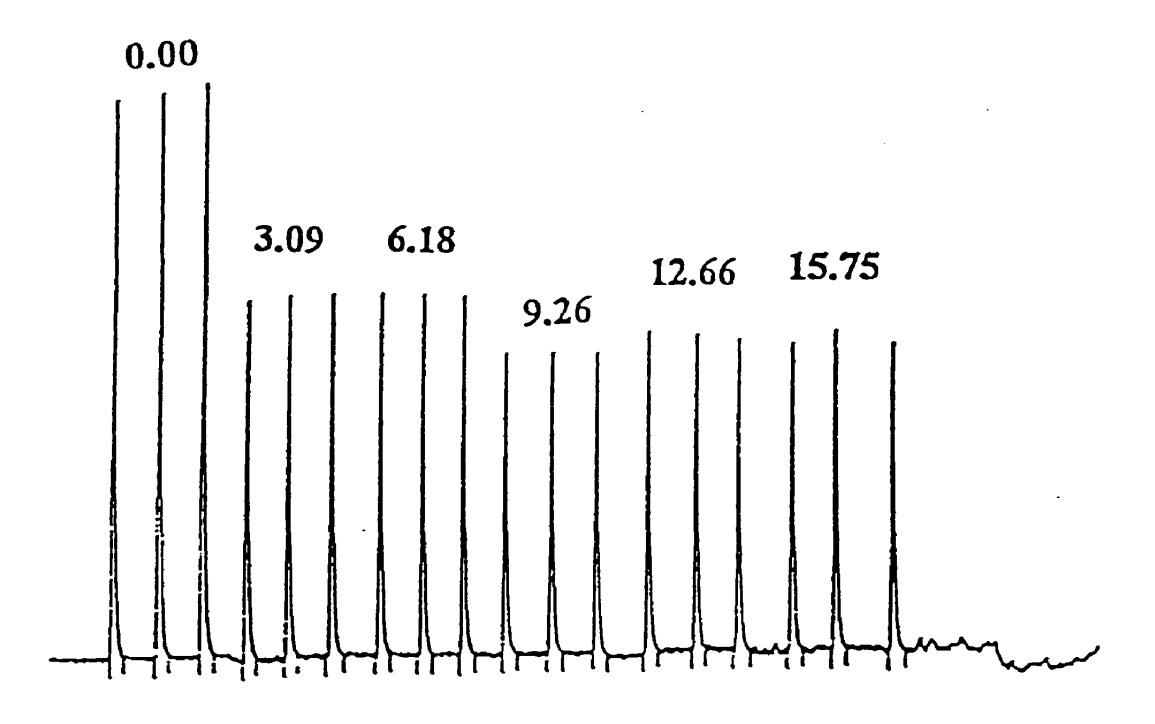


Figure 3.8

Effects of cadmium on the FPD response of 20 ng of sulfur as GSSG, in flow injection mode; mobile phase: 10 mM ammonium acetate.

3.3.7 Limit of Detection and Level of the Three Targets Analytes

Calibration plots for HPLC-THG-FPD response were obtained by the analysis of various standard solutions at various levels of MT, GSH, and taurine with a loop of 97 µL and 10 mM ammonium acetate as mobile phase. Interfacing the detection system with column eluate from of a Progel TSK G4000 PWxL provided a limit of detection of 30, 10 and 8 ng for MT, GSH and taurine respectively.

A recovery test was performed by spiking the horse kidney supernatant with standard MT, GSH, and taurine. Table 3.1 presents the recovery of each analyte determined by our system. In this table, the first column represents the analyte detected in the extract, the second column presents the amount of the detected analyte, the third column shows the respective amount of standard added to the extract, the fourth column represents the detected quantities in the spiked extract, whereas the last column shows the recoveries for two additions, which were near or exceed 90%.

Table 3.1

Recovery test by detection of MT, GSH, and Taurine in horse kidney tissues and sums of MT, GSH, and Taurine contents in kidney tissues plus respective additions

	Analyte detected (ng/g)	Analyte added (ng/g)	Quantity found (ηg/g)	Mean % recovery (± RSD)
MT	664.0 ± 0.6	181.2 422.6	779.4 ± 1.0 998.7 ±1.2	92.2 ±1.0 91.9 ± 1.2
GSH	322.4 ± 2.1	80.4 263.7	430.6 ± 1.5 601.9 ± 0.7	$106.9 \pm 1.5 \\ 102.7 \pm 0.7$
Taurine	1877.0 ± 0.6	505.0 1049.9	2187.8 ± 0.4 2592.1 ± 0.3	91.8 ± 0.4 88.6 ± 0.3

3.3.8 Application of the HPLC-FPD System for the Determination of Taurine, Glutathione and Metallothionein in Biological Matrices

The applicability of the HPLC-THG-FPD to high molecular weight sulfur compounds in biological samples was investigated by introducing a horse kidney supernatant fraction into the system. Figure 3.9 illustrates the distribution profile of several sulfur compounds in this matrix. Coinjection with authentic standards permitted tentative identification of GSH, MT, and taurine in the horse kidney supernatant fraction in the same run, despite the complex nature of the extract. In most case, these analytes (MT, GSH, taurine) are usually determined independently using separate methods (see above). SEC coupled with ICPES sulfur emission spectroscopy has been used in the past for the analysis, in a same run, of these sulfur species in horse kidney supernatant (Suzuki, 1991).

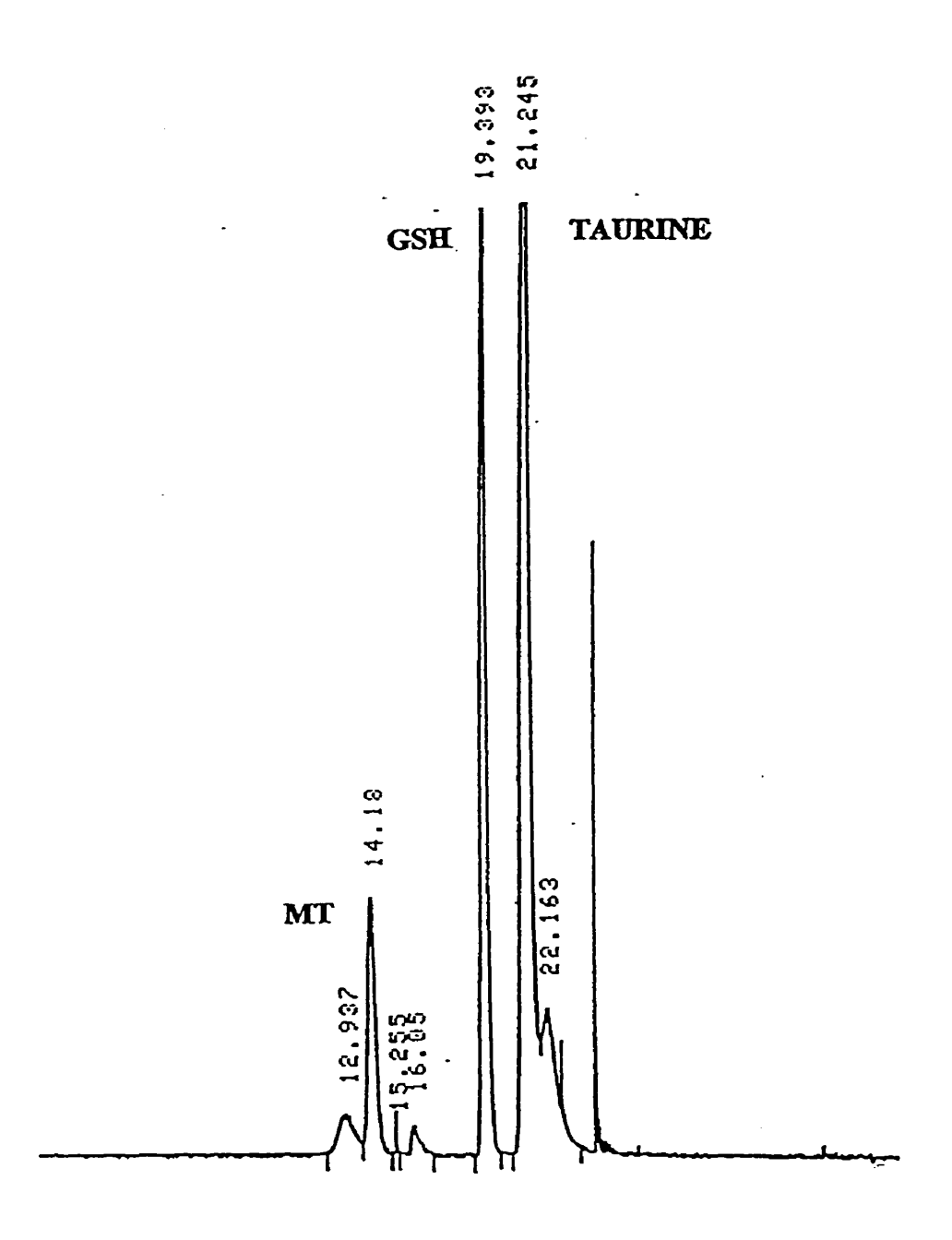


Figure 3.9

HPLC-THG-FPD response for sulfur compounds from horse kidney extract (1:100 dilution): mobile phase, 10 mM ammonium acetate at 0.65 mL/min; loop, 97 μL; column, TSK G4000 PW_{XL}.

3.3.9 Resolution of MT-I and MT-II, and Chromatographic Behaviour of MTs, GSH, and Taurine on a G2000SW Column

The TSK G4000 PW_{x1} column provides a simple sieving mechanism with regard to MTs (Figure 3.9), while silica based column packing are known to have both gel chromatographic and ion-exchange properties (Suzuki, 1979). A G2000SW column was used to achieve the resolution of the two MTs isoforms. The elution profile of the horse kidney supernatant is presented in Figure 3.10. In addition to the resolution of the two MT isoforms, the results provide another picture of what is normally observed when analytes of appreciable different molecular weight are eluted from a size exclusion column. This elution profile does not follow the ideal size-exclusion behaviour of large range of molecular weights solutes as predicted by the theory of size exclusion chromatography. The order of elution in Figure 3.10 does not correspond to decreasing molecular weights of MTs, GSH, and taurine. A non-ideal behaviour on the silica-based G2000SW column was observed. The principals of size-exclusion chromatography are well established and based upon molecular sieving behaviour of uniform packing of silica or polymer particles where the average residence time depends upon the size and the shape of the analytes. The theory of size exclusion chromatography predicts that compounds having a larger molecular size than the average pore size of the stationary phase are excluded and eluted in the void volume. However, small analytes can penetrate the network of the stationary phase. They are partially retained and eluted with retention times that increase with decreasing molecular weight. The TSK G4000 PW_{xl} profile of the kidney supernatant fraction (Figure 3.9) followed this behaviour.

The elution of GSH (M.W.= 307.33 g/mole), and taurine (M.W.= 110.13 g/mole) suggested that the mechanism of these two small molecules is adsorption independent, and follows a simple filtration mechanism, whereas the elution behaviour of MTs is governed principally by an adsorption-desorption mechanism on the same column. Identification of these peaks was based upon cochromatography standards. Suzuki and Maitani (1981) have obtained a similar chromatographic elution profile. In their work, these authors did not explain why glutathione eluted prior to metallothionein, which has an average molecular weight of thirty eight times bigger than that of reduced glutathione. This elution profile comes from the dual nature of the silica column, which acts as a typical exclusion stationary phase when we compare the retention time of 2aminoethanesulfonic acid with the retention time of glutathione or of MTs. However, the silica column behaves as a typical adsorbent relative to the retention time of glutathione, which is eluted more rapidly than metallothioneins. This situation is related to the fact that silica has a heterogeneous surface activity, which permits adsorption of polar molecules and thereby invalidates fractionation, which is directly related to molecular size and to some extent molecular shape. In this respect, MTs had to adopt a conformation allowing access of their polar residues to the polar moetly of the packing bead. For this reason, when silica-based particles are used in column packing, size exclusion chromatography may suffer from physical interactions between analytes and the stationary phase, even if efforts have been achieved in recent years to eliminate such interactions on silica matrix by modifying the siliceous particles with certain organic functional groups (Cooper and Deveer, 1978; Fukano et al., 1978; Rokushika et al., 1978; Kato et al., 1980; Regnier and Noel, 1976; Engelhardt and Mathes, 1977, 1979).

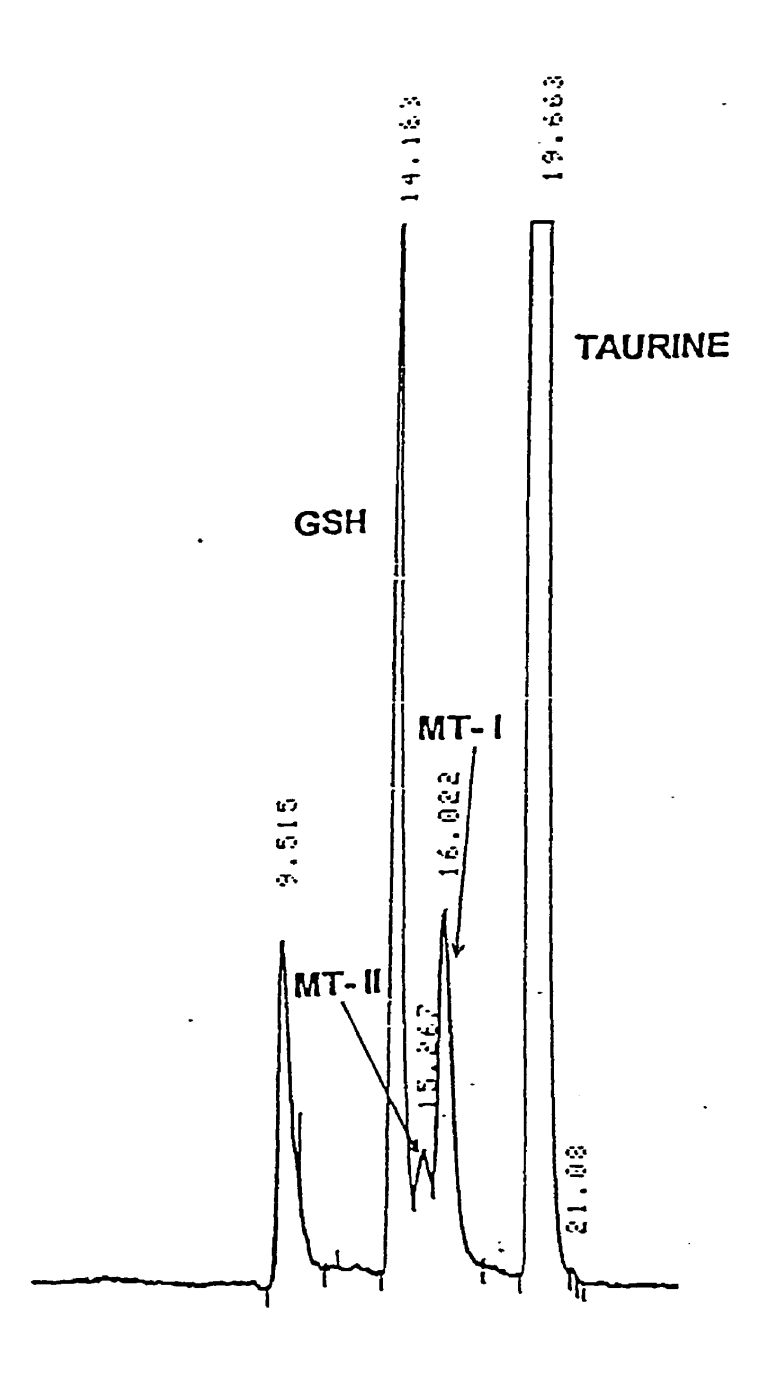


Figure 3.10

HPLC-THG-FPD response for sulfur compounds from horse kidney extract (1:100 dilution): mobile phase, 10 mM ammonium acetate at 0.65 mL/min; loop, 97 μ L; column, TSK G2000 SW_{XL}.

3.4 Determination of Allicin and Other Thiosulfinates from Garlic Homogenates

3.4.1 Limit of Detection of Allicin Using the Hydrogen Fuelled Interface

Calibration curves by HPLC-THG-FPD, using 60:40 methanol: water as mobile phase and a C_{18} column, were obtained by analysis of various standard solution of allicin. The limit of detection for allicin was calculated to be 2 ηg as sulfur from the calibration curves as three standard deviations above the average background noise.

3.4.2 Performance of the Hydrogen Fuelled Interface With Regard to Real Samples: Detection of Allicin and Other Thiosulfinates in Garlic Extracts

In the previous interface, the requirement of methanol as mobile phase limited the application of the THG interface for separation of sulfur compounds from garlic extracts. The behaviour of this hydrogen-fuelled interface was evaluated with garlic extracts. However a black deposit was observed within the combustion chamber, this limitation was overcome by interchanging the pyrolysis and hydrogen inlets for handling methanol based mobile phase. This configuration brought us back to the situation found in the methanol-fuelled interface. For this reason, the optimum flow rates used for that interface were applied to the hydrogen fuelled interface for the detection of thiosulfinates in garlic extracts which served as a good example to illustrate the capability of the system to analyse thermolabile sulfur compounds.

The HPLC-THG-FPD chromatogram obtained after injection of the aqueous garlic extract in the system is presented in the Figure 3.12. The application and the capability of the HPLC-THG-FPD system to thiosulfinates analysis is demonstrated by resolving

several thiosulfinates in the garlic extract (Figure 3.12). Allicin (Tr = 10.2 min.) determination has been performed by co-chromatography of garlic extracts with authentic standard. Allicin content of the garlic was evaluated to be 0.46% to wet weight. Quantification and identification of all other thiosulfinates detected by means of the system have not been performed, since the required standards were not available commercially. The allicin level found using the THG-FPD system is in agreement with the levels reported by several authors. As reported in the literature, the allicin content of fresh (wet) garlic ranges from 0.15% to 0.70% fresh weight (Lawson et al., 1990: Sendl and Wagner, 1990; Müller, 1990; Block and al., 1992, Jansen et al., 1987). This large range of allicin levels in garlic results from differences in growing and storage conditions of the bulbs, as concluded by Block and al. (1992).

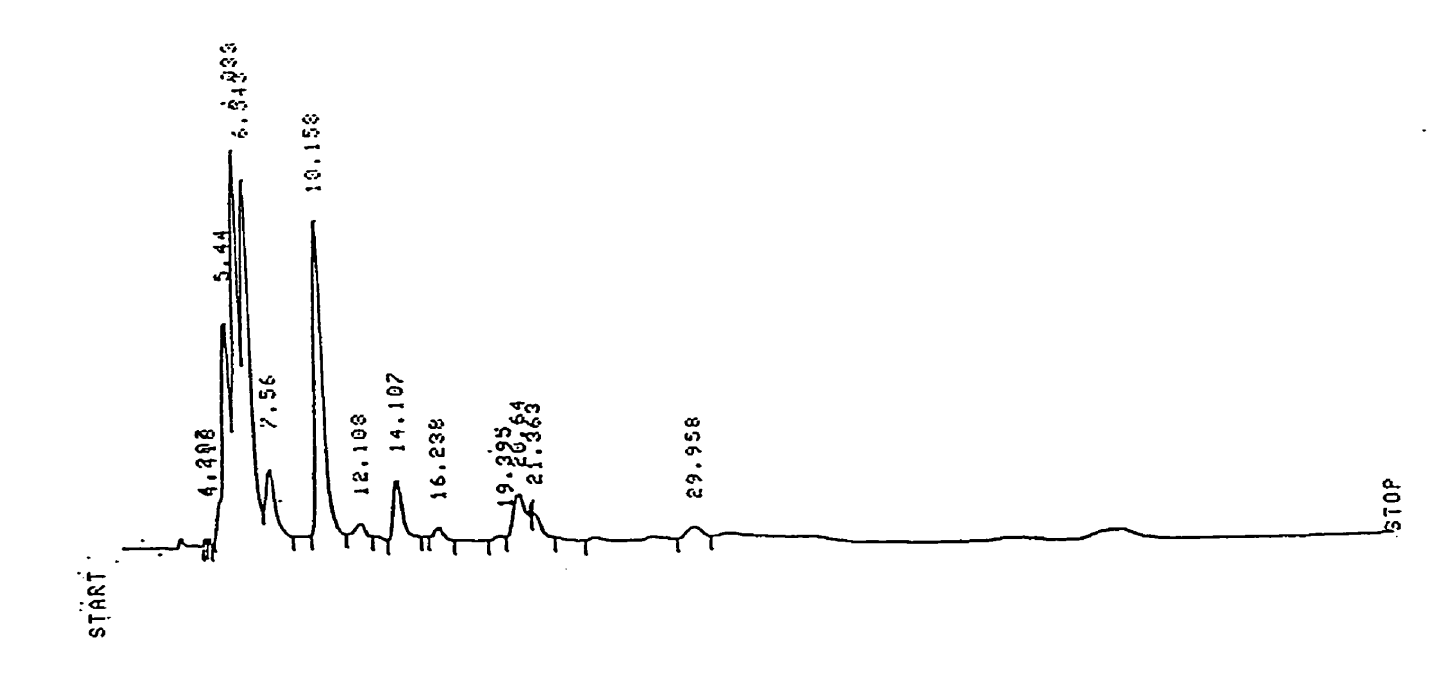


Figure 3.11

C₁₈ HPLC-FPD chromatogram of fresh aqueous garlic extract using methanol-water (60: 40) as eluent; loop: 20 µL.

3.5 Conclusion

A selective and reliable detection system for non-volatile/or and heat labile sulfur compounds was developed and applied to real samples. In the previous interface described in the Chapter II, the choice of the mobile phase was limited to methanol or methanol modified with up to 15% of water. Modification of that interface by using a coil to heat the hydrogen of the combustion chamber, led to an appreciable reduction in the system back pressure. This improvement provided a good separation of several sulfur compounds present in horse kidney and in garlic extracts. These results illustrate the capability for this technique to be applied for the selective analysis of sulfur compounds in real samples. The technique appears to be a suitable tool for the analysis of thermally unstable sulfur compounds in biological samples. The special utility of our technique lies in its low cost combined with its high selectivity with regard to hydrocarbon. The HPLC-THG-FPD system should be extremely attractive to the food industry for the analysis of garlic products.

The system permitted determination in a same run of reduced glutathione, metallothionein isoforms and taurine. To date, the proposed HPLC-THG-FPD is the only one molecular emission technique that permits, for the first time, the use of high performance liquid chromatography with flame photometric detection for the analysis of sulfur compounds in biological samples. From this study, it was demonstrated that MT, in spite of their high carbon content, can be easily determined using the THG-FPD detector after separation on a silica based column.

The system is relatively inexpensive to construct and operate and provides a highly selective detection procedure for sulfur compounds. The system can be operated with water and aqueous organic. It offers several advantages over current HPLC-FPDs: it is easy, fast, and inexpensive to perform. All the items needed for this system are inexpensive and readily available. The HPLC-THG-FPD turned out to be an economical alternative to HPLC-MS or HPLC-ICP and an excellent complement to GC-FPD when this latter cannot be used because of low volatility and/or thermolability nature of sulfur analytes.

CHAPTER IV

Original Contributions to Knowledge and Suggestions for Further
Studies on Thermolabile and Low Volatile Sulfur Compounds Using the
Developed HPLC-THG-FPD System

4.1 Contributions to Original Knowledge

- Development and optimization of thermospray microatomization interfaces for the high performance liquid chromatography detection of sulfur-containing analytes by flame photometric detector
- 2. Characterization of the intermediate involved in the formation of the sulfur dimer
- 3. Applications of the proposed HPLC-THG-FPD system to two different biological matrices: horse kidney and garlic homogenates

4.2 Suggestions for Further Research

4.2.1 Analysis of Garlic Products

The use of fresh garlic as an antithrombic in traditional folk medicine has led to the commercialization of garlic products in the non-prescription drug market. The isolation of these products often involves a steam distillation step, which is known to decompose the heat sensitive thiosulfinates. High-performance liquid chromatography with UV detection has been suggested as a more relevant method for the analysis for garlic products. Due to a lack of reliable analytical methods, the quality and the shelf-life of these increasingly popular products remain unclear. Given the unstable character of several sulfur species present in garlic extracts, a sulfur specific HPLC-FPD system would provide an attractive method for the speciation of sulfur in such extracts.

4.2.2 Determination of Taurine in Fluids and Tissues Homogenates.

Taurine has a low absorption of light in the low UV range. It is non fluorescent, and not volatile. These physicochemical features have lead to the development of a number of methods for determination of taurine. These methods include ion exchange chromatography, gas chromatography, and HPLC after derivatization for volatization or detection purposes. Due to the preparation of derivatives, these procedures are time-consuming. The high selectivity of the HPLC-THG-FPD system coupled with the high concentration of taurine in mammalian fluids and tissues suggests that the proposed system is ideally suited for direct determination of taurine without pre-/or post column derivatization, thus overcoming difficulties associated with formation and instability of derivatives.

CHAPTER V

APPENDIX

Statistical Analysis
Associated With the Optimization of the HPLC-THG-FPD

Table A-1 Obtained counts per minute for 35S

	Distance	Low O ₂	Med O ₂	High O ₂
	(cm)	(counts)	(counts)	(counts)
	0.00	5144	833	4761
	3.50	2871	66	48
	7.00	3907	169	138
	10.50	7190	2693	885
	14.00	15036	2923	3316
	17.50	6071	3273	1745
	21.00	1128	2211	1464
	24.50	2531	30055	71892
Total	Trap 1	5537140	5308192	128717
Total	Trap 2	199111	201766	24251

Table A-2 Matrix of the 2⁴ factorial design

1 1 1 1 1 1 1 1 1 1 2 2 2 2 2 2 2 2 2 2	-1 -1 -1 1 1 1 1 0 0 -1 -1 -1 1 1 1 0 0 0 0	-1 -1 1 -1 -1 1 0 0 -1 -1 1 1 0 0 0 0 0	-1 1 -1 1 -1 1 -1 1 -1 1 -1 1 0 0 0 0 0	1 -1 -1 1 -1 1 -1 1 -1 1 -1 1 0 0 0 0 0

Table A-3 Observed and Predicted Results of the factorial Experiment for the Methanol Fuelled Interface

Point	Oox	Oanal	H ₂	He	Re	esponse	D *
	mL/min	mL/min	mL/min	mL/min	Observed	Predicted	%
1	337.5	95.0	1025.0	7133.8	72735	76458	-5.12
2 3	337.5	95.0	1025.0	7133.8	69047	76458	-10.73
3	337.5	95.0	1025.0	7133.8	70091	76458	-9.08
4 5	337.5	95.0	1225.0	6376.7	84921	93983	-0.67
5	337.5	95.0	1225.0	6376.7	86510	93983	-8.64
6	337.5	95.0	1225.0	6376.7	86389	93983	-8.79
7	337.5	115.0	1025.0	6376.7	96238	86226	10.40
8	337.5	115.0	1025.0	6376.7	83687	86226	-3.03
9	337.5	115.0	1025.0	6376.7	97613	86226	11.67
10 11	337.5	115.0	1225.0	7133.8	116800	113945	2.44
12	337.5 337.5	115.0 115.0	1225.0 1225.0	7133.8 7133.8	117025 112112	113945 113945	2.63 -1.63
13	337.5 397.5	95.0	1025.0	6376.7	79614	79042	0.72
13	397.5 397.5	95.0 95.0	1025.0	6376.7	78351	79042 79042	-0.88
15	397.5 397.5	95.0 95.0	1025.0	6376.7	77369	79042 79042	-2.16
16	397.5 397.5	95.0 95.0	1225.0	7133.8	97550	105247	-7.89
17	397.5	95.0 95.0	1225.0	7133.8	99340	105247	- 5.95
18	397.5	95.0	1225.0	7133.8	102303	105247	-2.88
19	397.5	115.0	1025.0	7133.8	49079	40493	17.49
20	397.5	115.0	1025.0	7133.8	51342	40493	21.13
21	397.5	115.0	1025.0	7133.8	47500	40493	14.75
22	397.5	115.0	1225.0	6376.7	112770	108588	3.71
23	397.5	115.0	1225.0	6376.7	113588	108588	4.40
24	397.5	115.0	1225.0	6376.7	119220	108588	8.92
25	365.0	105.0	1150.0	6755.2	118980	124109	-4.31
26	365.0	105.0	1150.0	6755.2	116552	124109	-6.48
27	365.0	105.0	1150.0	6755.2	118784	124109	-4.48
28	365.0	105.0	1150.0	6755.2	114805	124109	-8.10
29	365.0	105.0	1150.0	6755.2	114711	124109	-8 .19
30	365.0	105.0	1150.0	6755.2	117174	124109	-5.92
31	337.5	95.0	1025.0	6376.7	91431	96192	-5.21
32	337.5	95.0	1025.0	6376.7	95013	96192	-1.24
33	337.5	95.0	1025.0	6376.7	88694	96192	-8.45
34	337.5	95.0	1225.0	7133.8	98694	110778	12.24
35	337.5	95.0	1225.0	7133.8	103829	110778	-6.69
36	337.5	95.0	1225.0	7133.8	101617	110778	-9.02
37	337.5	115.0	1025.0	7133.8	110785	106590	3.79
38	337.5	115.0	1025.0	7133.8	113360	106590	5.97
39	337.5	115.0	1025.0	7133.8	110421	106590	3.47
40	337.5	115.0	1225.0	6376.7	140494	137422	2.19
41	337.5	115.0	1225.0	6376.7	140137	137422	1.94
42 43	337.5	115.0	1225.0	6376.7	139803	137422	1.70
43 44	397.5	95.0 95.0	1025.0	7133.8	104462	105877	-1.35
44 45	397.5 397.5	95.0 95.0	1025.0 1025.0	7133.8 7133.8	105792	105877 105877	-0.08 -4.29
43 46	397.5 397.5	95.0 95.0	1225.0	6376.7	101522 121325	126396	-4.29 -4.18
10	ر. ۱ ر د	75.0	1445.0	0370.7	12132	120370	-7.10

Table A-3 Observed and predicted results of the factorial experiment for the methanol fuelled interface (continued)

Point	Oox	Oanal	H_2	He	Res	sponse	D*
	mL/min	mL/min	mL/min	mL/min	Observed	Predicted	%
47	397.5	95.0	1225.0	6376.7	122200	126396	-3.43
48	397.5	95.0	1225.0	6376.7	123178	126396	-2 .61
49	397.5	115.0	1025.0	6376.7	142196	128549	9.60
50	397.5	115.0	1025.0	6376.7	142705	128549	9.92
51	397.5	115.0	1025.0	6376.7	131253	128549	2.06
52	397.5	115.0	1225.0	7133.8	142084	138375	2.61
53	397.5	115.0	1225.0	7133.8	140944	138375	1.82
54	397.5	115.0	1225.0	7133.8	147847	138375	6.41
55	365.0	105.0	1150.0	6755.2	131383	124109	5.54
56	365.0	105.0	1150.0	6755.2	134502	124109	7.73
57	365.0	105.0	1150.0	6755.2	137920	124109	10.01
58	365.0	105.0	1150.0	6755.2	129375	124109	4.07 3.95
59	365.0	105.0	1150.0	6755.2	129211	124109	
60	365.0	105.0	1150.0	6755.2	122154	124109 110289	-1.60 -9.79
61	425.0	105.0	1150.0	6755.2 6755.2	100456 101333	110289	-9.19 -8.84
62	425.0	105.0	1150.0	6755.2	101333	110289	-6.59
63	425.0 282.5	105.0 105.0	1150.0 1150.0	6755.2	112193	107546	14.14
64 65	282.5 282.5	105.0	1150.0	6755.2	119180	107546	9.76
66	282.5	105.0	1150.0	6755.2	112243	107546	4.18
67	365.0	125.0	1150.0	6755.2	72274	97398	<i>-</i> 34.76
68	365.0	125.0	1150.0	6755.2	75605	97398	-28.82
69	365.0	125.0	1150.0	6755.2	77407	97398	-25.83
70	365.0	85.0	1150.0	6755.2	101835	80844	20.61
71 71	365.0	85.0	1150.0	6755.2	100154	80844	19.28
72	365.0	85.0	1150.0	6755.2	102826	80844	21.38
73	365.0	105.0	1350.0	6755.2	148149	140682	5.04
74	365.0	105.0	1350.0	6755.2	144700	140682	2.78
75	365.0	105.0	1350.0	6755.2	148270	140682	5.11
76	365.0	105.0	950.0	6755.2	77897	86855	-11.50
77	365.0	105.0	950.0	6755.2	81608	86855	-6.43
78	365.0	105.0	950.0	6755.2	77361	86855	-12.27
79	365.0	105.0	1150.0	7512.3	94880	94404	0.50
80	365.0	105.0	1150.0	7512.3	98208	94404	3.87
81	365.0	105.0	1150.0	7512.3	65941	94404	1.60
82	365.0	105.0	1150.0	5998.1	104490	109063	-4.38
83	365.0	105.0	1150.0	5998.1	103256	109063	-5.82
84	365.0	105.0	1150.0	5998.1	109003	109063	-0.06
85	365.0	105.0	1150.0	6755.2	126950	124109	2.24
86	365.0	105.0	1150.0	6755.2	121853	124109	-1.85
87	365.0	105.0	1150.0	6755.2	125898	124109	1.42
88	365.0	105.0	1150.0	6755.2	127421	124109	2.60
89	365.0	105.0	1150.0	6755.2	121723	124109	-1.96
90	365.0	105.0	1150.0	6755.2	124572	124109	0.37

^{*} D : Deviation of observed from predicted values: (obs.-pred.)/obs. X 100

Table A-4 Analysis of variance for the full regression of observed on predicted values (sulfur emission for the optimization of the methanol fuelled interface)

Parameter	Estimate	Standard Error	T value	Prob. level
Intercept	-335204	4607.37	-7.28X10 ⁻⁵	0.99994
Slope	1	0.04	23.8022	0.00000

Source	Sum of Squares	DF	Mean Square	F-Ratio	P-value
Model	4.17X10 ¹⁰	1	4.17 X10 ¹⁰	5.67X10 ²	0.0000
Error	6.48X10 ⁹	88	7.36X10 ⁷		
Total (corr.)	4.82 10 ¹⁰	89		4 C T T T T T T T T T T T T T T T T T T	

Correlation Coefficient = 0.9304 Stnd. Error of est. = 8583.62 R-squared = 86.56 percent

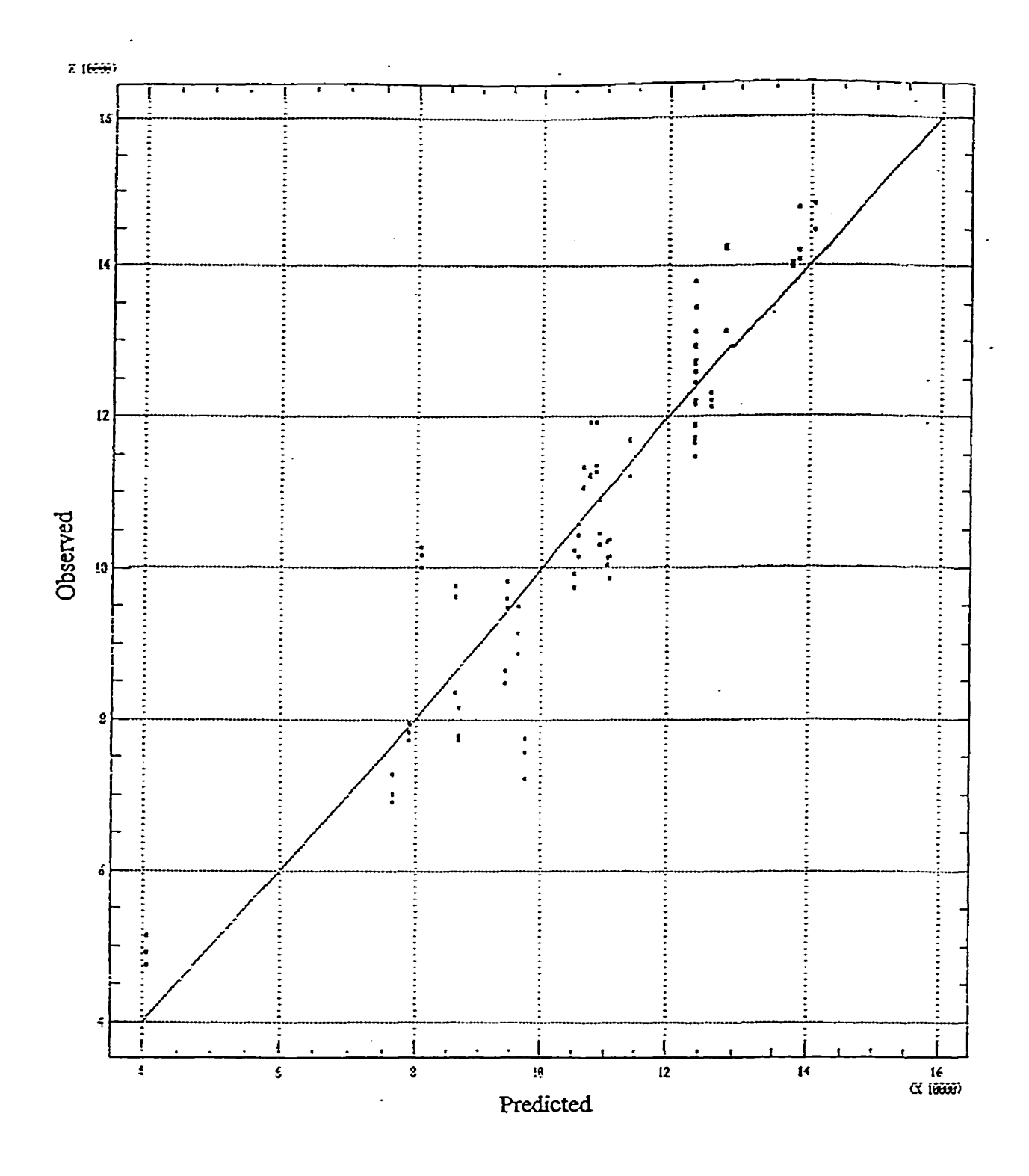


Figure A-1. Regression of Observed on Predicted Values for the Factorial Optimization of the Pure Methanol Fuelled Interface

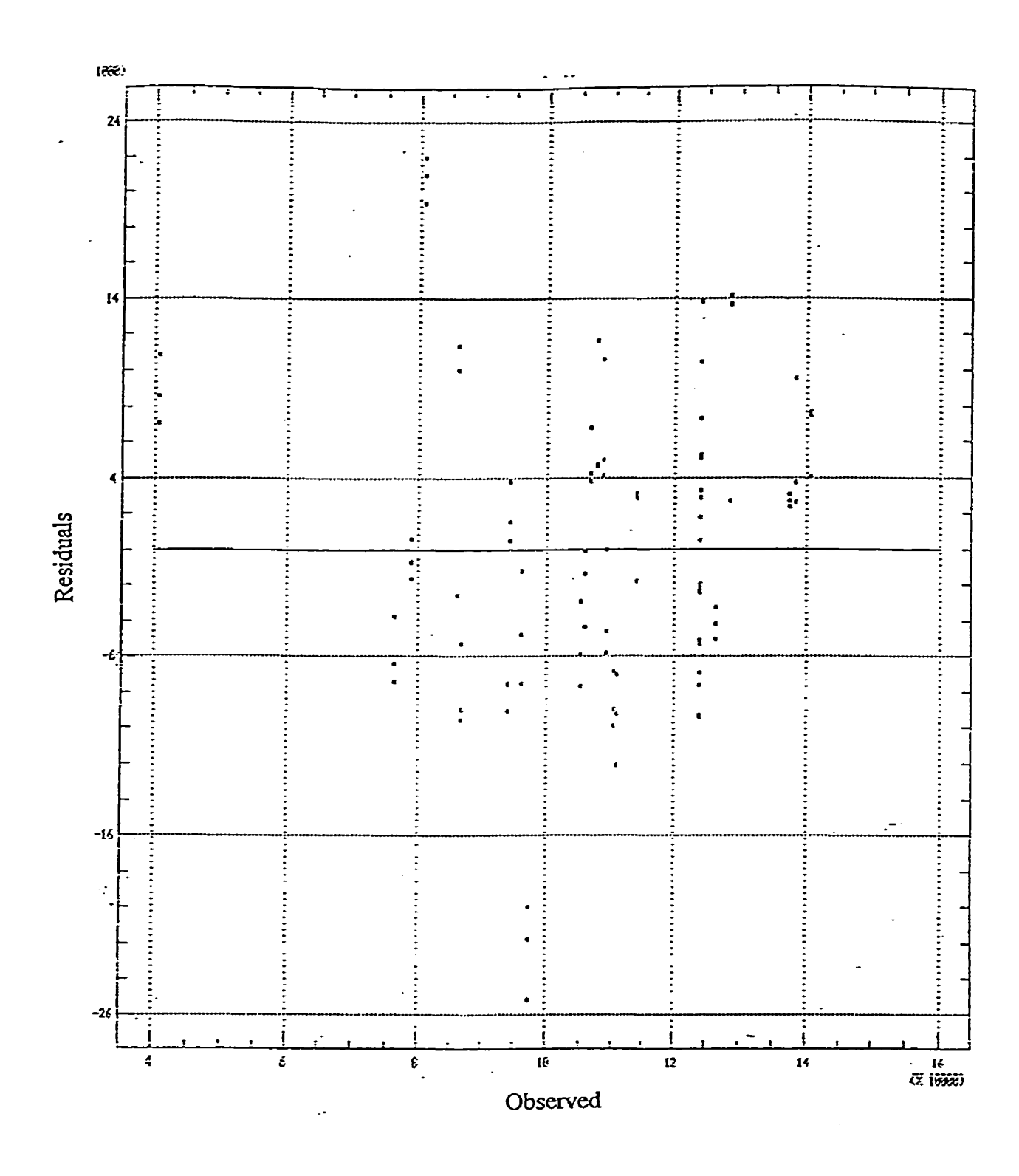


Figure A- 2. Residuals of observed on predicted values for the factorial Optimization of the Pure Methanol Fuelled Interface

Table A-5

Factorial second order equations predicting the effects of selected variables on the emission intensity of sulfur dimer for the pure methanol fuelled interface.

1) (H₂) and (He) versus Emission Intensity

Conditions:
$$(Oox) = 365.0 \text{ mL/min}$$

(Oanal) =
$$115.0 \text{ mL/min}$$

Emission Intensity = $124109 + 13457 \text{ H}_2 - 3665 \text{ He} - 2585 \text{ H}_2^2 - 5594 \text{ He}^2 + 3909 \text{ H}_2\text{He}$

2) Oanal and H₂ versus Emission Intensity

Conditions:
$$Oox = 365.0$$
 mL/min

He =
$$6755.2 \text{ mL/min}$$

Emission Intensity =
$$124109 + 13457 H_2 + 4138 Oanal - 2585 H_2^2 - 8747 Oanal^2 + 3602 OanalH_2$$

3) Oox and H₂ versus Emission Intensity

He =
$$6755.2$$
 mL/min

Emission Intensity =
$$124109 + 686 \text{ Oox} + 13457 \text{ H}_2 - 3798 \text{ Oox}^2 - 2585 \text{ H}_2^2 + 2124 \text{ OoxH}_2$$

4) He and Oanal versus Emission Intensity

Conditions :
$$Oox = 365.0 \text{ mL/min}$$

$$H_2 = 1150.0 \text{ mL/min}$$

Emission Intensity =
$$124109 + 3665 \text{ He} + 4138 \text{ Oanal} + 5594 \text{ He}^2 - 8747 \text{ Oanal}^2$$

- 4008 HeOanal

Table A-6

Regression analysis for the square roots of the peak integration versus amounts of sulfur injected as 2-methylthiophene – Linear model: y = a + bx

Dependent va	riable: Square	ty. Independ	dent variable : μgS.	
Parameter	Estimate	Standard Error	T value	Prob. level
Intercept	-6.871	1.561	-4.402	0.0004
Slope	146.462	1.982	73.891	0.0000

Source	Sum of Squares	DF	Mean Square	F-Ratio	P-value
Model	29932.965	1	29932.965	5460.227	0.0000
Error	87.706	16	5.482		
Total (Corr.)	30020.671	17			

Correlation Coefficient = 0.9985

R-squared = 99.71 percent

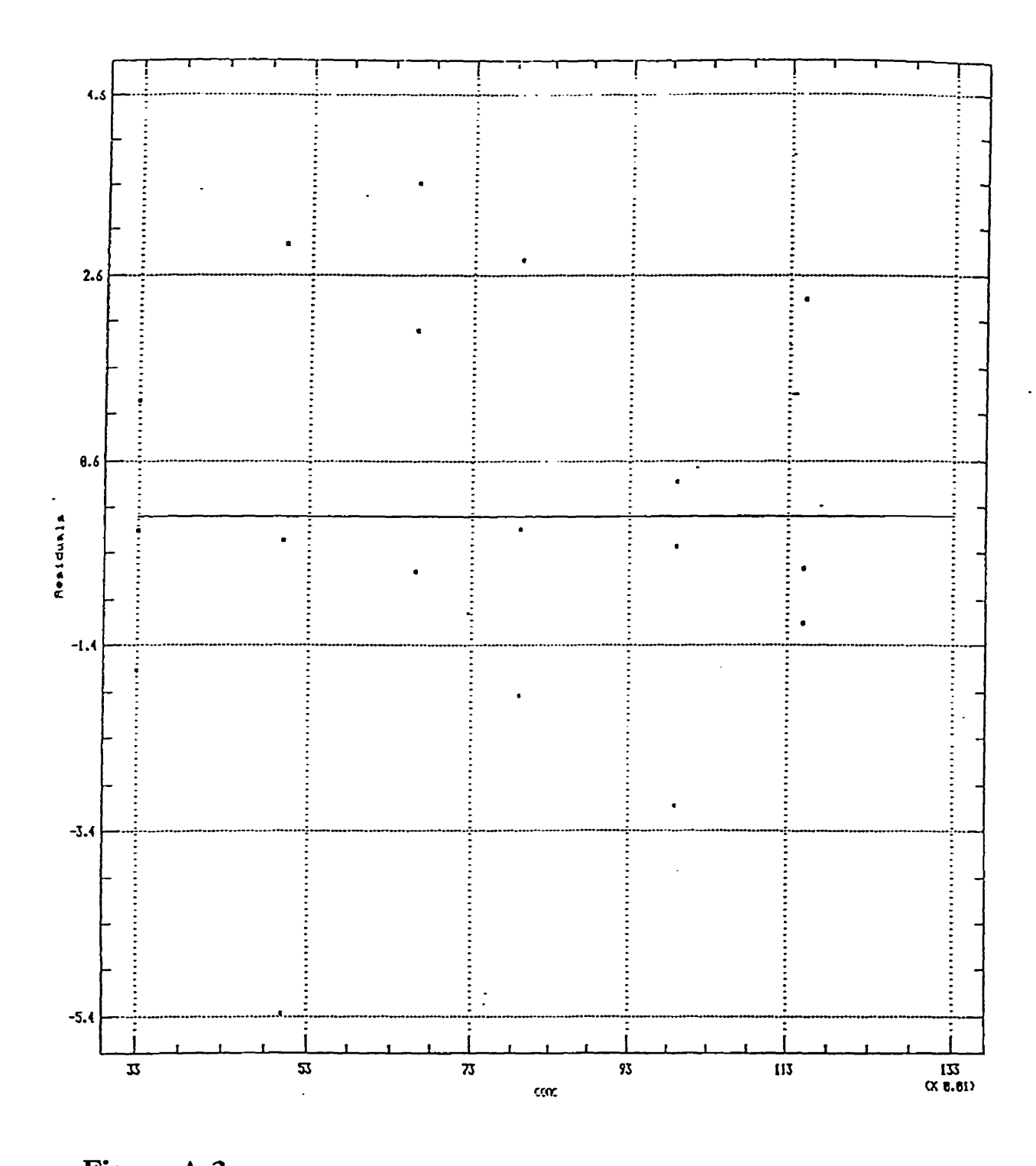


Figure A-3

Residuals for the square root emission intensity on amounts of sulfur injected as 2-methylthiophene

Table A-7

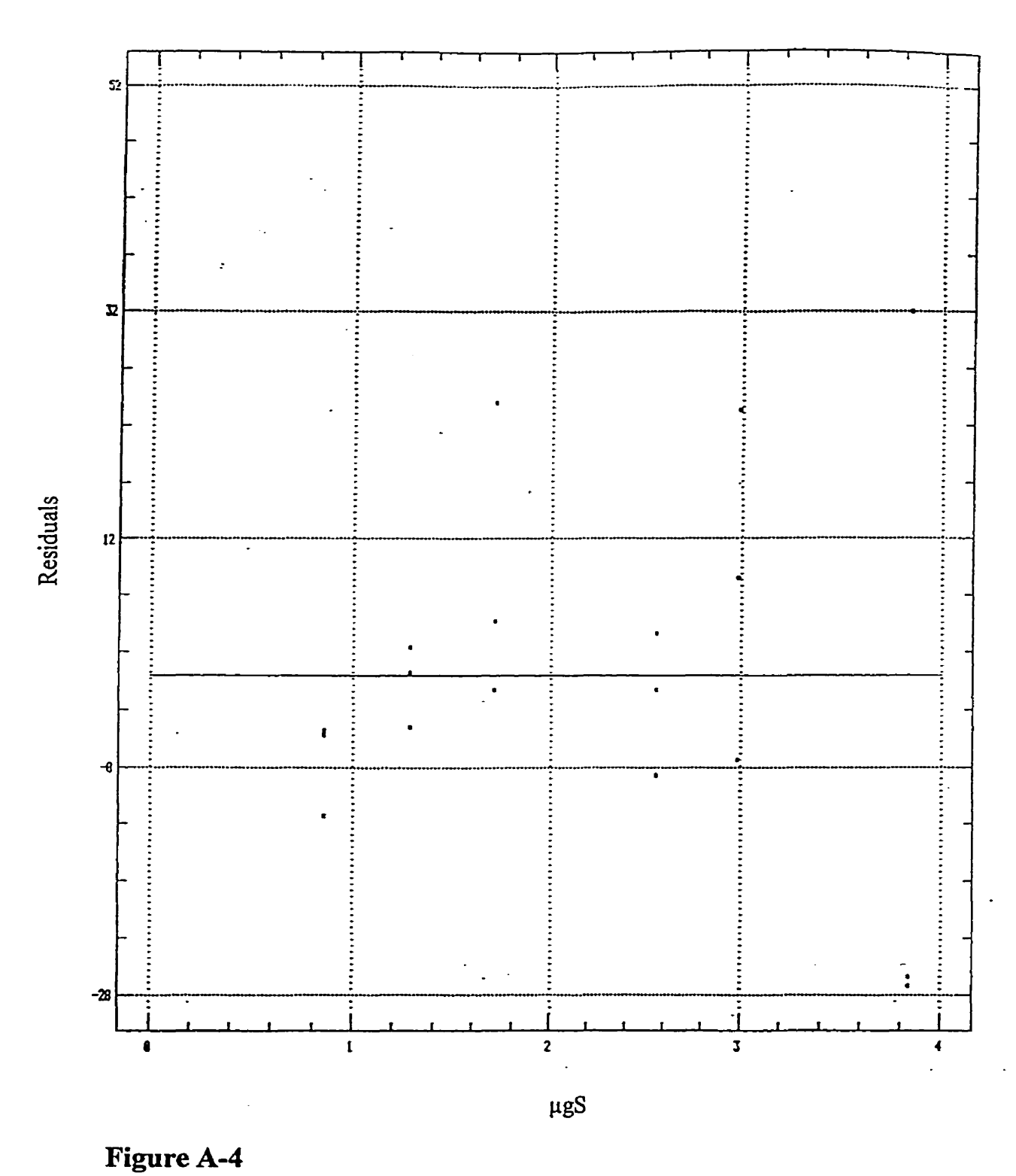
Regression analysis for the square roots of the peak integration versus amounts of sulfur injected as carbon disulfide – Linear model: y = a + bx

Dependent varia	ble: Square Ro	Independent variable: µgS.		
Parameter	Estimate	Standard Error	T value	Prob. level
Intercept	-18.172	8.877	-2.047	0.0574
Slope	146.216	3.648	40.081	0.0000

Source	Sum of Squares	DF	Mean Square	F-Ratio	P-value
Model	407408.97	1	407408.97	1606.44	0.0000
Error	4057.71	16	253.61		
Total (Corr.)	411466.68	17		~~~~~~~~~	

Correlation Coefficient = 0.9950

R-squared = 99.01 percent



Residuals for the square root of emission intensity on amounts of sulfur injected as carbon disulfide

Table A-8

Regression analysis for the square roots of the peak integration's versus amounts of sulfur injected as ethanesulfonic acid – Linear model: y = a + bx

Dependent var	riable: Square Ro	Independent variable : μgS.		
Parameter	Estimate	Standard Error	T value	Prob. level
Intercept	-9.077	1.535	-5.913	0.0000
Slope	118.196	1.456	81.178	0.0000

Source	Sum of Squares	DF	Mean Square	F-Ratio	P-value
Model	32505.974	1	32505.974	6589.494	0.0000
Егтог	93.738	19	4.933		
Total (Corr.)	32599.712	20			

Correlation Coefficient = 0.9986

R-squared = 99.71 percent

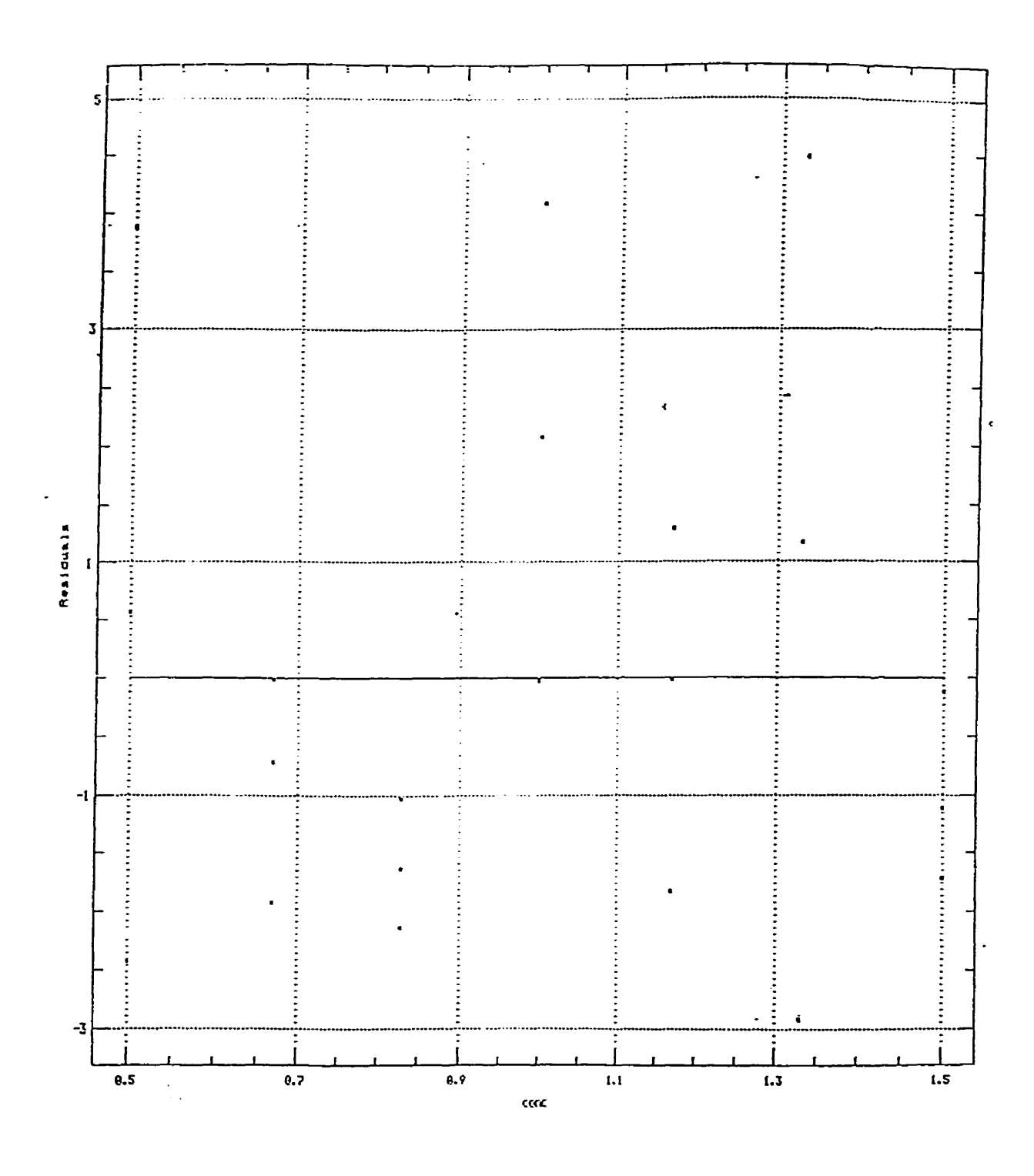


Figure A-5

Residuals for the square root of emission intensity on amounts of sulfur injected as ethanesulfonic acid

Table A-9

Regression analysis for the log emission intensity versus log amounts of sulfur injected as 2-methylthiophene – Linear model: y = a + bx

Dependent variable: log Emission Intensity.			Independent variable :log µgS.		
Parameter	Estimate	Standard Error	T value	Prob. level	
Intercept	4.291	9.35X10 ⁻³	458.930	0.0000	
Slope	2.189	0.038	54.605	0.0000	

Source	Sum of Squares	DF	Mean Square	F-Ratio	P-value
Model	2.871	1	2.871	2871	0.0000
Егтог	0.014	16	0.001		
Total (Corr.)	2.885	17			

Correlation Coefficient = 0.9976

R-squared = 99.52 percent

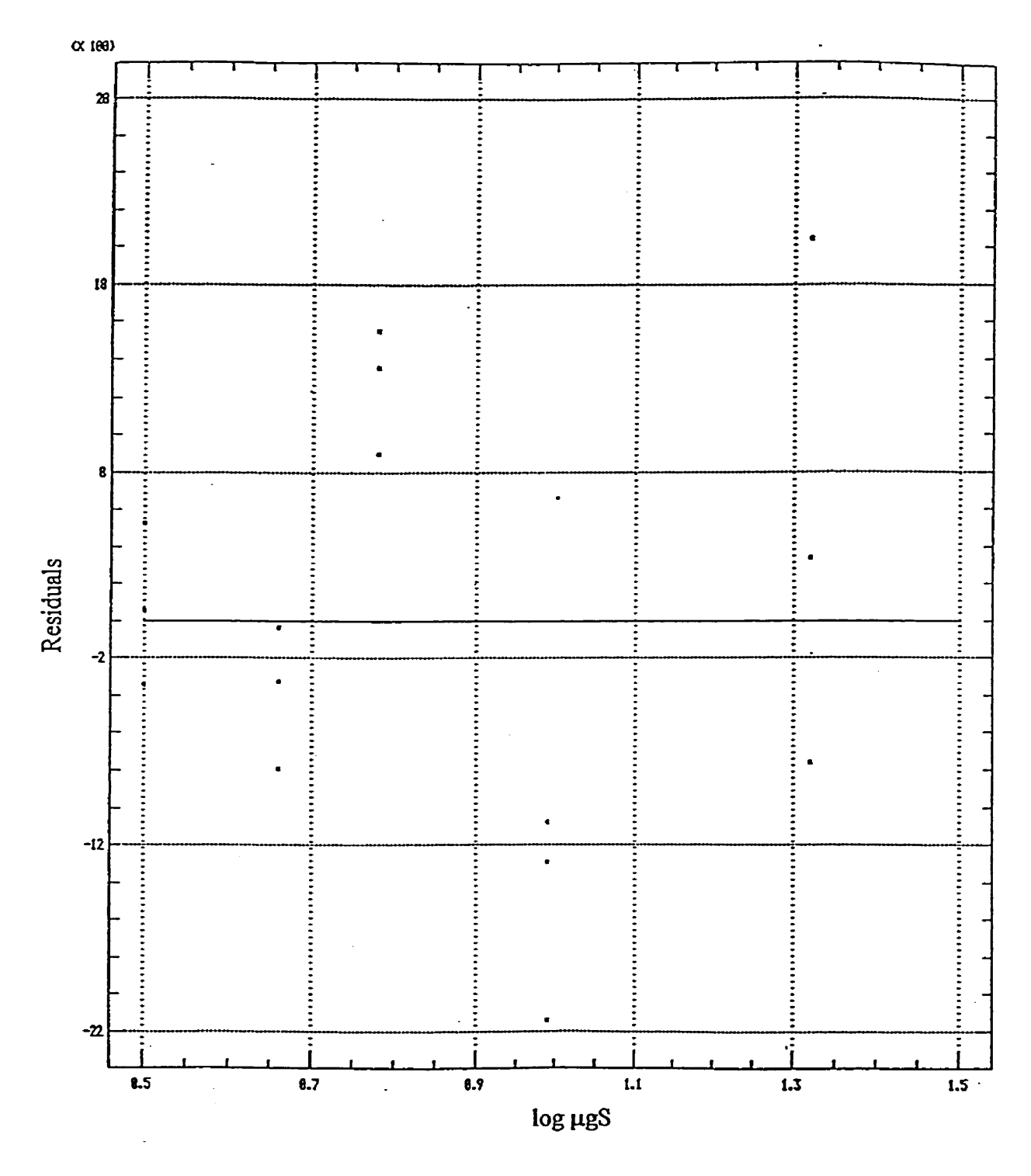


Figure A-6

Residuals for the log emission intensity versus log amounts of sulfur injected as 2-methylthiophene

Table A-10

Regression analysis for the log emission intensity versus log amounts of sulfur injected as carbon disulfide – Linear model: y = a + bx

Dependent variable: log Emission Intensity.			Independent variable :log μgS.		
Parameter	Estimate	Standard Error	T value	Prob. level	
Intercept	4.180	0.014	298.571	0.0000	
Slope	2.238	0.039	57.385	0.0000	

Source	Sum of Squares	DF	Mean Square	F-Ratio	P-value
Model	4.511	1	4.511	4511	0.0000
Error	0.022	16	0.001		
Total (Corr.	.) 4.533	17			

Correlation Coefficient = 0.9975

R-squared = 99.51 percent

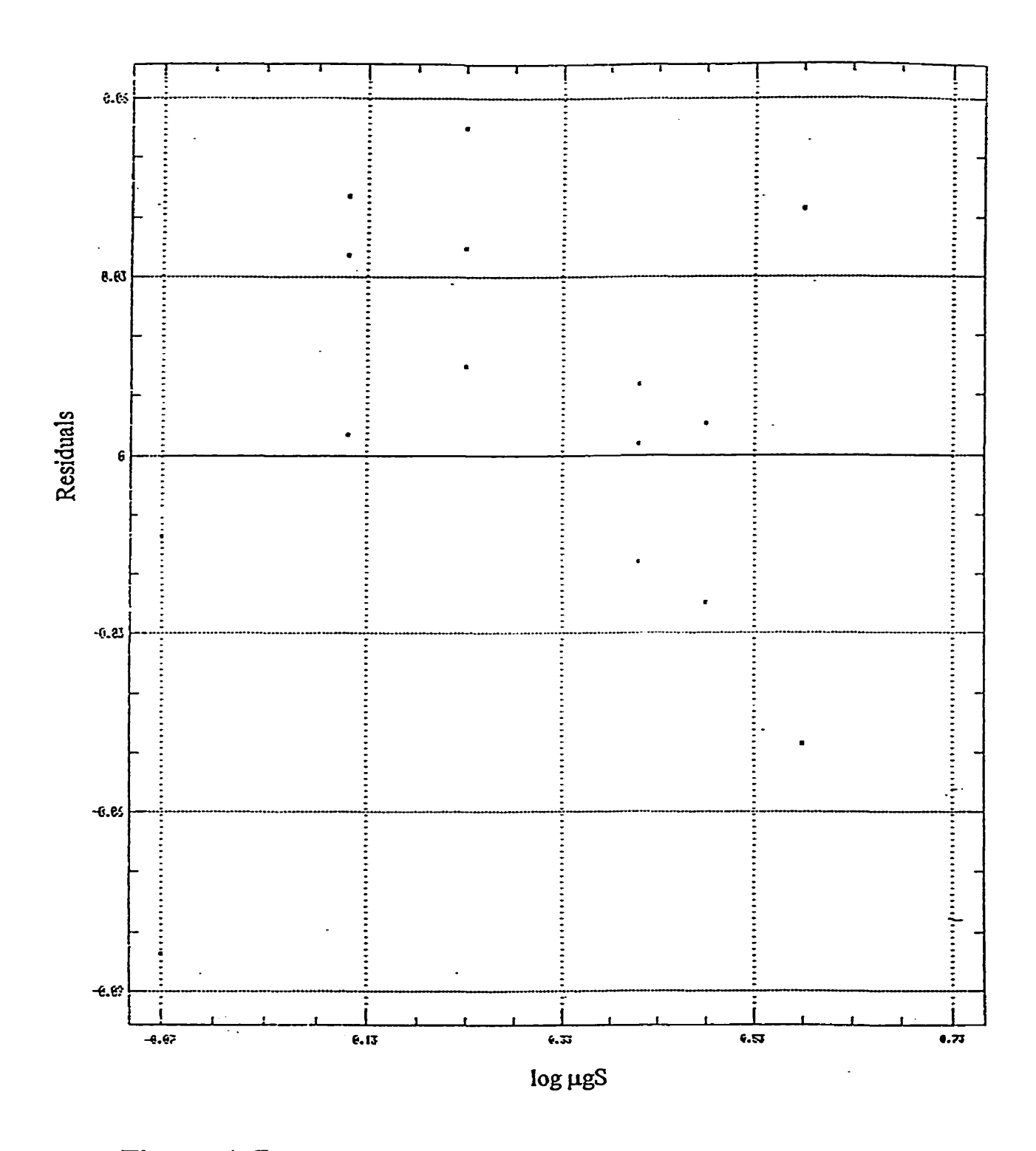


Figure A-7 Residuals for the log emission intensity versus log amounts of sulfur injected as carbon disulfide

Table A-11

Regression analysis for the log emission intensity versus log amounts of sulfur injected as ethanesulfonic acid – Linear model: y = a + bx

Dependent variable : log Emission Intensity.			Independent variable :log µgS.		
Parameter	neter Estimate Standard Error		T value	Prob. level	
Intercept	4.068	5.65X10 ⁻³	708	0.0000	
Slope	2.214	0.035	63.257	0.0000	

Analysis of Variance

Source	Sum of Squares	DF	Mean Square	F-Ratio	P-value
Model	2.534	1	2.534	2534	0.0000
Error	0.012	16	0.001		
Total (Corr.)	2.546	17		,.,,,,,,,,,,,,,,,,,,,,,,,,,,,,,,,,,,,,	

Correlation Coefficient = 0.9976

R-squared = 99.51 percent

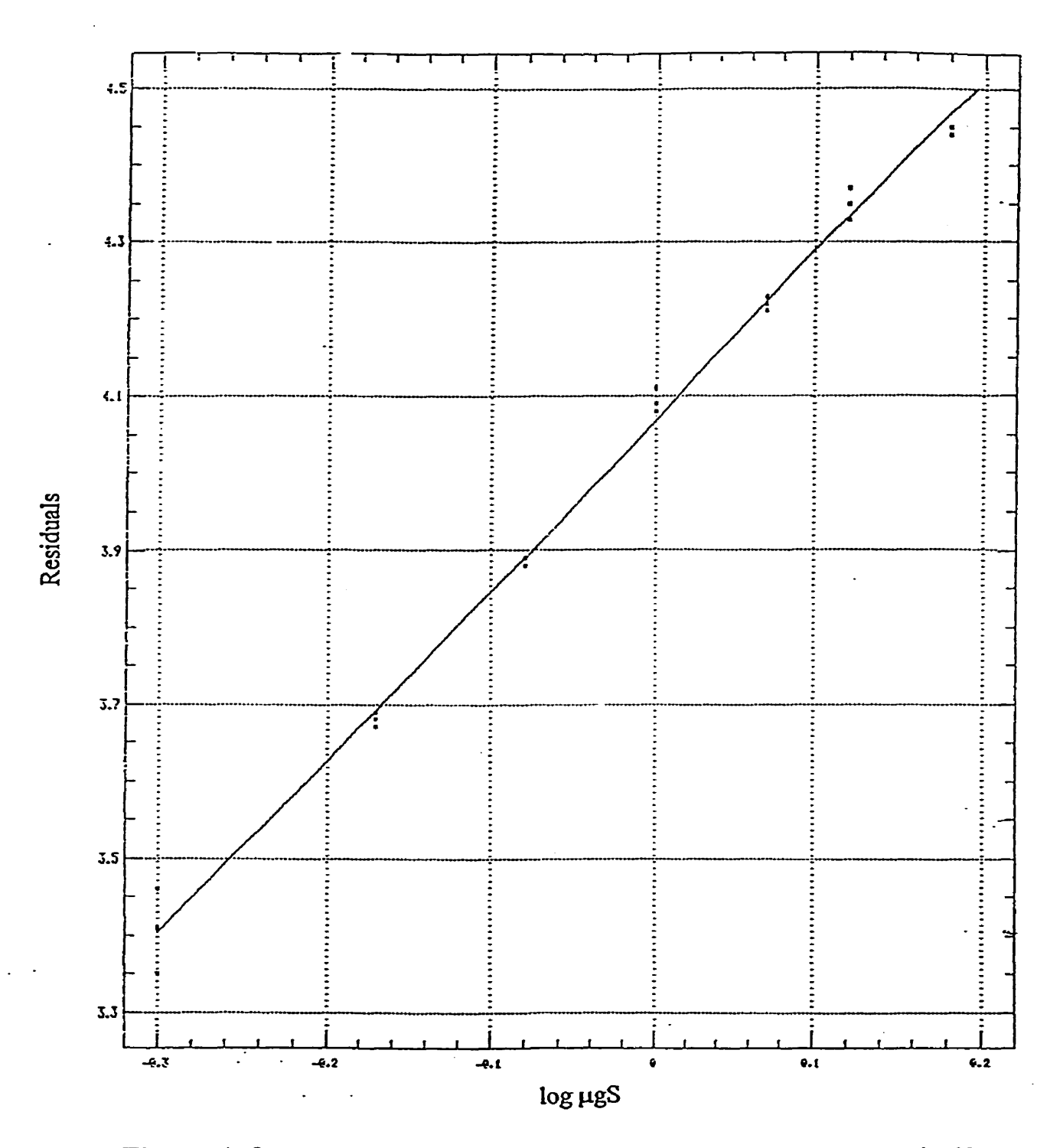


Figure A-8 Residuals for the log emission intensity versus log amounts of sulfur injected as ethanesulfonic acid

Table A-12

Regression analysis for the emission intensity versus amounts of sulfur injected as 2-methylthiophene (mobile phase doped with 20 ppm of 2-methylthiophene) – Linear model: y = a + bx

Dependent variable: Emission Intensity.			Independent variable: μgS.		
Parameter	Estimate	Standard Error	T value	Prob. level	
Intercept	-20414	971	-21	0.0000	
Slope	55359	1083	51	0.0000	

Analysis of Variance

Source	Sum of Squares	DF	Mean Square	F-Ratio	P-value
Model	3.71X10°	1	3.71X10°	$2.63X10^{3}$	0.0000
Error	1.84X10 ⁷	13	1.41X10 ⁶		
Total (Corr.)	3.73X10 ⁹	14			

Correlation Coefficient = 0.9975

R-squared = 99.50 percent

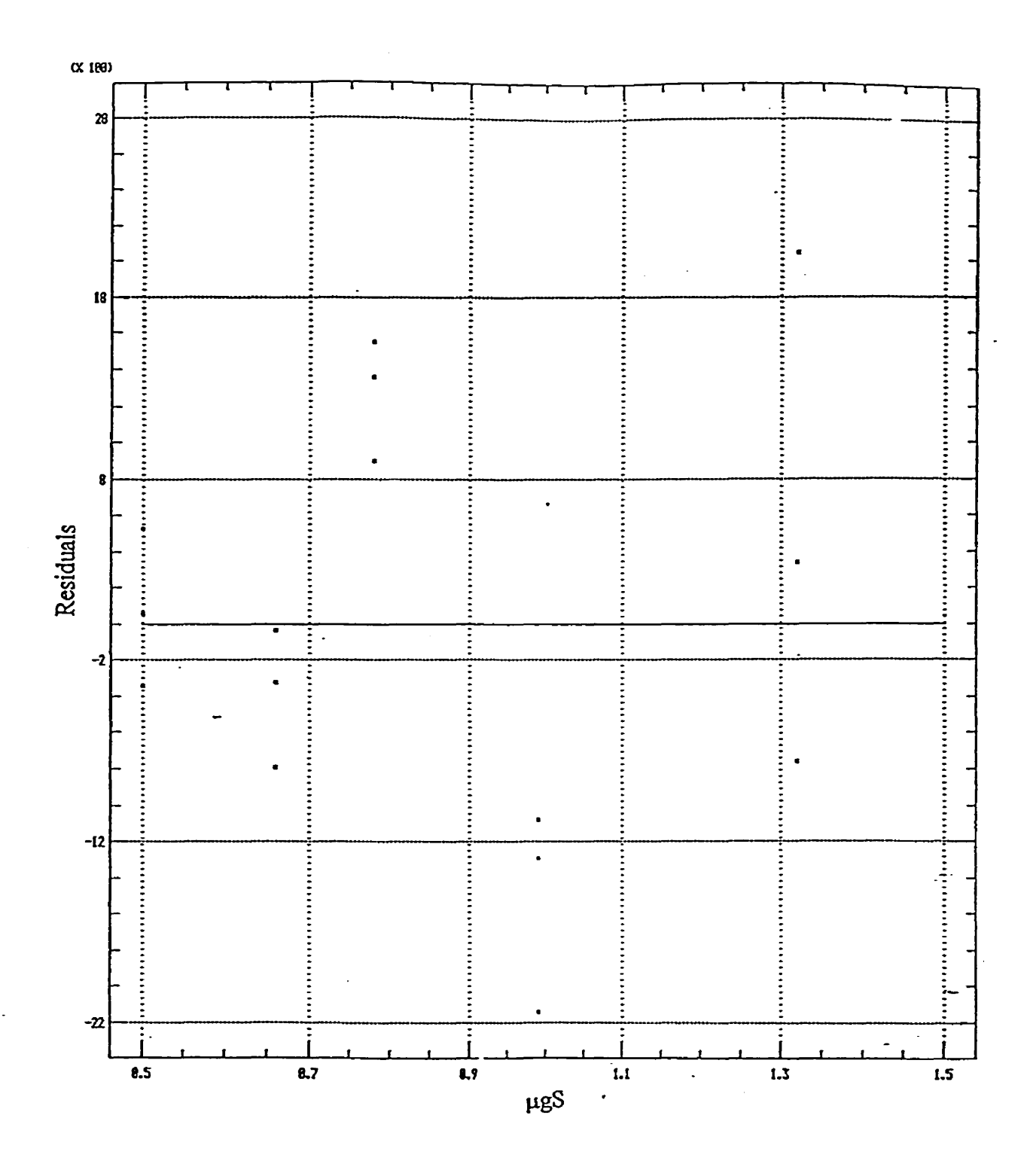


Figure A-9

Residuals for the emission intensity *versus* amounts of sulfur injected as 2-methylthiophene (mobile phase doped with 20 ppm of 2-methylthiophene)

Table A-13 Matrix of the 2² factorial design

1 1 1 1	-I -1 1 1	-1 1 -1 1
1	0	0
1	0	0
1	0	0
2	1.41421	0
2	-1.41421	0
2	0	1.41421
2	0	-1.41421
2	0	0
2	0	0
2	0	0

Table A-14

Observed and predicted results of the factorial experiment for the optimization of the hydrogen fuelled interface using pure water as eluent (Emission Intensity for sulfur).

Point	Oanal	He	Emissio	Emission Intensity	
	mL/min	mL/min	Observed	Predicted	%
1	10	130	294222	339237	-15.30
2	10	130	296013	339237	-14.60
2 3 4 5 6 7 8 9	10	130	298916	339237	-13.49
4	10	1720	213419	223570	-4.76
5	10	1720	217094	223570	-2.98
6	10	1720	223908	233570	0.15
7	15	130	357386	391146	-9.45
8	15	130	366754	391146	-6.65
	15	130	362887	391146	<i>-</i> 7.79
10	15	1720	202602	201941	0.33
11	15	1720	207037	201941	2.46
12	15	1720	222042	201941	9.06
13	13	930	289392	292684	-1.14
14	13	930	291479	292684	-0.41
15	13	930	290519	292684	-0.75
16	13	930	297462	292684	1.61
17	13	930	304072	292684	3.75
18	13	930	297227	292684	1.53
19	13	930	287903	292684	-1.66
20	13	930	286489	292684	-2.16
21	13	930	311079	292684	5.91
22	38	930	267492	260622	2.57
23	38	930	258549	260622	-0.80
24	38	930	277373	260622	6.04
25 26	8	930	259116 267655	239211 239211	7.68
26 27	8 8	930	267655	239211	10.63 12.06
		930	272017		
28	13 13	0	215176 207337	220242 220242	-2.35 -6.22
29 30		0	210178		
30	13	0 930		220242	-4 .79
31	13 13	930 930	484131	435818	9.98
32 33	13		479475	435818	9.11
		930	474584 300254	435818 292684	8.17 2.52
34 35	13	960 930	295876	292684 292684	1.08
	13				-4.78
36 37	13 13	930 930	279333 286235	292684 292684	-4.78 -2.25
37 38	13	930 930	280233 295312	292684 292684	0.89
36 39	13	930 930	293712 299753	292684 292684	2.36
40	13	930 930	299753 283944	292684 292684	-3.08
40	13	930 930	283944 287704	292684 292684	-3.08 -1.73
41	13	930 930	28770 4 284282	292684 292684	-1.73 -2.96
42	13	930	204282	272004	-2.90

^{*} D : Deviation of observed from predicted values: (obs.-pred.)/obs. X 100

Table A-15

Analysis of variance for the regression of observed on predicted values (sulfur emission for the optimization of the hydrogen fuelled interface using pure water as eluent)

Parameter	Estimate	Standard Error	T value	Prob. level
Intercept	0.961	15766.3	6.0899X10 ⁻⁵	0.99995
Slope	1.000	0.053	18.849	0.00000

Analysis of Variance

Source	Sum of Squares	DF	Mean Square	F-Ratio	P-value
Model	1.6330X10 ¹¹	1	1.6330X10 ¹¹	3.553X10 ²	0.0000
Error	1.8385X10 ¹⁰	40	4.5962X10 ⁸		
Total (corr.)	1.8168X10 ¹¹	41			

Correlation Coefficient = 0.948051 Stnd. Error of est. = 21438.9 R-squared = 89.88 percent

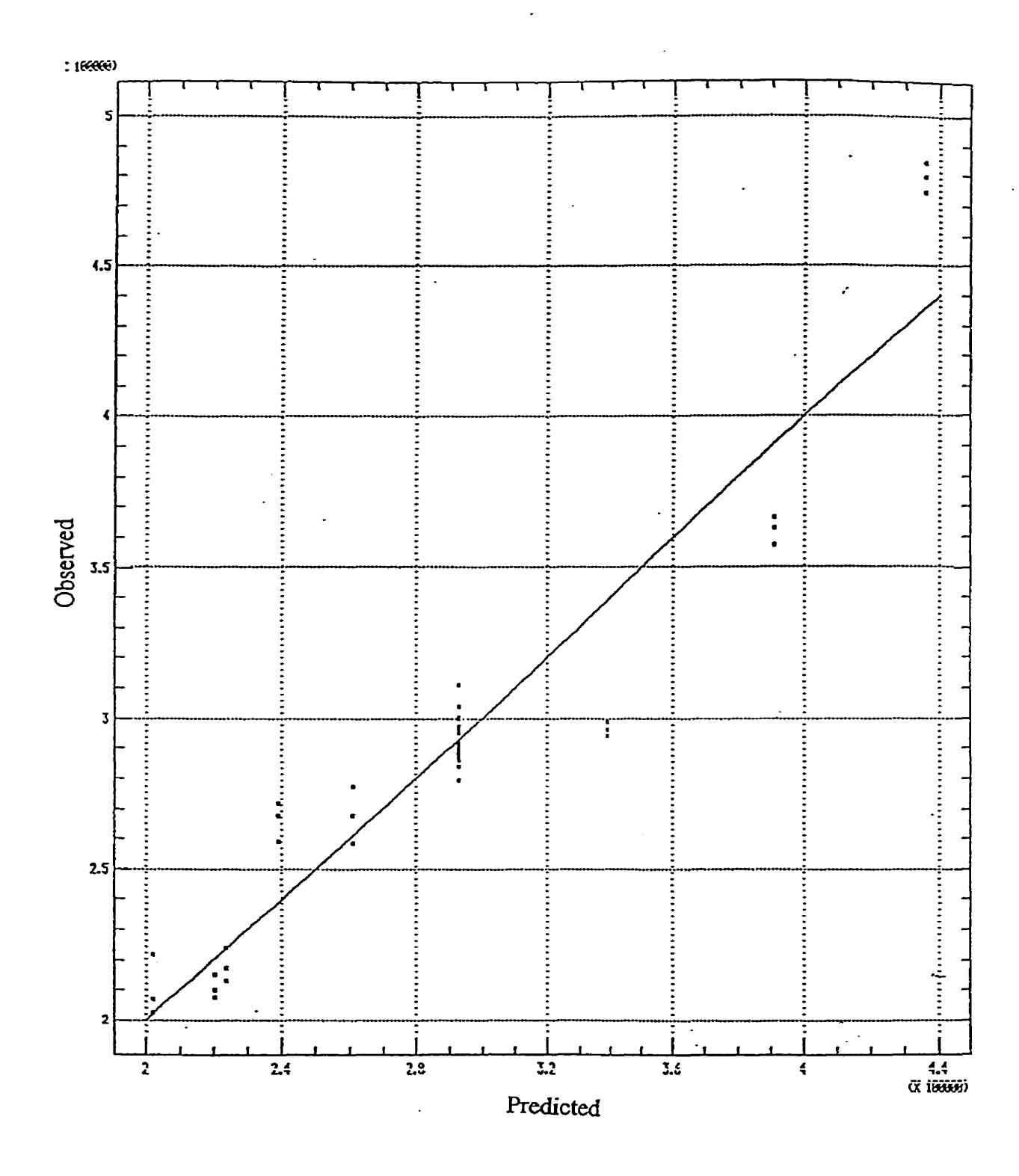


Figure A-10

Regression of observed versus predicted values (Emission intensity for sulfur using pure water as mobile phase in flow injection mode)

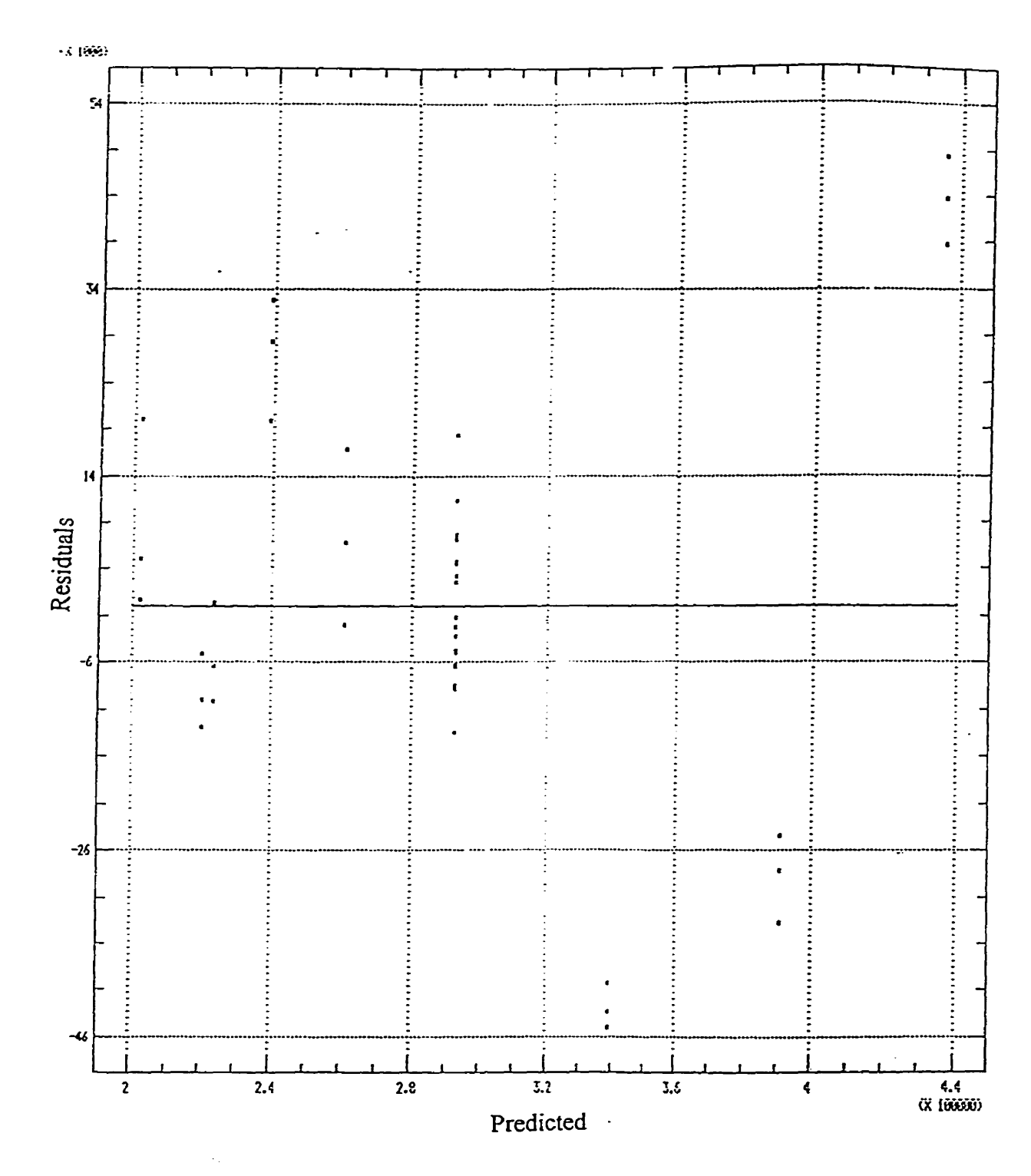


Figure A-11
Residuals of observed versus predicted values (Emission intensity for sulfur using pure water as mobile phase in flow injection mode)

Table A-16

Observed and predicted results of the factorial experiment for the optimization of the hydrogen fuelled interface using pure water as eluent (Emission Intensity for carbon)

Point	Oanal	Не	Emission	n Intensity	D*
	mL/min	mL/min	Observed	Predicted	%
1	10	130	8783	9863	12.30
2	10	130	72 98	9893	35.56
2 3 4 5 6 7 8 9	10	130	8745	9893	13.13
4	10	1720	9720	11858	22.00
5	10	1720	11577	11858	2.43
6	10	1720	9931	11858	19.40
7	15	130	30704	35474	15.54
8	15	130	29770	35474	19.16
	15	130	30602	35474	15.92
10	15	1720	31649	36243	14.52
11	15	1720	30916	36243	17.23
12	15	1720	31327	36243	15.69
13	13	930	23765	24124	1.51
14	13	930	24251	24124	-0.52
15	13	930	23494	24124	2.68
16	13	930	23645	24124	2.03
17	13	930	23747	24124	1.59
18	13	930	23548	24124	2.45
19	13	930	23954	24124	0.71
20	13	930	22635	24124	6.58
21	13	930	24336	24124	-0.87
22	38	930	48625	43149	-11.26
23	38	930	48632	43149	-11.27
24	38	930	49454	43149	-12.75
25	8	930	8874	7818	-11.90
26	8 8 8	930	8477	7818	<i>-7.77</i>
27	8	930	8531	7838	-8.36
28	13	0	25595	22218	-13.19
29	13	0	25113	22218	-11.53
30	13	0	25433	22218	-12.64
31	13	930	23071	20284	-12.08
32	13	930	24078	20284	-15.76
33	13	930	23907	20284	-15.15
34	13	960	25261	24124	-4.50
35	13	930	24752	24124	-2.54
36	13	930	24709	24124	-2.37
37	13	930	24049	24124	0.31
38	13	930	23996	24124	0.53
39	13	930	24481	24124	-1.46
40	13	930	24635	24124	-2.07
41	13	930	24521	24124	-1.62
42	13	930	24443	24124	-1.31
		750	6 ∃∃∃J	# 11#T	-1.51

^{*} Deviation of observed from predicted values: (obs.-pred.)/obs. X 100

Table A-17

Analysis of variance for the full regression of observed on predicted values (carbon emission for the optimization of the hydrogen fuelled interface using pure water as

Parameter	Estimate	Standard Error	T value	Prob. level
Intercept	-0.037	1211.9	-3.1X10 ⁻⁵	1.0000
Slope	1.000	0.047	21.276	0.0000

Analysis of Variance

Source	Sum of Squares	DF	Mean Square	F-Ratio	P-value
Model	3.82X10 ⁹	1	3.82X10 ⁹	4.44X10 ²	0.0000
Error	3.44X10 ⁸	40	8.60X10 ⁶		
Total (corr.)	4.16X10 ⁹	41		*******	

Correlation Coefficient = 0.9578

eluent)

R-squared = 91.74 percent

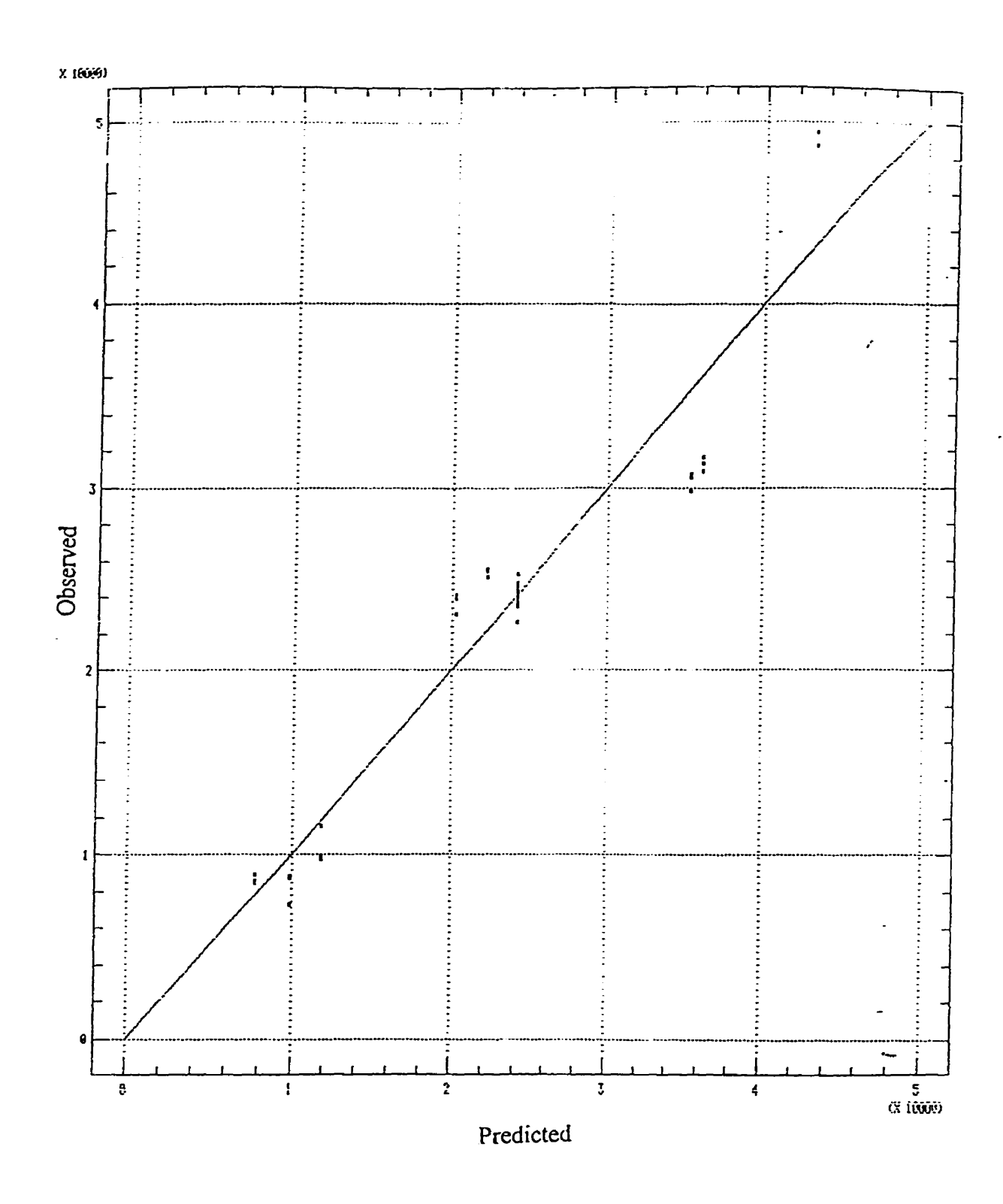


Figure A-12

Regression of observed *versus* predicted values (Emission intensity from carbon using pure water as mobile phase in flow injection mode)

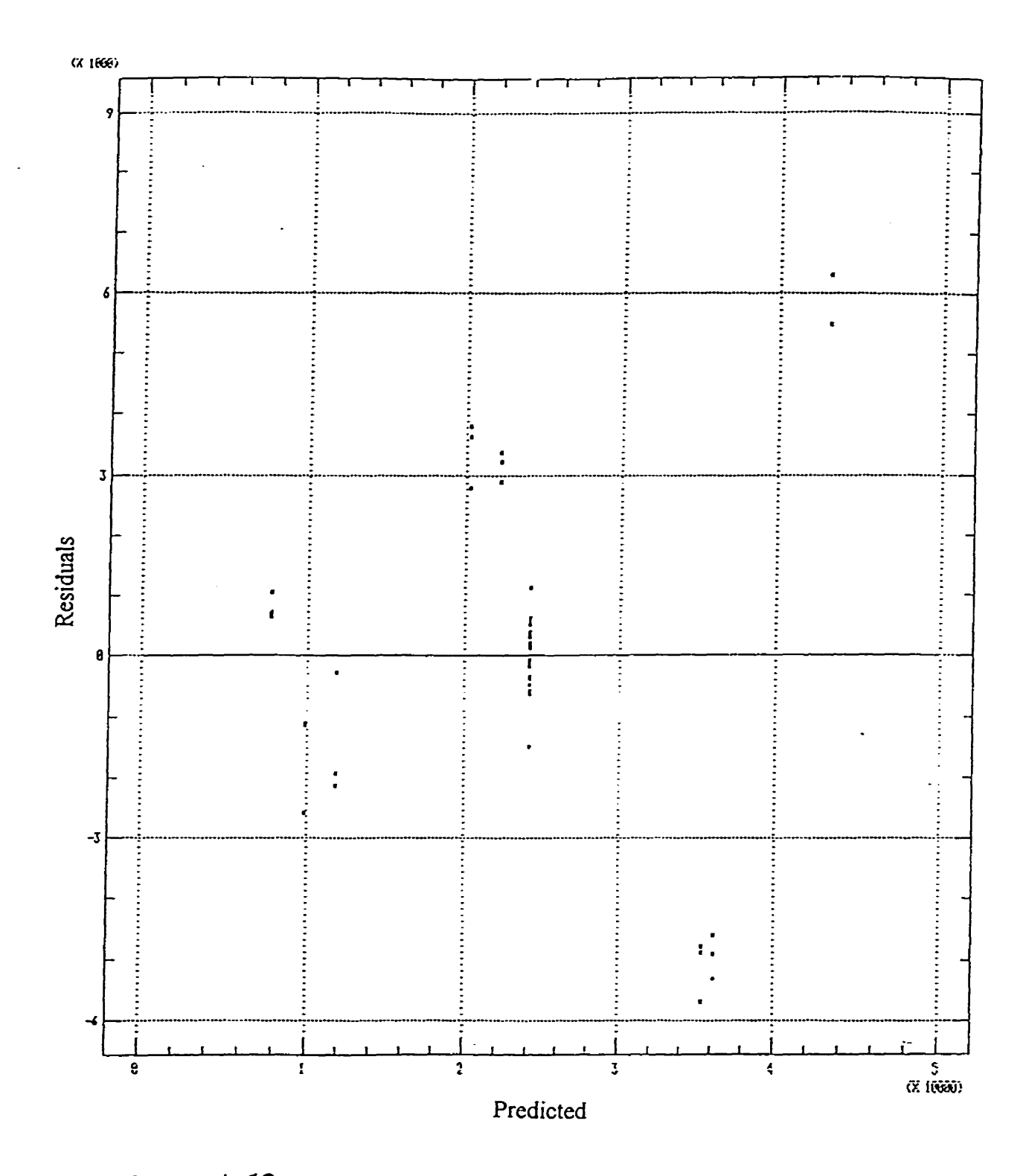


Figure A-13

Residuals of observed *versus* predicted values (Emission intensity from carbon using pure water as mobile phase in flow injection mode)

Table A-18

Observed and predicted results for the optimization of the hydrogen fuelled interface for 10mM ammonium acetate as mobile phase.

Point	Oanal	Не	Res	ponse	D*
	mL/min	mL/min	Observed	Predicted	%
1	10	750	65521	69249	5.69
1 2 3 4	10	750	65418	69249	5.86
3	10	750	64595	69249	7.21
4	10	4910	390981	385845	-1.31
5 6	10	4910	384635	385845	0.31
6	10	4910	399580	385845	-3.44
7	15	750	185117	228651	23.52
8	15	750	196079	228651	16.61
9	15	750	181182	228651	26.20
10	15	4910	466278	494503	6.05
11	15	4910	461646	494503	7.12
12	15	4910	461886	494503	7.06
13	13	2830	371902	424130	14.04
14	13	2830	363814	424130	16.58
15	13	2830	371655	424130	14.12
16	13	2830	420214	424130	0.93
17	13	2830	437085	424130	-2.96
18	13	2830	447431	424130	-5.21
19	13	2830	431854	424130	-1.79
20	13	2830	440914	424130	-3.81
21	13	2830	417899	424130	1.49
22	38	2830	430014	412673	-4.03
23	38	2830	463861	412673	-11.04
24	38	2830	475846	412673	-13.28
25	8	2830	214087	223127	4.22
26	8	2830	226563	223127	-1.52
27	8	2830	202944	223127	9.95
28	13	5800	457298	477151	4.34
29	13	5800	499967	477151	-4.56 6.10
30	13	5800	506020	477151	-6.10
31	13	0	88846	65299 65200	-26.50
32	13	0	102377 78754	65299 65200	-36.22
33	13	0		65299 424120	-17.08
34	13	2830	452328	424130 424130	-6.23
35 36	13	2830	429832 430399	424130 424130	-1.33
36 27	13	2830		424130 424130	-1.46
37 38	13 13	2830 2830	429817 450562	424130 424130	-1.32 -5.87
38 39	13	2830 2830	430302 426918	424130	-3.87 -0.65
39 40	13	2830 2830	440227	424130 424130	-0.65 -3.66
41	13	2830 2830	448174	424130	-5.36
42	13	2830	423312	424130	0.19
72	13	2030	72JJ 12	727130	0.17

^{*} D : Deviation of observed from predicted values: (obs.-pred.)/obs. X 100

Table A-19

Analysis of variance for the full regression of observed on predicted values (sulfur emission for the optimization of the hydrogen fuelled interface using 10 mM ammonium acetate as mobile phase)

Parameter	Estimate	Standard Error	T value	Prob. level	
Intercept	-37.03	12004.5	-3.1X10 ⁻³	0.9976	
Slope	1.00	0.03	33.33	0.0000	

Analysis of Variance

Source	Sum of Squares	DF	Mean Square	F-Ratio	P-value
Model	7.98X10 ¹¹	1	7.98X10 ¹¹	9.83X10 ²	0.0000
Error	3.25X10 ¹⁰	40	8.12X10 ⁸		
Total (corr.)	8.31X10 ¹¹	41			********

Correlation Coefficient = 0.9802

R-squared = 96.09 percent

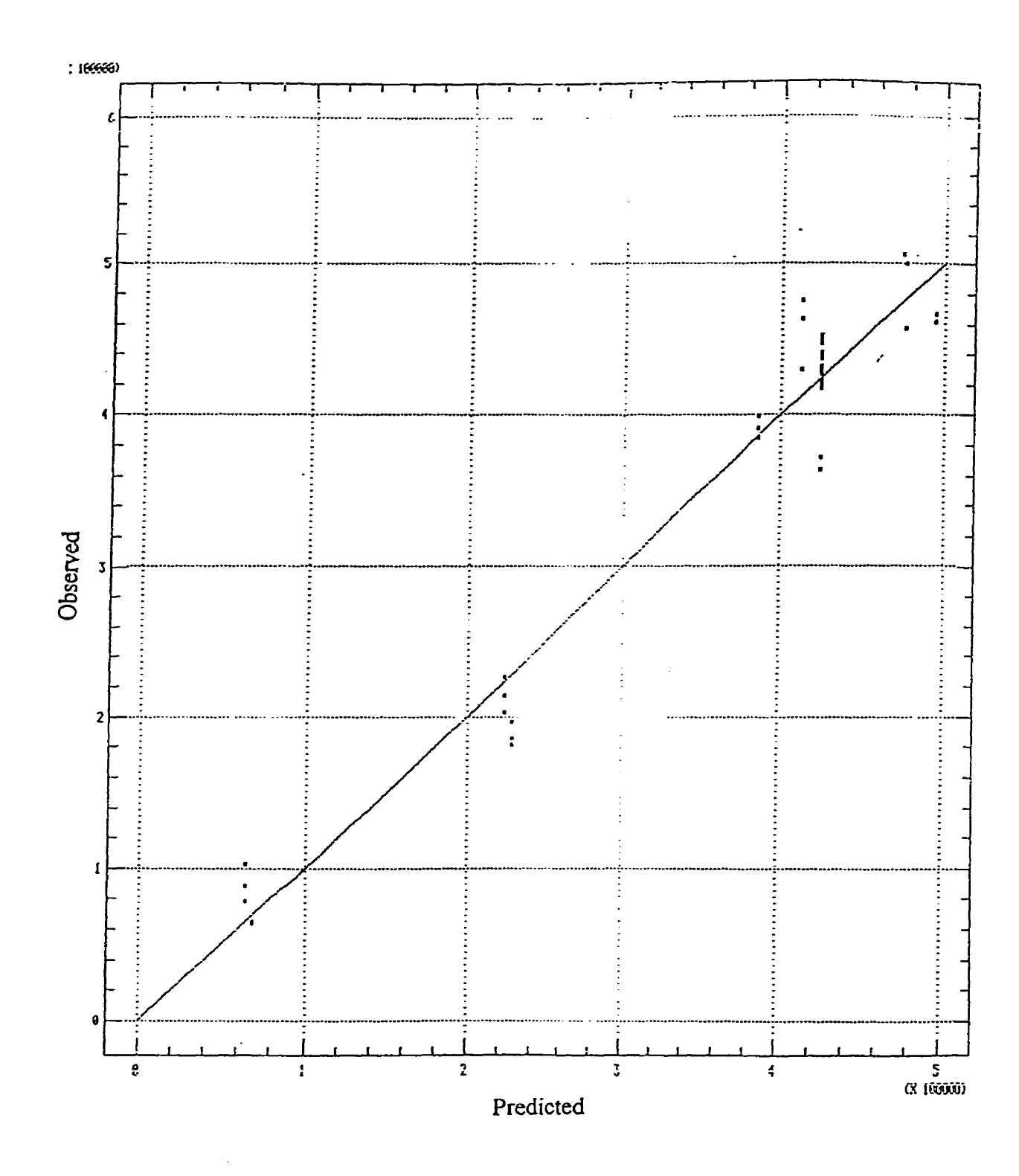
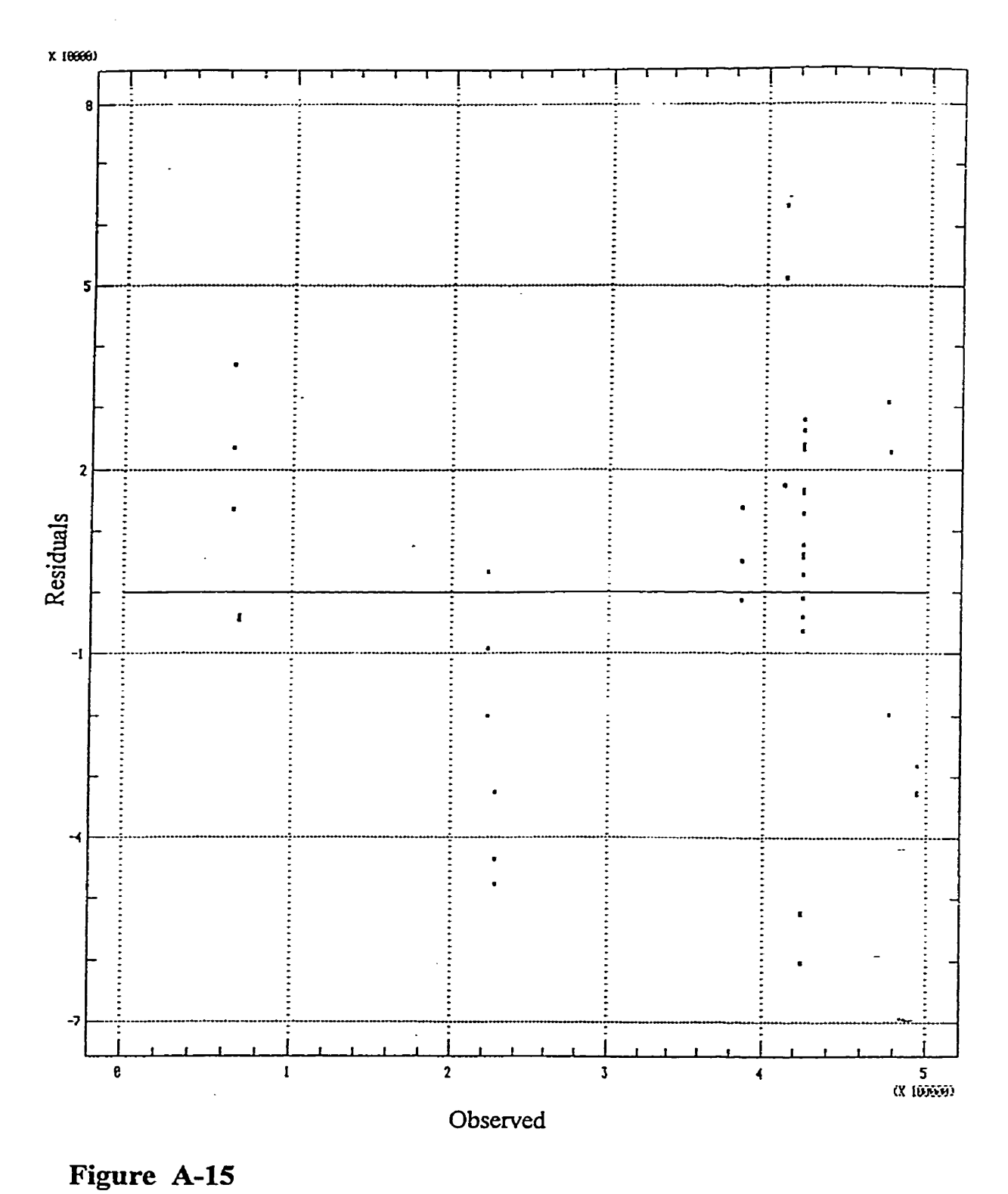


Figure A-14

Regression of observed versus predicted values (Emission intensity from sulfur dimer using 10 mM ammonium acetate as mobile phase)



Residuals of observed versus predicted values (Emission intensity from sulfur dimer using 10 mM ammonium acetate as mobile phase)

Table A-20

Observed and predicted results for the optimization of the hydrogen fuelled interface for 10mM ammonium acetate as mobile phase. (Emission from carbon).

Point	Oanal	Не	Response		D*
	mL/min	mL/min	Observed	Predicted	%
1	13	9	27014	28075	1.67
2 3 4 5 6	13	9	30270	28075	-7.25
3	13	9	29457	28075	-4.49
4	13	51	14875	18117	21.79
5	13	51	16400	18117	10.47
6	13	51	17291	18117	4.78
7	22	9	88302	102927	16.56
8 9	22	9	91003	102927	13.10
10	22	9	84252	102927	22.17
11	22 22	51 51	36611 42704	58247 58247	59.10 36.40
12	22	51	41301	58247 58247	41.03
13	20	30	55405	54248	-2.09
14	20	30	56381	54248	-2.0 9 -3.78
15	20	30	53342	54248	1.70
16	20	30	52133	54248	4.06
17	20	30	54296	54248	-0.09
18	20	30	52738	54248	2.86
19	20	30	54410	54248	-0.30
20	20	30	53970	54248	0.52
21	20	30	54128	54248	0.22
22	30	30	124458	102376	-17.74
23	30	30	122405	102376	-16.36
24	30	30	119952	102376	-14.65
25	10	30	18741	21070	12.43
26	10	30	19840	21070	6.20
27	10	30	15950	21070	32.10
28	20	60	32363	22642	-30.04
29	20	60	35001	22642	-35.31
30	20	60	32363	22642	-30.04
31	20	0	68483	61278	-10.52
32	20	0	69644	61278	-12.01
33	20	0	64917	61278	-5.61
34	20	30	55914	54248	-2.98
35	20	30	53539	54248	1.32
36	20	30	54282	54248	-0.06
37	20	30	54910	54248	-1.21
38	20	30	55010	54248	-1.39
39	20	30	53762	54248	0.90
40	20	30	53147	54248	2.07
41 42	20 20	30	54165 54032	54248 54248	0.15 -1.25
44	20	30	54932	34240	-1.23

^{*} D : Deviation of observed from predicted values: (obs.-pred.)/obs. X 100

Table A-21

Analysis of variance for the regression of observed on predicted values (Emission from carbon for the optimization of the hydrogen fuelled interface using 10 mM ammonium acetate as mobile phase)

Parameter	Estimate	Standard Error	T value	Prob. level	
Intercept	-0.12	3342.47	-3.53X10 ⁻⁵	1.0000	
Slope	1	0.06	16	0.0000	

Analysis of Variance

Source	Sum of Squares	DF	Mean Square	F-Ratio	P-value
Model	2.64X10 ¹⁰	1	2.64X10 ¹⁰	3.066X10 ²	0.0000
Error	3.45X10 ⁹	40	8.75X10 ⁷		
Total (corr.)	2.89X10 ¹⁰	41			

Correlation Coefficient = 0.9405

R-squared = 88.46 percent

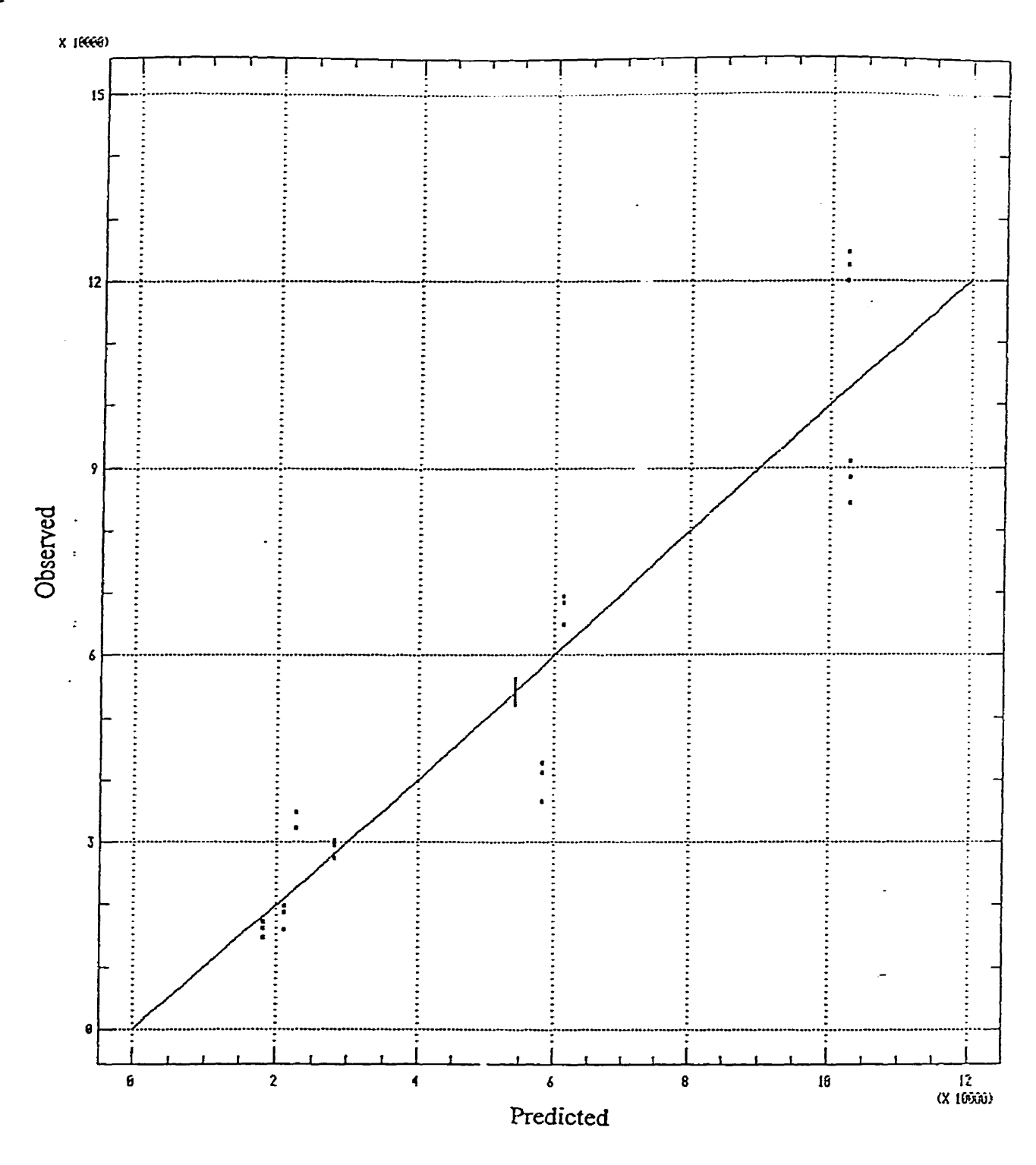


Figure A-16

Regression of observed *versus* predicted values (Emission intensity from carbon using 10 mM ammonium acetate as mobile phase)

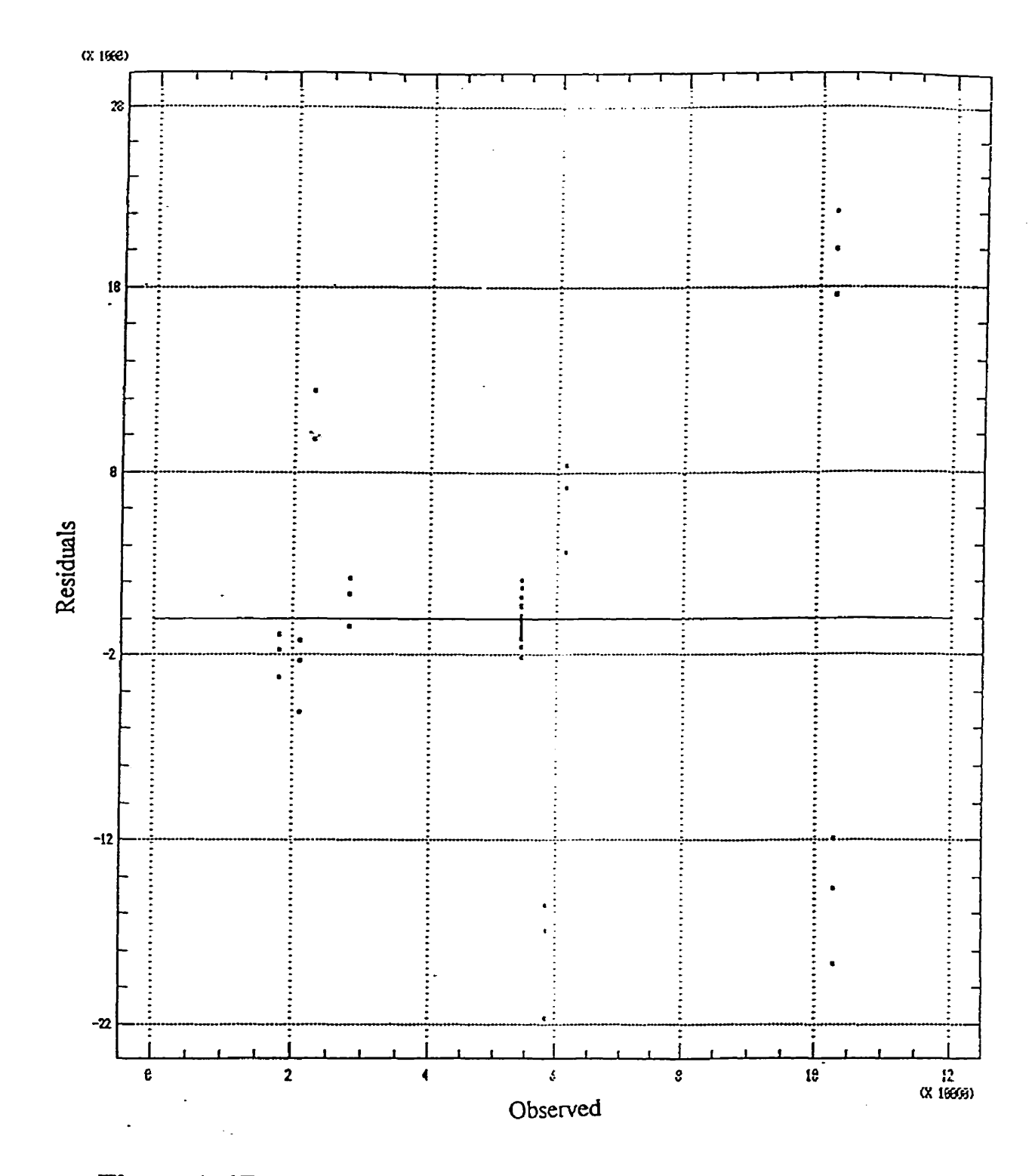


Figure A-17

Residuals of observed *versus* predicted values (Emission intensity from carbon using 10 mM ammonium acetate as mobile phase)

CHAPTER VI

REFERENCES

- Aldous, K.M.; Dagnall, R.M.; and West, T.S. 1970. The Flame-spectroscopic Determination of Sulfur and Phosphorus in Organic and Aqueous Matrices by Using a Simple Filter Photometer. Analyst. 95: 417-424.
- Allaway, W.H. and Thompson, J.F. 1966. Sulfur in the Nutrition of Plants and Animals. Soil Sciences. 101: 240-247.
- Alvarez, J.G., Storey, B.T.1983. Taurine, Hypotaurine and Albumin Lipid Peroxidation in Rabbit Spermatozoa and Protect Against Loss of Mobility. Biol. Reprod. 29: 548-555.
- Anderson, M.E. 1985. Determination of Glutathione and Glutathione disulfide in Biological Samples. Methods in Enzymologies. 113: 548-553.
- Ariyoshi, T. Shiiba, S., Hasegawa, H., and Arizono, K. 1990. Profile of Metal-binding Proteins and Heme Oxygenase in Red Carp Treated with Heavy Metals, Pesticides and Surfactants. Bull. Environ. Contam. Toxicol. 44: 643-649.
- Asaoka, K and Takahashi, K. 1981. An enzymatic assay of reduced glutathione using S-aryltransferase with O-dinitrobenzene as a substrate. J. Biochem. 90: 1237-1242.
- ASTM D 5623-94: Sulfur Compounds in Light Petroleum Liquids by Gas Chromatography and Sulfur Selective Detection. *Annual Book of Standards*, Vol. 5. ASTM. West Conshohoken, PA, 1994, pp 791-95.
- Bayer, T.; Breu, W.; Seligmann, O.; Wray, V.; Wager, H. 1989. Biologically Active Thiosulfinates and α-Sulphinyl-disulfides from Allium Cepa. Phytochemistry. 28: 2373-2377.
- Beaton, J.D., Leitch, R.H., Macallister, and Nyborg, M. Preprint Can. Sulfur Symposium., Calgary, May 1974. "The projected Need for Sulfur Fertilizers in Westhern Canada. Their Integration in Soil Fertility Programs".
- Bebiano, M.J., and Langston, W.J. 1989. Quantification of metallothioneins in marine Invertebrates using differential pulse polarography. Port Electrochemical Acta. 7: 59-64.
- Belcher, R., Bogdanski, S.L., and Townshend, A. 1973. Molecular Emission Cavity Analysis.-A New Flame Analytical Technique. Part I. Description of the Technique and the Development of a Method for the Determination of Sulfur. Anal. Chim. Acta. 67: 1-16.
- Belcher, R., Bogdanski, S.L., Ghonaim, S.A., and Townshend, A. 1974. MECA Spectroscopy. A New Flame Analytical Technique .Anal. Lett. 7:133-146.
- Belcher, R., Bogdanski, S.L., Knowles, D.J., and Townshend, A. 1975. Molecular Emission Cavity Analysis A New Flame Analytical Technique. Part VI. The

- Simultaneous Determination of Sulphate and Sulphite or Thiosulphate ions. Anal. Chim. Acta. 79: 292-295.
- Benner, R.L., and Stedman, D.H. 1990. Field Evaluation of the Sulfur Chemiluminescence Detector. Environ. Sci. Technol. 24: 1592-1596.
- Bernt, E. and Bergmeyer, H.U. 1974. Glutathione, in Methods of Enzymatic Analysis. vol.4, 2nd ed., Bergmeyer, H.U.Ed., Academic Press, New York, pp 1643-1647.
- Beutler, E. and West, C. 1977. Comment concerning a fluorometric assay for glutathione. Anal. Biochem. 81: 458-460.
- Bixby, D.W., and Beaton, J.D. Sulfur Institute Tech. Bull. 1970, 17.
- Blais, J.S., Momplaisir, G.M., and Marshall, W.D. 1990. Determination of arsenobetaine, arsenocholine, and tetramethylarsonium cations by High-Performance Liquid Chromatography-Thermochemical Hydride Generation-Atomic Absorption Spectrometry. Anal. Chem. 62:1161-1166.
- Blais, J.S., Hughues-Despointes, A., Momplaisir, G.M., and Marshall, W.D. 1991. An HPLC-AAS interface for the determination of selenonium choline and trimethyl-selenium cation-application to human urine. J. Anal. Atom. Spectrom. 6: 225-232.
- Block, E. 1992. The Organosulfur Chemistry of the Genus Allium. Implications for Organic Sulfur Chemistry. Angew. Chem., Int. Ed. Engl. 31: 1135-1178.
- Block, E., Iyer, R., Grisoni, S., Saha, C., Belman, S., Lossing, F.P. 1988. Lipoxygenase Inhibitors from the Essential Oil of Garlic. Markovnikov Addition of the Allyldithio Radical to Olefins. J. Am. Soc. 110: 7813-7827.
- Block, E., Negenathan, S., Putman, D., and Zhao, S.H. 1992. Allium Chemistry: HPLC Analysis of Thiosulfinates from Onion, Garlic, Wild Garlic (Ramsoms), Leek, Scallion, Shallot, Elephant (Great-Headed) Garlic, Chive, and Chinese Chive. Uniquely High Allyl to Methyl Ratios in Some Garlic Samples. J. Agr. Food Chemistry. 40. 2418-2430.
- Bloomfield, C. 1967. Effect of Some Phosphate Fertilizers On The Oxidation of Elemental Sulfur in Soil. Soil Sciences. 103: 219-223.
- Bogdanski, S.L., Calokerinos, A.C., and Townshend, A. 1982. Spectral Studies in Molecular Emission Cavity Analysis. Canadian Journal of Spectroscopy. 27: 10-16.
- Boulanger, Y., Armitage, I.M., Miklossy, K,-A and Winge, D.R. 1982. ¹¹³Cd NMR Study of a Metallothionein Fragment. Evidence for a two domain structure. J. Biol. Chem. 257: 13717-13719.

- Brewster, H. D. and Robinowitch, H. D. Eds., Onions and Allied Crops, Vol. 1-3, CRC Press, Boca Raton, Fl., 1990.
- Brodnitz, M. H; Pascale, J.V.; Van Derslice, L. 1971. Flavor Components of Garlic Extracts J. Agric. Food Chem., 19: 273-275.
- Brody, S.S. and Chaney, J.E. 1966. Flame Photometric Detector. The application of a specific detector for phosphorus and sulfur compounds-sensitive to subnanogram quantities. J. Gas Chromatogr. 4: 42-46.
- Brotter, P., Negretti V.E., Rosick, V., Jaff, W.G., Mendez, H., and Tov, G. 1984. Anal. Chem., Biol., 3, 29
- Buiatti, E., Blot, W. 1989. A case-control study of Gastric cancer and diet in Italy. Int. J. Cancer . 44. 611-616.
- Burnett, C.H., Adams, D.F., and Farwell, S.O. 1977. Potential error in linearization FPD responses for sulfur. J. Chromatogr. Sci. 15: 230-232.
- Calvey, E.M., White, K.D., Matusik, J.E. Sha, D., and Block, E. 1998. Allium Chemistry: Identification of Organosulfur Compounds in Ramp (Allium tricoccum) Homogenates. Phytochemistry. 49: 359-364.
- Carvalho, F.D., Remiao, F., Vale, P., Timbrell, J.A., Bastos, M.L., Ferreira, M.A. 1994. Glutathione and Cysteine Measurement in Biological Samples by HPLC With a Glassy Carbon Working Detector. 8: 134-136.
- Cavallito, C.J. and Bailey, J.H. 1944. Allicin, The Antibacterial Principle of *Allium sativum*. I. Isolation, Physical Properties and Antibacterial Action. J. Am. Chem. Soc. 66: 1950-1951.
- Cavallito, C.J., Buck, J.S., and Suter, 1944. Allicin, The Antibacterial Principle of Allium sativum. II. Determination of the Chemical Structure. J. Am. Chem. Soc. 66: 1952-1954.
- Carson, J.F., Wong, F.F. 1959. A colour reaction for thiosulfinates. Nature. 183: 1673.
- Cherian, M.G. 1988. An evaluation of methods of estimation of metallothioneins. In: Environmental Toxin Series, Vol.2. Cadmium. M. Stoeppler and M. Piscator (Eds). Springer-Verlag, Berlin. pp 227-235.
- Chester, T.L. 1980. Dual Flame Photometric Phosphorus-Selective Detector for High Performance Liquid Chromatography. Anal. Chem. 52: 1621-1624.
- Cohn, V.H. and Lyle, J. 1966. A fluometric assay for glutathione. Anal. Biochem. 14: 434-440.

- Conchillo, A., Camps, A.F., and Messeguer, A. 1990. Versality of reversed phase chromatographic techniques on the separation and purification of complex glutathione conjugates mixtures from synthetic origin. J. Liquid Chromtogr. 13: 569-581.
- Corbrigde, D. Phosphorus. An Outline of its Chemistry, Biochemistry and Technology. Second edition, edited by Elsevier Scientific Company, Netherlands, 1980.
- Cousins, R.J. 1985. Absorption, transport, and hepatic metabolism of copper and zinc: Special reference to metallothionein and ceruloplasmin. Physiol. Rev. 65: 238-309.
- Crider, W.L., and Slater, R.W. Jr. 1969. Flame-Luminescent Intensification and Quenching Detector (FLIQD) in Gas Chromatography. Anal. Chem. 41: 531-533.
- Dagnall, R.M. Tompson, K.C., and West, T.S. 1967. Molecular-emission Spectroscopy in Cool Flame. Part I. The Behaviour of Sulfur Species in a Hydrogen-Nitrogen Diffusion Flame and in a Shield Air-Hydrogen. Analyst. 92: 506-512.
- Dagnall, R.M., Smith, DJ Thompson, K.C., and West, T.S. 1969. Emission Spectra Obtained from Combustion of Organic Compounds in Hydrogen Flames. Analyst. 94: 871-878.
- Dalinger, R., Berger, B., and Bauer-Hilty. 1989. Purification of cadmium-binding proteins from related species of terrestrial helicidae (gastropoda, molusca): A comparative study. A. Mol. Cell. Biochem. 85: 135-145.
- Dasenbrock, C.O. and Lacourse, W.R. 1998. Assay for Cephapirin and Ampicillin in Raw Milk by High-Performance Liquid Chromatophy-Integrated Pulsed Amperometric Detection. Anal. Chem. 70: 2415-2420.
- Dasenbrock, C.O. and Lacourse, W.R. 1998. Measuring traces of antibiotics in milk. CHEMTECH (1). 26-32.
- **Dedina, J.** 1992. Quartz tube atomizers for hydride generation atomic absorption spectrometry: mechanism of selenium hydride atomizer and fate of free atoms. Spectrochim. Acta, Part B., 47: 689-700.
- Demarcay, H. 1838. Ueber die Natur der Galle. Ann. Pharm. 27: 270 291.
- Denis, W., and Reed, L. 1927. The Action of Blood on Sulfides. J. Biol. Chem. 72: 385-394.
- Dent, C.E. 1948. A study of the behaviour of some sixty amino acids and other ninhydrin-reacting substances on phenol-"collidine" filter paper chromatograms. Biochem. J. 43: 169-180.

- Dieter, H.H., Muller, L., Abel, J., and Summer, K.H. 1987. Metallothionein Determination in biological materials: inter-laboratory comparison of 5 current methods. Exp. Suppl. 52: 351-358.
- Dressler, M. J. 1983. Hydrocarbon and Water Quenching of the Flame Photometric Detector response. J. of Chromatogr. 270: 145-150.
- Dressler, M. J. 1986. Selective Gas Chromatographic Detectors. Elsevier, Amsterdam, 1986, Chapters 7-9.
- Dziewiatkowski, D., "in Mineral Metabolism, An Advanced Treatise", Vol. 2, CL Comar and F. Bronner, Eds., Part B, The elements, Academic Press, New York, 1962. "Sulfur".
- Eaton, D.L. and Toal, B.F. 1982. Evaluation of Cd/hemoglobin affinity assay for rapid determination of metallothionein in biological tissues. Toxicol. Appl. Pharmacol. 66: 134-142.
- Eaton, D.L. 1985. Effects of various trace metals on the binding of cadmium to rat hepatic metallothionein determined by the Cd/hemoglobin affinity assay. Toxicol. Appl. Pharmacol. 78: 158-162.
- Ebdon, L., Hill, S., and Ward, R.W. 1986. Direct Coupled Chromatography-Atomic Spectroscopy. Part 1. Directly coupled Gas Chromatography-Atomic Spectroscopy. A Review. Analyst. 111: 1113-1138.
- Ebdon, L., Hill, S., and Ward, R.W. 1987. Direct Coupled Chromatography-Atomic Spectroscopy. Part 2. Directly coupled Liquid Chromatography-Atomic Spectroscopy. A Review. Analyst. 112: 1-16.
- Ellman, G.L. 1959. Tissue sulfhydryl groups. Arch. Biochem. Biophys. 82: 70-77.
- Ericson, L.-E. and Carlson, B. 1954. Studies on the occurrence of amino acids, niacin, and pantothenic acid in marine algae. Ark. Kemi. 6: 51-522.
- Ettre, L.S. 1978. Selective Detection in Column Chromatography. J. Chromatogr. Sci. 16: 396-417.
- Evans, P.D. 1974. Amino acid distribution in the nervous system of the crab, Carcinus maenas L J. Neurochem. 21: 11-17.
- Farwell, S.O., Gage, D.R., and Kagel, R.A. 1981. Current status of prominent selective gas chromatographic detector: A critical assessment. J.Chromatogr. Sci.19: 358-376.

- Farwell, S.O., and Barinaga, C. J. 1986. Sulfur-Selective Detection with the FPD: Current Enigmas, Practical usage, and Future Directions. J. Chromatogr. Sci. 24: 483-494.
- Fay, L.B. Métairon, S., Montigon, F., and Ballèvre, O. 1998. Evaluation of Taurine Metabolism in Cats by Dual Stable Isotope Analysis. Anal. Biochem. 260: 85-91.
- Fowler, J.C. and Vaidya, M.W. 1931. The spectrum of the flame of carbon disulfide. Proc. Roy. Soc. (London), Ser. A. A132: 310-330.
- Fowler, B.A., Hildelbrand, C.E., Kojima, Y., and Webb, M. 1987. Nomenclature of metallothionein. In Metallothionein II, J. HR Kägi and Y. Kojima, eds. Birkhauser-Verlag, Basel, pp. 19-22.
- Franconi, F., Stendardi, I., Failli, P, Matucci, R., Baccardo, C., Montorsi, L., Bandinelli, R., and Giotti, A. 1985. The protective effects of taurine on hypoxia (performed in the absence of glucose) and on reoxygenation (in the presence of glucose) in guinea-pig heart. Biochem. Pharmacol. 34: 2611-2616.
- Fredriksson, S.A. and Cedergren, A. 1981. Effect of Carrier Gas Flow Geometry on the response of Sulfur Flame Photometric Detector for Gas Chromatography. Anal. Chem. 53: 614-618.
- Frontali, N. Brain glutamic acid decarboxylase and synthesis of GABA in vertebrate and invertebrate species. In: Comparative Neurochemistry, edited by D. Richter. Oxford. UK: Pergamon, 1964, p. 185-192.
- Fujiwara, M., Yoshimura, M., Tsono, S. 1955. "Allithiamine", A Newly found Derivative of Vitamin B1. III. On The Allicin Homologues in the Plants the Allium Species. J. Biochem (Tokyo). 42: 591-601.
- Futani, S., Ubuka, T., and Abe, T. 1994. High-performance liquid chromatographic determination of hypotaurine and taurine after conversion to 4-dimethylaminoazobenzene-4'-sulfonyl derivatives and its application to the urine of cysteine-administered rats. J. Chromatography B. 660: 164-169.
- Glyn, J. R. and Lipton J.M. 1981. Effects of central administration of alanine on body temperature of the rabbit: comparisons with the effects of serine, glycine and taurine. Brain Res. Bull. 6: 467-472.
- Goodman, H.O., and Shihabi, Z.K. 1987. Automated and Synthesis of a Naturally Occurring Selenucleoside in Bacteria tRnas: 5[(Methylamino)methyl]-2-Selenoudine. Clin. Chem. 33: 835-837.
- Gotti, R., Andrisana, V., Gatti, R., Cavrini, V., and Candeletti, S. 1994.

 Determination of Glutathione in Biological Samples by High-Performance-Liquid Chromatography With Fluorescence Detection. 8: 306-308.

- Guftafson, J.M., Dodds, S.J., Burgrd, R.C., and Mercer, L.P. 1986. Prediction of brain and serum free amino acid profiles in rats fed graded levels of protein. J. Nutr. 116: 1667-1681.
- Han, J., Lawson, L., Han, G., and Han, P. 1995. A Spectrophotometric Method for Quantitative Determination of Allicin and Total Garlic Thiosulfinates. Anal. Biochem. 225: 157-160.
- Hayes, K.C., Carey, R.E., and Schmidt, S.Y. 1975. Retinal degeneration associated with taurine deficiency in the cat. Science. 188: 949-951.
- Hayes, K.C., 1985. Taurine requirements in primates. Nutr. Rev. 43: 65-71.
- Hayes, K.C., Pronczuk, A., Addesa, A. E., and Stephan Z.F. 1989. Taurine modulates platelet aggregation in cats and human. Am. J. Clin. Nutr. 49: 1211-1216.
- High, K.A., Azani, R., Fazekas, A. F, Chee, Z.A., and Blais, J.S. 1992. Thermochemical-Microatomizer Interface for the Determination of Trace Cadmium and Cadmium Metallothioneins in Biological Samples with Flow Injection-and High-Performance Liquid Chromatography-Atomic Absorption Spectrometry. Anal. Chem. 64: 3197-3201.
- Hills, A.J., Lenschow, D.H., and Birks, J.W. 1998. Dimethyl Sulfide Measurement by Fluorine-Induced Chemiluminescence. Anal. Chem. 70: 1735-1742.
- Hissin, P.J. and Hilf, R. 1976. A fluorometric method for determination of oxidized and reduced glutathione in tissues. Anal. Biochem. 74: 214-226.
- Huxtable, R.J. Metabolism and function of taurine in the heart. In: *Taurine*, edited by R.J. Huxtable and A. Barbeau. New York: Raven, 1976, p 99-119.
- Huxtable, R.J. 1982. Taurine: epilepsy, inotropy and eyesight. Trends Pharmacol. Sci. 3: 21-25.
- Huxtable, R.J. Taurine and the oxidation metabolism of cysteine. In: Biochemistry of Sulfur, edited by R.J. Huxtable. New York: Plenum, 1986, p.1-10.
- Huxtable, R.J. 1992. Physiological Actions of Taurine. Physiological reviews. 7: 101-163.
- Iberl, B., Winkler, G., and Knobloch. 1990. Products of Allicin Transformation: Ajoenes and Dithiins, Characterization and their Determination by HPLC. Planta Medica. 56: 202-211.

- Iwata, K., Kakuta, I., Ikeda, M., Kimoto, S., and Wada, N. 1981. Nitrogen metabolism in the mudskipper, Periophthalmus cantonensis: a role of free amino acids in detoxication of ammonia produced during its terrestrial life. Comp. Biochem. Physiol. A Comp. Physiol. 68: 589-596.
- Jacobsen, J.G. and Smith, L.H. Jr., 1968. Biochemistry and physiology of taurine and derivatives. Physiol. Rev. 48: 424-511.
- Jäger, H. Quantitative Bestimmung von Allicin in frischem Knoblauch. 1955. Arch. Pharm. 288: 145-148.
- Jansen, H., Muller, B., and Knobloch, K. 1987. Allicin Characterization and its Determination by HPLC. Planta Medica. 53: 559-562.
- Johansen, R.L. and Birks, J.W. 1991. Am. Lab. 23: 112-119.
- Johnson, D.W., Saba, C.S., Wolf, J.D., and Wright, R.L. 1997. Time-Resolved Molecular Emission Spectroscopy: an Analytical Technique for Solid Materials. Anal. Chem. 69: 532-535.
- Jones, D.P., Carlson, J.L., Samiec, P.S., Sternberg, P.J., Mody, J.V.C., Reed, R.L., and Brown, L.A.S. 1998. Glutathione Measurement in Human Plasma: Evaluation of Sample Collection, Storage and Derivatization Conditions for Analysis of Dansyl Derivatives by HPLC. Clinica Chemica Acta. 275: 175-184.
- Julin, B.C., Vandenborn, H.W., and Kirkland J.J. 1975. Selective Flame Emission Detection of Phosphorus and Sulfur In High-Performance Liquid Chromatography. J.Chromatogr. 112: 443-453.
- Kägi, J.H.R. and Kojima, Y. 1987. Chemistry and biochemistry of metallothionein. Experentia. Suppl. 52: 25-61.
- Kataoka, H., and Ohnishi, N. 1986. Occurrence of taurine in plants. Agric. Biol. Chem. 50: 1887-1888.
- Khatter, J.C., Soni, P.L., Hoeschen, L.E., Alto, L.E., and Dhalla, N.S. Subcellular effects of taurine on guinea pig heart. In: The effects of taurine on Excitable Tissues, edited by S.W. Schaffer, S.I. Baskin, and J.J. Kocsis. New York: Spectrum, 1981, p. 281-294.
- Karnicky, J.F., Zitelli, L.T., and van der Wal, Sj. 1987. Ultrasonic Micronebulizer Interface for High-Performance Liquid Chromatography with Flame Photometric Detection. Anal.Chem. 59: 327-333.
- Kientz, C.E., Verweij, A., de Jong, G.J., and Brinkman, U.A. Th. 1989. The Potential of On-Line Flame Photometric Detection in Microcolumn Liquid Chromatography. J.High Resol.Chromatogr. 12: 793-796.

- Kientz, C.E., Verweij, A. 1987. The Application of a Flame Photometric Detector in Packed Microcapillary Liquid Chromatography: Detection of Organophosphates. Intern. J. Environ. Anal. Chem. 30: 255-263.
- Kientz, C.E., Verweij, A., Boter, H.L. Poppema, A., Frei, R. W., de Jong, G.J., and Brinkman, U.A. 1989. On-Line Flame Photometric Detector In Micro-Column Liquid Chromatography. J. Chromatogr. 467: 385-394.
- Kirkbright, G.F., and Marshall, M. 1972. Direct Determination of Sulfur by Atomic Absorption Spectrometry in a Nitrogen Separated Nitrous Oxide-Acetylene Flame. Anal. Chem. 44: 1288-1290.
- Koivusalo, M. and Uotila, L. 1974. Enzymatic methods for the quantitative determination of reduced glutathione. Anal. Biochem. 59: 34-45.
- Kramer, J.H., Chovan, J.P., and Schaffer, S.W. 1981. Effect of taurine on calcium paradox and ischemic heart failure. Am. J. Physiol. 240 (Heart Circ.Physiol. 9):H238-H246.
- Kramlich, J.C. 1980. The fate and behaviour of fuel-sulfur in combustion systems. Ph.D. thesis, Washington State University.
- Kulakowski, and E.C. Maturo, J. 1984. Hypoglycemic properties of taurine: not mediated by enhanced insulin release. Biochem. Pharmacol. 33: 2835-2838.
- Lack, L. and Smith M. 1964. An enzymatic determination of reduced glutathione. Anal. Biochem. 8: 217-222.
- Lancaster, J.E.; Collin, H.A. 1981. Presence of Alliinase in Isolated Vacuoles and of Alkyl Cysteine Sulfoxides in the Cytoplasm of Bulbs of Onions (Allium Cepa). Plant Sci. Lett. 22:169-176.
- Lavoisier, A., "Elements of Chemistry", R. Kerr, Transl., Creech & Son, Edinburgh, 1794.
- Lawson, L.D.; Wang, Z.Y.J.; and Hugues, B.G. 1991. Identification and HPLC Quantification of the Sulfides and Dilk(en)yl Thiosulfinates in Commercial Garlic Products. Planta Medica. 57: 363-370.
- Lawson, L.D.; Wood, S.G.; Hugues, B.G. 1991b. HPLC Analysis of Allicin and other Thiosulfinates in Garlic Cloves Homogenates. Planta Medica. 57: 263-270.
- Lehman, L.D., and Klaassen, C.D. 1986. Separation and Quantification of Metallothioneins by High-Performance Liquid Chromatography Coupled With Atomic Absorption Spectrophotometry. Anal. Biochem. 153: 305-314.

- Lemoine, M. "Le Soufre en Agriculture". L'office de Publicité Générale, Paris, Société du Superphosphate, Paris, 1973.
- Li, P., and Caldwell. 1966. The Oxidation of Elemental Sulfur in Soil. Soil Sci. Soc. Amer. Proc. 30: 370-372.
- Liu, S., Ansari, N.H., Wang, L., and Srivastava, S.K. 1996. A Rapid HPLC Method For the Quantification of GSH and GSSG in Ocular Lens. Current Eye Research. 15: 726-732.
- Lobel, P.B., and Payne, J.F. 1987. The Mercury-203 Method for evaluating Metallothioneins: interference by Copper, Mercury, Oxygen, Silver and Selenium. Comp. Biochem. Physiol C: Comp. Pharmacol. Toxicol. 86C: 37-39.
- Lombardini, J.B. 1985. Effects of taurine on calcium ion uptake and protein phosphorylation in rat retinal membrane preparations. J. Neurochem. 45: 268-275.
- L'Vov, in Atomic Spectroscopy, eds. R.M. Dagnall and G.F. Kirkbright, Butterworths, London, 1970, p. 28.
- Marafante, E., Walter, M., and Dencker, L. 1984. Sci. Total Environ. 34: 223.
- Margoshes, M. and Vallee, B.L. 1957. A cadmium protein from equine kidney cortex. J. A. Chem. Soc., 79: 4813-4814.
- Markides, K.E., Lee, E.D., Bolick, R., and Lee, M.L. 1986. Capillary Supercritical Fluid Chromatography with Dual-Flame Photometric Detection. Anal. Chem. 58: 740-743.
- Marriott, P. J. and Cardwell, T.J. 1981. Chromatographic parameters derived for the non-linear response of a flame photometric detector. Chromatographia. 14:279-284.
- Mason, A.Z., Storms, S.D., and Jenkins, K.D. 1990. Metalloprotein Separation and Analysis by Directly Coupled Size Exclusion High-Performance Liquid Chromatography Inductively Coupled Plasma Mass Spectroscopy. Anal. Biochem. 186: 187-201.
- Masuoka, N., Yoa, K., Kinuta, M., Ohta, J., Wakimoto, M., and Ubuka, T. 1994. High-performance liquid chromatographic determination of taurine and hypotaurine using 3,5-dinitrobenzoyl chloride as derivatizing reagent. J. of Chromatography. 660: 31-35.
- Matsubara, J., Tajima, Y., Karasawa, M. 1987. Promotion of Radioresistance by Metallothionein Induction prior to Irradiation. Environmental Research. 43: 66-74.

- McCrea, P.F., and Light, T.S. 1967. Emission Response of Some Hydrocarbon-Methanol Solutions in Hydrogen Flames. Anal. Chem. 39: 1731-1736
- McGaughey and Gangwal, S.K. 1980. Comparison of three commercially available gas chromatographic-flame photometric detectors in the sulfur mode. Anal.Chem. 52: 2079-2083.
- McGuffin, V.L., and Novotny, Milos. 1981. Flame Emission Detection in Microcolumn Liquid Chromatography. Anal. Chem. 53: 946-951.
- Meister, A and Take, S.S. 1976. Glutathione and related γ-glutamyl compounds: Biosynthesis and utilization. Ann. Rev. Biochem. 45: 559-604.
- Meister, A. 1981. Metabolism and functions of glutathione. Trends in Biochemical Sciences. 6: 231-239.
- Meister, A. and Anderson, M.E. 1983. Glutathione. Ann. Rev. Biochem. 52: 711-760.
- Meister, A. 1983. Selective modification of glutathione metabolism. Science. 220: 472-477.
- Meyer, B. 1976. The structures of elemental Sulfur. Adv. Inorg. Chem. and Radiochem. 18: 287-317.
- Meyer, B. Sulfur, Energy, and Environment. Edited by Elsevier Scientific Company. Netherlands, 1977.
- Michelet, F., Gueguen, R., Leroy, P., Wellman, M., Nicolas, A., and Sies, G. 1995. Blood and Plasma Glutathione Measured in Healthy Subjets by HPLC: Relation to Sex, Aging, Biological Variables, and Life Habits. Clinical Chemistry. 41: 1509-1517.
- Miron, T., Rabinkov, A., Mirelman, D., Weiner, L., and Wilchek, M. 1998. A Spectrophotometric Assay for Allicin and Alliinase (*Aliin lyase*) Activity: Reaction of 2-Nitro-5-thiobenzenoate with Thiosulfinates. Anal. Biochem. 265: 317-325.
- Mitton, K.P. and Trevithick, J.R. 1994. High-Performance Liquid Chromatography-Electrochemical Detection of Antioxidants in Vertebrate Lens: Glutathione, Tocopherol, and Ascorbate. Methods in Enzymology. 233: 523-539.
- Miyairi, S., Shibata, S., and Naganuma, A. 1998. Determination of Metallothionein by High-Performance Chromatography with Fluorescence Detection Using an Isocratic Solvent System. Anal. Biochem. 258: 168-175.
- Müller, B. 1990. Garlic (Allium sativum): Quantitative Analysis of the Tracer Substances Alliin and Allicin. Planta Medica. 56: 589-590.

- Nelson, J.K., Getty, R.H., and Birks J.W. 1983. Florine Induced Chemiluminescence Detector for Reduced Sulfur Compounds. Anal. Chem. 55: 1767-1770.
- Nemer, M., Wilkinson, D.G., Travaglini, E.C., and Sternberg, E.J. 1985. Sea urchin metallothionein sequence: Key to an evolutionary diversity. Proc. Natl. Acad. Sci. USA. 82: 4992-4994.
- Newton, G.L., Dorian, R., and Fahey, R.C. 1981. Analysis of biological thiols: derivatization with monobromobimane and separation by reverse-phase high performance liquid chromatography. Anal. Biochem. 114: 383-387.
- Norey, C.G., Cryer, A., and Kay. 1990. A comparison of cadmium-Induced Metallothionein Gene expression and Me⁺² Distribution in the Tissues of Cadmium-Sensitive (Rainbow Trout; Salmo Gairdneri) and Tolerant (Stone Loach); Noecheilus Barbatulus) Species of Fresh water Fish. Comp. Biochem. Physiol. 97 C: 221-225.
- Norey, C.L., Less, W.E., Darke, B.M., Stark, J.M., Barker, T.S., Cryer, A., and Kay, J. 1990. Immunological Distinction Between Piscine and Mammalian Metallothioneins. Comp. Biochem. Physiol. 95 B: 597-601.
- Oja, S.S., and Kontro, P., In "Taurine and Neuropharmacological Disorders, Barbeau, A., and Huxtable, R.J., Eds Raven Press, New York, N.Y., 1978, pp 181-200.
- Olesik, S.V., Pekay, L.A. and Paliwoda, E.A. 1989. Characterization and Optimization of Flame Photometric Detector in Supercritical Fluid Chromatography. Anal. Chem. 61: 58-65.
- Onosaka, S. and Cherian, M.G. 1981. The Induced Synthesis of Metallothionein in Various Tissues of Rat in Response to Metals. I. Effect of Repeated Injection of Cadmium. Toxicology. 22:91-101.
- Onosaka, S. and Cherian, M.G. 1982. Comparison of metallothionein determination by polarographic and cadmium-saturation methods. Toxicol. Appl. Pharmacol. 63: 270-274.
- Otvos, J.D. and Armitage, I.M. 1980. Structure of the metal clusters in rabbit liver metallothionein. Proc. Natl. Acad. Sci. USA. 91: 1219-1223.
- Otvos, J.D., Olafson, R.W., and Armitage, I.M. 1982. Structure of an invertebrate metallothionein Scylla serrata. J. Biol. Chem. 257:2427-2431.
- Otvos, J.D., Engeseth, I.M., and Wehrli, S. 1985. Preparation and ¹¹³Cd NMR Studies of Homogeneous Reconstituted Metallothionein: Reaffirmation of the two-Cluster Arrangement of Metals. Biochemistry. 24: 6735-6740.

- Owens, C.W.I. and Belcher, R.V. 1965. A colorimetric micro-method for the determination of glutathione. Biochem. J. 94: 705-711.
- Ozasa, H., and Gould, K.G. 1982. Protective effect of taurine from osmotic stress on chimpanzee spermatozoa. Arch. Androl. 9: 121-126.
- Parmentier, C., Leroy, P., Wellman, M., and Nicolas, A. Determination of Cellular Thiols and Glutathione-related enzyme Activities: Versatility of High-Performance Liquid Chromatography-Spectrochemical Detection. Journal of Chromatography B. Issue 1-2. 719: 37-46.
- Pasantes-Morales, H., and Cruz, C. 1984. Protective effect of taurine on peroxidation-induced damaged in photoreceptor outer segments. J. Neurosci. Res. 11:303-311.
- Pasantes-Morales, H., Quesada, O., Alcocer, L., and Sánchez-Olea. 1989. Taurine content in foods. Nutr. Rep. Int. 40: 793-801.
- Patierno, S.R., Pellis, N.M., Evans, R.M. and Costa, M. 1983. Application of a Modified ²⁰³Hg Binding Assay for Metallothionein. Life Sci. 32: 1629-1636.
- Patterson, P.L., Howe, R.L., and Abu-Shumays, A. 1978. Dual-Flame Photometric Detector for Sulfur and Phosphorus Compounds in Gas Chromatograph Effluents. Anal. Chem. 50: 339-344.
- Patterson, P.L. 1978. Comparison of Quenching Effects In Single-and Dual Flame Photometric Detectors. Anal. Chem. 50: 345-348.
- Pauling, Linius, "The Nature of the Chemical Bond, 3rd ed., Cornell University Press, Ithica, N.Y., 1960.
- Pentz, E.I., Davenport, C.H., Glover, W., and Smith, D.D. 1957. A test for the determination of taurine in urine. J.Biol. Chem. 228: 433-445.
- Piao, J.H., Hill, K.E., Hunt, R.W. Jr., and Burk, R.F. 1990. Effect of selenium deficiency on tissue taurine concentration and urinary taurine excretion in the rat. J. Nutr. Biochem. 1: 427-430.
- Piotrowski, J.K., Trojanowska, B., Wisniewska-Knypl, and Bolanowska, M. 1974. Mercury binding in the kidney and liver of rats repeatedly exposed to mercury chloride: Induction of metallothionein by mercury and cadmium. Toxicol. Appl. Pharmacol. 27: 11-19.
- Racci, J.M., and Welton, B. 1985. Operation of the Sigma 2000 Flame Photometric detector. Instrum. Res. 1: 30-35.

- Raggi, M.A., Mandrioli, Bugamelli, F., and Sabbioni, C. 1997. Comparison of Analytical Methods for Quality Control of Pharmaceutical Formulations Containing Glutathione. Chromatographia. 46: 17-22.
- Raggi, M.A., Mandrioli, R., Casamenti, G., Musiani, D., and Marini, M. 1998. HPLC Determination of Glutathione and Thiols in Human Mononuclear Blood Cells. Biomedical Chromatography. 12: 262-266.
- Reynoso, G.T. and D.E. Gamboa, B.A. 1982. Salt tolerance in the freshwater algae Chlamydomonas reinhardii: effect of proline and taurine. Comp. Biochem. Physiol. 73: 95-100.
- Richards, M.P. 1989. Characterization of the Metals Composition of Metallothionein Isoforms using Reversed-Phase High Performance Liquid Chromatography with Atomic Absorption Spectrophotometric Detection. J.Chromatogr. 482: 87-97.
- Roesijadi, G. 1981. The significance of low molecular weight metallothionein-like proteins in marine invertebrates: current status. Mar. Environ. Res. 4: 167-179.
- Rupprecht, W.E., and Phillips, T.R. 1969. The Utilisation of Fuel-Rich Flames as Sulfur Detectors. Anal. Chem. Acta. 47: 439-449.
- Rupp, H. and Weser, U. 1978. Circular dichroism of metallothioneins: a structural approach. Biochem. Biophys. Acta. 533: 209-226.
- Rydén, L., and Deutsch. 1978. Preparation and Properties of the Major Copper-bearing Component in Human Fetal Liver. Its identification as Metallothionein. The journal of Biological Chemistry. 253: 519-524.
- Ryerson, T.B., Dunham, A.J., Barkley, R.M., and Sievers, R.E. 1994. Sulfur Selective Detector for Liquid Chromatography Based on Sulfur Monoxide Ozone Chemiluminescence. Anal. Chem. 66: 2841-2851.
- Sakaguchi, M., Murata, M., and Kawai, A. 1982. Taurine levels in some tissues of yellowtail (Seriola quiqueradiata) and markeral (Scomber japonicus). Agric. Biol. Chem. 46: 2857-2858.
- Schubert, S.A., Clayton, J.W. Jr, and Fernando, Q. 1979. Determination of Sulfite and Sulfate by Time-Resolved Molecular Emission Spectrometry. Anal. Chem. 51: 1297-1301.
- Schmidt, S.Y., Berson, E.I., Hays, K.C. 1976. Retinal degeneration in cats fed casein. I. Taurine deficiency. Invest. Ophthal. Mol. 15: 47-62.
- Schultz, O.E., Mohrmann, H.L. 1965. Beitragzur Analyse der Inhaltsstoffe von Knoblauch-Allium Savativum L. Die Pharmazie. 20: 441-447.

- Schwartz, S.A. and Meyer, G.A. 1986. Characterization of aerosols generated by thermospray nebulization for atomic spectroscopy. Spectrochimica Acta.. 41B: 1287-1298.
- Schwimmer, S., Mazelis M. 1963. Characterization of Allium Cepa (onion). Arch. Biochem. Biophys. 100: 66-73.
- Semmler, F.W. 1892. Arch. Pharm. 230: 434.
- Sendl, A and Wagner, H. 1990. Comparative Chemical and Pharmacological Investigations of Extracts of Allium Ursinum (Wild Garlic) and Allium sativum (Garlic). Planta Medica. 56: 588-589.
- Sendl, A., Schliack, M., Loser, R. Stanislaus, F., and Wager, H. 1992. Inhibition of cholesterol synthesis in vivo by extracts and isolated compounds from garlic and wild garlic. Artherosclerosis. 94: 79-85.
- Shearer, R.L. 1992. Development of Flameless Sulfur Chemiluminescence Detector: Application to Gas Chromatography. Anal. Chem. 64: 2192-2196.
- Shihabi, Z.K., Goodmam, H.O., and Holmes, R.P., in "Taurine", Eds. J.B. Lombardini, Plenum Press, New York, 1989.
- Sorbo, B. 1961. A method for the determination of taurine in urine. Clin. Chem. Acta. 6: 87-90.
- Sparla, A.M. and Overnell, J. 1990. The binding of cadmium to crab cadmium metallothionein. Biochem. J. 267: 539-540.
- Stadtman, T.C. 1979. Some Selenium-Dependent Biochemical processes. Adv. Enzymol. 48:1-28.
- Starkey, R.L. 1966. Oxidation and Reduction of Sulfur Compounds in Soils. Soil Sci. 101: 297-306.
- Streitwieser, A., and Heathcock, C. Introduction to organic Chemistry, Mcmillan Publishing Company, N.Y., U.S.A, 1976, p.409
- Sturman, J.A., Moretz, R.C., French, J.H., and Wisniewski, H.M. 1985. Taurine deficiency in the developing cat: persistence of the cerebellar external granule cell layer. J. Neurosci. Res. 13: 408-416.
- Sturman, J.A. 1986. Taurine in infant physiology and nutrition. Pediatr. Nutr. Rev. 1-11.
- Sturman, J.A., Messing, J.M., Rossi, S.S., Hofmann, A.F., and Neuringer, M.D. 1988. Tissue taurine content and conjugated bile acid composition of rhesus

- monkey infants fed a human soy-protein formula with or without taurine supplementation for 3 months. Neurochem. Res. 13:311-316.
- Sugden, T.M., Bulewicz, E.M., and Demerdache, A. Some observations on oxides and hydrides of nitrogen and sulfur in flame gases containing atomic hydrogen, atomic oxygen, and hydroxyl radicals. In Chemical Reactions in the Lower and Upper Atmosphere. Wiley, New York, 1962, pp 99-108.
- Sugiyama, T., Suzuki, Y., and Takeuchi, T. 1973. Characteristics of S₂ Emission Intensity With a Flame Photometric Detector. J. Chromatog. 77: 309-316.
- Sunaga, H., Kobayashi, E., Shimojo, N., and Suzuki, K.T.1987. Detection of Sulfur-Containing Compounds in Control and Cadmium-Expoxed Rat Organs by High-Performance Liquid Chromatography-Vacuum-Ultraviolet Inductively Coupled Plasma-Atomic Emission Spectrometry (HPLC-ICP). Anal. Biochem. 160:160-168.
- Suzuki, T.K. 1991. Detection of Metallothioneins by High-Performance Liquid Chromatography-Inductively Coupled Plasma Emission spectroscopy. In Method in Enzymology, Academic Press, vol. 205, pp 198-205
- Suzuki, T.K. and Maitani, T. 1981. Metal-dependent Properties of metallothionein. Biochem. J., 199: 289-295.
- Suzuki, K.T. 1980. Direct Connection of High-Speed Liquid Chromatograph (Equipped with Gel Permeation Column) to Atomic Absorption Spectrophotometer for Metalloprotein Analysis: Metallothionein. Anal. Biochem. 102: 31-34.
- Syty, A., and Dean, J. 1968. Determination of Phosphorus and Sulfur in Fuel Rich Air-Hydrogen Flames. Applied Optics.7: 1331-1336.
- Takahashi, H., Nara, Y., Meguro, H., and Tuzimura, K. 1979. A sensitive fluorometric method for determination of glutathione and some thiols in blood and mammalian tissues by high performance liquid chromatography. Agric. Biol. Chem. 43: 1439-1445.
- Thomas, E.L., Grisham, M.B., and Jefferson, M.M. 1983. Evidence for a role of taurine in the in vivo oxidative toxicity of neutrophils toward erythrocytes. J. Biol. Chem. 260: 3321-3329.
- Tietze, F. 1969. Enzymatic method for quantitative determination of nanogram amounts of total and oxidized glutathione. Anal. Biochem. 27: 502-522.
- Tokarska, B., Karwowska, K. 1983. Nahrung. 27: 443-447.

- Toshiaki, Y. 1998. Determination of Reduced and Oxidized Glutathione in Erythrocytes by High-Performance Liquid Chromatography With Ultraviolet Absorbance Detection. Journal of Chromatography B. 678: 157-164.
- Toshiaki, S., Yoshito, S., and Tsugio, T. 1973. Interferences of S₂ Molecular Emission In a Flame Photometric Detector. J. of Chromatogr. 80: 61-67.
- Vernin, G., Metger, J., Fraisse, D., Scharff, C. 1986. GC-MS (EI, PCI, NCI) Computer Analysis of Volatile Sulfur Compounds in Garlic Essential Oils. Application of the Mass Fragmentometry SIM Technique. Planta Medica. 52: 96-101.
- Verthein, T. Untersuchung des Knoblauchöls. 1844. Ann. Chem. 51: 289-315.
- Virtanen, A.I. 1962. Some Organic Sulfur Compounds in Vegetables and Fodder Plants and their Significance in Human Nutrition. Angew. Chem. Int. Ed. Eng. 1: 299-306.
- Virtanen, A.I. 1965. Study of Organic Sulfur Compounds and other Labile Substances in Plants. Phytochemistry. 4: 207-228.
- Wade, J. V., Olson, J.P., Samson, F.E., Nelson, S.R., and Pazdernik, T.L. 1988. A possible role for taurine in osmoregulation within the brain. J. Neurochem. 51: 740-745.
- Watanabe, T., Komade, K. 1966. Agr. Biol. Chem. (Tokyo). 9:418.
- Weinberg, D.S., Manier, M.L., Richardson, M.D., and Haibach, F.G. 1993. Identification and Quantification of Organosulfur Compliance Markers in a Garlic Extract. J. Agric. Food Chem. 41: 37-41.
- Whitaker, J.R. 1976. Development of flavor, odor, and pungency in onion and garlic. Adv. Food Res. 22: 73-133.
- White, P.C. 1984. Recent Developments in Detection Techniques for High-performance Liquid Chromatography. Part I. Spectroscopic and Electrochemical Detectors. Analyst. 109: 677-697.
- Whittwer, A.J., Stai, L., Ching, W.M., and Stadtman, T.C.1984. Identification and Synthesis of a Naturally Occurring Selenonucleoside in Bacterial tRNAs: 5[(Methylamino)methyl]-2-Selenouridine. Biochemistry. 23: 4650-4655.
- Winge, D.R. and Miklossy, K,-A. 1982. Domain Nature of Metallothionein. J. Biol. Chem. 257: 3471-3476.
- Woodward, G.E. 1935. Glyoxalase as a reagent for the quantification microestimation of glutathione. J. Biol. Chem. 109: 1-10.

- Worden, J.A., and Stipanuk, M.H. 1985. A comparison by species, age and sex of cysteinesulfinate decarboxylase activity and taurine concentration in liver and brain animals. Biochem. Physiol. 82B: 233-239.
- Wu, J.L.; Wu, C.M. 1981. High-performance liquid chromatographic separation of shallot volatile oil. J. Chromatog. 214: 234-236.
- Xing, M.; Mei-ling, W.; Hai-xiu, X.,X.; Xi-pu, P.; Chun-yi,G.; Na, H.; Mei-yun, F. 1982. Acta Nutrimenta Sinica. 4: 53.
- Yang, G.Q., Wang, S., Zhou, R., and Sun, R. 1983. Endemic selenium Intoxication of humans in China. Am. J. Clin. Nutr. 37: 872-881.
- You, W. C.; Blot, W. J.; Chang, A.; Ershow, A.; Z. T.; An, Q.; Henderson, B. E.; Fraumani, J. F.; Wang, T. G. 1989. Allium Vegetables and Reduced Risk of Stomach Cancer. J. Natl. Cancer Inst. 81: 162-164.
- Yu, T.H., Wu, C.M., Liou, Y.C. 1989. Volatile compounds from garlic. J. Agric. Food Chem. 37: 725-730.
- Zelazowski, A. and Piotrowski, J.K. 1977. A modified procedure for determination of metallothionein-like proteins in animal tissues. Acta Biochem. Pol. 24: 77-103.